



University of
Salford
MANCHESTER

**EXPERIMENTAL INVESTIGATION OF THE EFFECT OF
NANOPARTICLES AND POLYMER ON INTERFACIAL
TENSION BETWEEN OIL AND WATER DURING
ENHANCED OIL RECOVERY (EOR)**

by

FAHAD RASHID

Master by Research

Dissertation 2019

Declaration

I hereby declare that the work in this Thesis is my own, except for quotations and summaries that have been duly acknowledged. The thesis has not been accepted for any degree and is not concurrently submitted for the award of another degree.

Signature:

Name:

ID Number:

Date:

Abstract

Nanotechnology has been generally used in several other industries, and the interest in it within the oil industry is increasing, due to its potential to deeply change enhanced oil recovery (EOR) and to improve the mechanism of recovery. With the decline in oil discoveries during the last decades, it is believed that EOR technologies will play a key role to meet the energy demand in years to come. New materials and additives are needed to make EOR economical in challenging reservoirs or harsh environments. Nanoparticles have been widely studied for EOR, but nanoparticles with polymer chain joined to the surface, known as polymer-coated nanoparticles (PNPs), are an emerging class of materials that may be better than nanoparticles for EOR due to enhanced solubility and stability, greater maintenance of foams and emulsions, and more facile conveyance through porous media.

This research study experimentally investigates the interfacial tension (IFT) of silica/gum-Arabic) in the presence brine at different temperature to enhanced and improve oil recovery. The study also investigate experimentally the pH value of brine and in combination with nanoparticles and polymer for liquid characterization.

The results obtained for the prepared nano polymer fluid by dispersion of hydrophilic Silica and Gum Arabic in three different concentrations of brine (15%, 10%, 5%) showed variability and agglomeration. The nanopolymer fluids became cloudy due to the aggregation and sedimentation of nanopolymer particles, and this demonstrates that NaCl concentrations exceeded the critical salt concentrations (CSC) in the solution. However, the stability would not be controlled by decreasing the concentrations of NaCl, since the size of the nanopolymer particles that have been used in this experiment is 20nm, which is greater than 15nm particles that has a CSC of 0.5wt%.

Additionally, the results of the interfacial tension between the brine 1.5wt% and oil decreased from 17.48mN/m to 12.58mN/m when the temperature increased from 30°C to 50°C. Similar behaviour was observed at 70°C, 90°C and 100°C with a recorded IFT of 12.1, 5.75 and 5.74mN/m. The IFT between oil and 1.5wt.% brine-based combinations (silica (0.15wt%) + Gum Arabic (0.4wt%) particles was 17.48mN/m at 30°C. It then decreased to 12.58mN/m at 50°C and to 5.75mN/m and 5.74mN/m at 90°C and 100°C, demonstrating that the best results are at the lower temperature 30°C and at the higher temperature of 100°C, where interfacial tension reduced from 17.48mN/m to 5.74mN/m, with a reduction of almost 67.17%.

Conclusively, The IFT tends to decrease significantly even with increasing and decreasing the combination of silica nanoparticles and gum Arabic polymer concentration. Although, fluid 5 with 15% brine shows more efficient in lowering IFT compared with the other combinations, fluid 5 solutions were able to reduce IFT the most at 100°C, thus, fluid 5 solution also gives the lowest IFT values at 30°C. Therefore, these percentage of Brine 15% + (silica (0.15wt%) + Gum Arabic (0.4wt%) could be a very good combination for enhance oil recovery.

Acknowledgements

I would like to pay special thanks, warmth and appreciation to the persons below who made my research successful, and who assisted me at every point to cherish my goal:

My Supervisor, Dr Abubakar Abbas, for his vital support and assistance. His encouragement made it possible to achieve my goal.

My Assistant Supervisor, Professor Ghasem Nasr, whose help and sympathetic attitude at every point during my research helped me to work in time.

All the faculty, staff members and lab technicians, whose services turned my research a success.

My Mom and Dad and family members, without whom I was nothing; they not only assisted me financially, but also extended their support morally and emotionally.

Contents

Declaration	ii
Abstract	iii
Acknowledgements	iv
List of Figures	x
List of Tables	xiii
Chapter 1 Introduction	1
1.1 Preface	1
1.2 Overview	1
1.3 Explanation of the Research	2
1.4 Applications and Significance of Interfacial Tension	2
1.5 Research Contributions	3
1.6 Aim and Objectives	3
Chapter 2 Theoretical Background and Literature Review	4
2.1 Preface	5
2.2 Introduction	5
2.3 Basic Concepts and Definition in Reservoir Engineering	4
2.4 Reservoir Properties	5
2.4.1 Porosity	5
2.4.2 Saturation	6
2.4.3 Surface and Interfacial Tension	..5
2.4.4 Wettability	8
2.4.5 Permeability	9

2.5	Fluid Properties	10
2.5.1	Density	12
2.5.2	Viscosity	12
2.6	Introduction to Nanotechnology for Enhanced Oil Recovery	11
2.6.1	Nanofluids	12
2.6.2	Potential Nanoparticles	13
2.7	Mechanism for Increased Recovery	14
2.7.1	Structural Disjoining Pressure	14
2.7.2	Effect on Interfacial Tension	16
2.7.3	Effect on Wettability	17
2.7.4	Effect on Viscosity	18
2.8	Polymer (Gum Arabic)	18
2.8.1	Introduction	19
2.8.2	Polymer Types	20
2.8.3	Effects of Salinity on Polymer Rheology	19
2.8.4	Effects of Temperature on Polymer Rheology	20
2.8.5	Effects of Concentration on Polymer Rheology	20
2.8.6	Effects of Concentration on Polymer Absorption	21
2.8.7	Choosing the Best Polymer	21
2.9	Mobility Ratio	22

Chapter 3	Experimental, Materials and Methods of IFT	24
3.1	Introduction	24
3.2	Measuring Principle	31
3.3	Making a Measurement	33
3.3.1	Preparing for the Measurement	33
3.3.2	Choice of Needle Diameter	33
3.3.3	Determining the Image Magnification	33
3.3.4	Generating the Pendant Drop and Drop Image Optimisation	35
3.3.5	Excluding Evaporation Effects	37
3.3.6	Recording the Stationary Value	32
3.4	Carrying out the Drop hape Analysis	32
3.4.1	Required System Parameters	38
3.4.2	The sensibility of profile recognition in the analysis software	38
3.4.3	Setting the Baseline for the Analysis	39
3.5	Sample Preparation	34
3.5.1	Materials Used in the Present Study	
	Error! Bookmark not defined.	
3.5.2	Preparation of Salt Water (Brine)	26
3.5.3	Brine Preparation Procedure	26
3.5.4	Combination (Silica and Gum Arabic) Preparation Procedure	27
3.6	Liquid Characterisation	37
3.6.1	PH Measurement	29
3.6.2	Equipment Description:	29
3.6.3	PH Calibration Procedure	30

Chapter 4	Results and Discussion	41
4.1	Introduction	41
4.2	Combination of Silica and Gum Arabic Results	41
4.3	Interfacial Tension Results	41
4.3.1	Fluid 3 Brine 5% (Silica 0.15wt% + Gum Arabic 0.4wt%)	42
4.3.2	Fluid 5 Brine 5% (Silica 0.25wt% + Gum Arabic 0.2wt%)	43
4.3.3	Fluid 4 Brine 5% (Silica 0.2wt% + Gum Arabic 0.3wt%)	43
4.3.4	Fluid 3 Brine 10% (Silica 0.15wt% + Gum Arabic 0.4wt%)	44
4.3.5	Fluid 5 for Brine10% (Silica 0.25wt% + Gum Arabic 0.2wt%)	44
4.3.6	Fluid 4 for Brine10% (Silica 0.2wt% + Gum Arabic 0.3wt%)	44
4.3.7	Fluid 3 Brine 15% (Silica 0.15wt% + Gum Arabic 0.4wt%)	46
4.3.8	Fluid 5 Brine 15% (Silica 0.25wt% + Gum Arabic 0.2wt%)	46
4.3.9	Fluid 4 Brine 15% (Silica 0.2wt% + Gum Arabic 0.3wt%)	46
4.3.10	Fluid 4 Distilled Water (Silica 0.2wt% + Gum Arabic 0.3wt%)	47
4.3.11	Fluid 3 Distilled Water (Silica 0.15wt% + Gum Arabic 0.4wt%)	48
4.3.12	Fluid 5 Distilled Water (Silica 0.25wt% + Gum Arabic 0.2wt%)	48
4.4	PH Results	48
4.5	The Effect of Pressure and Temperature on IFT	48
4.6	The Effect of Salinity on IFT Reduction	49
Chapter 5	Conclusion and Recommendations	51
5.1	Introduction	50
5.2	Conclusions	50
5.3	Recommendations	51
References		54

Appendix A	Drop Image Advanced Software	59
Appendix B	Pendant Drop Method Results	66

List of Figures

Figure 2.1	Droplet on the Surface (Torsæter, 2012)	7
Figure 2.2	How the Interfacial Tensions Work on a Droplet/Bubble (Hiemenz and Rajagopalan, 1997)	9
Figure 2.3	Connected Pores Gives Permeability (MPG Petroleum, 2003)	10
Figure 2.4	Typical Relative Permeability Curves for Water Wet Sandstone (Zolotukhin and Ursin, 2000)	11
Figure 2.5	Two-Phase Diagram of Reservoir Fluids Showing How They Will Vary With Different Pressures and Temperatures (Whitson and Brul`e, 2000)	11
Figure 2.6	Nanoparticles Establishing a Wedge-Film, Resulting in a Structural Disjoining Pressure. (Wasan et al., 2011)	14
Figure 2.7	Disjoining Pressure in the Wedge Structure (Wasan and Nikolov, 2003)	16
Figure 2.8	Breakup of Oil Droplets Due to Absorption of Nanoparticles (Frijters et al., 2012)	17
Figure 2.9	Effect of Viscosity and Relative Permeability on Fisplacement.	19
Figure 2.10	Fingering Effect Promoted by the Unfavorable Mobility Ratio (top), and Good Oil Recovery Facilitated by the use of Polymer Flooding (bottom) (G. Zerkalo)	22
Figure 3.1	Pendant Drop (A); Curved Surface Segment (B), Radii of the Horizontal (green) and Vertical (blue) Circles of Curvature Define the Surface Curvature at Point P	31
Figure 3.2	Influence of Tilted Needle on the Magnification Factor. In (A) the Correct Factor is Measured; in (B) the Result Varies by 0.5%	34
Figure 3.3	Proper Distance Between the two Measuring Lines for Determining the Magnification	35
Figure 3.4	Adequately (A) and Inadequately (B) Deformed Pendant Drops	35

Figure 3.5	Drops with Correct (A) and Too Low (B) Magnification	36
Figure 3.6	Correct (A) and Incorrect (B) Focus Setting.	36
Figure 3.7	Drop Image with Suitable (A), Too Dark (B) and Too Bright (C) Background Illumination	31
Figure 3.8	Grey Level Values of the Drop and Surrounding Phase Under Optimal Illumination	37
Figure 3.9	Influence of the ‘Profile Detection’ Value on Profile Recognition: (A) Correct Value, Profile Found Completely; (B) Value Too Low, No Profile Found; (C) Value Too High, Profile only Partly Found	39
Figure 3.10	(A) Fit Depicts Drop Profile Correctly and Provides an Accurate Result; (B) Fit Clearly Varies from Drop Profile and Provides Inaccurate Result.	39
Figure 3.11	Materials and Equipment Used for Salt-Water: (A) Sodium chloride, (B) Tared mass balance with Petri dish, (C) Magnetic stirrer with brine contained	27
Figure 3.12	Preparing Brine by Mixture	28
Figure 3.13	PH Measuring Device	30
Figure 3.14	Schematic Presentation of the Experimental Validation Stage	40
Figure 4.0.1	Fluid 3 IFT -Brine 5% - Oil Details at Five Temperature Ranges (30°C, 50°C, 70°C, 90°C and 100°C)	42
Figure 4.2	Fluid 5 IFT - Brine 5% - Oil Details at Five Temperature Ranges (30°C, 50°C, 70°C, 90°C and 100°C)	49
Figure 4.3	Fluid 4 IFT - Brine 5% - Oil Details at Five Temperature Ranges (30°C, 50°C, 70°C, 90°C and 100°C)	43
Figure 4.4	Fluid 3 IFT - Brine 10% - Oil Details at Five Temperature Ranges (30°C, 50°C, 70°C, 90°C and 100°C)	43
Figure 4.5	Fluid 5 IFT - Brine 10% - Oil Details at Five Temperature Ranges (30°C, 50°C, 70°C, 90°C and 100°C)	44

Figure 4.6	Fluid 4 IFT - Brine 10% - Oil Details at Five Temperature Ranges (30°C, 50°C, 70°C, 90°C and 100°C)	44
Figure 4.7	Fluid 3 IFT - Brine 15% - Oil Details at Five Temperature Ranges (30°C, 50°C, 70°C, 90°C and 100°C)	45
Figure 4.8	Fluid 5 IFT - Brine 15% - Oil Details at Five Temperature Ranges (30°C, 50°C, 70°C, 90°C and 100°C)	45
Figure 4.9	Fluid 4 IFT - Brine 15% - Oil Details at Five Temperature Ranges (30°C, 50°C, 70°C, 90°C and 100°C)	46
Figure 4.10	Fluid 4 IFT - Distilled Water - Oil Details at Five Temperature Ranges (30°C, 50°C, 70°C, 90°C and 100°C)	46
Figure 4.11	Fluid 3 IFT - Distilled Water - Oil Details at Five Temperature Ranges (30°C, 50°C, 70°C, 90°C and 100°C)	47
Figure 4.12	Fluid 5 IFT - Distilled Water - Oil Details at Five Temperature Ranges (30°C, 50°C, 70°C, 90°C and 100°C)	47
Figure 4.13	Showing the Results Between IFT and Pressure	49
Figure 4.14	Influence of NaCl Concentration	49
Figure A 1	Display Screen Showing Capillary Tube in the Chamber	61
Figure A 2	Screen Displayed for Setting up a New Experiment Dialogue Box	61
Figure A 3	Screen Displayed Dialogue Box for Naming the New Experiment	62
Figure A 4	Dialogue Box Indicating Phase Input Data for the IFT Measurement	62
Figure A 5	Dialogue Box Indicating Timing Input Data for the IFT Measurement	63
Figure A 6	Information Display Showing Final Step in Setting the New Experiment	63
Figure A 7	Drop Film Showing the Crosshair Lines	64
Figure A 8	IFT/Surface Tension Results Window	65

List of Tables

Table 3.1	Structure, Types and Properties of the Salt used for the Investigations	
	Error! Bookmark not defined.	
Table 3.2	Types of Nanoparticles (Silica) used for the Investigations	
	Error! Bookmark not defined.	
Table 3.3	Different Concentrations of Combinations used for the Investigations	27
Table 4.1	Results for all Fluid with 15% Brine used for Investigations	41
Table 4.2	Results for PH for Fluids 3, 4 and 5 at Brine and Distilled Water Combination	48

Chapter 1 Introduction

1.1 Preface

Section 1.1 of this Chapter introduces the Chapter, while Section 1.2, gives the overview of the research. Sections 1.3 and 1.4 detail the explanation, and the applications and significance of the research. Research contributions are in Section 1.5 and Section 1.6 gives the research questions, aim and objectives. Section 1.7 details the Thesis structure.

1.2 Overview

The October 1973 Arab Oil embargo was not the first warning of impending energy shortages, nor was it the first embargo. Farsighted individuals had earlier called attention to the inevitability of an 'energy crunch'. The October 1973 embargo did, however, bring the problem to 'front and centre'.

Since then, countries, administration, industries and consumers have increasingly realised that new sources of energy, new attitudes and disciplines must be developed and adopted. Clearly, a comprehensive energy programme is complex, and a unified and complete programme must encompass the consideration of all options. The potential of each needs to be explored. Most oil fields around the world have reached, or will soon reach, the phase where the production rate is nearing the decline period.

Energy consumption worldwide is expected to increase by 50% relative to current levels by the end of 2030 (Ghauri, 1976). This growth is unlikely to be met by renewable resources and, thus, there is a strong and growing demand for oil as a predominant energy resource. Hence, the current main challenge is how to delay abandonment by extracting more oil economically. Primary and secondary oil recovery methods, typically produce only 15% to 30% of the original in place, depending on the compressibility of fluids and initial pressure of the reservoir (Goolsby, 1967). This leaves a large amount of trapped oil in reservoirs, which in some cases is agreeable to tertiary or enhanced oil recovery (EOR) processes.

One such option to produce more oil and to enhance the recovery from domestic oil fields is enhanced oil recovery (EOR); this is one of the 'building blocks' and an overall energy structure. Increasing production from existing fields may well be a good source of future domestic energy supply. The term 'enhanced oil recovery' refers, in the broadest sense, to any method used to recover more oil from a petroleum reservoir than would be obtained by primary recovery.

1.3 Explanation of the Research

Despite some works to understand the subtleties of the different interfaces, such as liquid-liquid connections, most of the reservoir fluids come along with water containing various concentrations of different salts, with NaCl being the major salt present. Presence of salt in the system alters or affects the IFT measured. Further, surfactants are used in enhanced oil recovery to reduce the interfacial tension between the fluids in the reservoir and the reservoir rock. Therefore, knowledge of interfacial surface tension plays a crucial role in carefully selecting and designing the best options. The present research is designed to investigate the concentration combination of nanoparticles (silica) with polymer (Gum Arabic). Also, the produced water comes with different salts, those, for example, being the major components. Therefore, in this research, sodium salt, NaCl was used.

1.4 Applications and Significance of Interfacial Tension

In many of the earlier mentioned industrial processes, understanding of interfacial tension (IFT) is critical in mass and energy transfer across the interfaces of the fluids involved and, hence, it therefore dramatically influences the design of process equipment (Sattari-Najafabadi *et al.*, 2018). This property also influences the quality of products such as coatings, paints, agrochemicals, drugs and detergents, as well as many other industrial processes associated with the formation of emulsions, foams, micelles, thin films and gels (Ciriminna *et al.*, 2013).

As for the petroleum industry, fluid–fluid interfacial tension affects most, if not all, processes involved in the extraction and refining of petroleum and natural gas, from the optimisation of reservoir engineering schemes to the design of petrochemical equipment. For instance, the (Abubakar *et al.*, 2015) report showed that oil–water IFT influences, significantly, the flow characteristics in the horizontal geometry of pipes. Others (Asadollahzadeh *et al.*, 2016; Amani *et al.*, 2017) demonstrated that the pressure drop in horizontal-vertical pulsed sieve-plate column and fluid hold up, characteristic velocity and slip velocity in multi impeller column are also affected by interfacial tension. Moreover, it is well established that several rock properties such as wettability, capillary pressure and relative permeabilities strongly depend on the IFT between fluid phases. Thus, IFT is a crucial parameter that determines the displacement of hydrocarbons in the pore spaces of reservoir rock and, in turn, the amount of oil produced (Arabloo, Ghazanfari and Rashtchian, 2016; Liang *et al.*, 2017).

Therefore, as observed above, accurate determination and understanding of IFT and its response to change in pressure, temperature and surfactant/polymer are necessary, more

especially in the design and optimisation of oil and gas production pipelines and enhanced recovery processes. Decreases in interfacial tension increase the tendency of hydrates plug in a pipeline, and increase the recovery of more oil from the reservoir. The decrease or increase of IFT is a function of pressure, temperature, the presence of salts and polymer-surfactants.

1.5 Research Contributions

The present research provides the following contribution to the academia and the industry in general. It provides a quantitative knowledge database concerning the interfacial tension of a combination of (silica and Gum Arabic) in liquid water and separately of both with:

- a. Nanoparticles (silica)
- b. Polymer (gum Arabic)
- c. With different concentrations of combination (silica and Gum Arabic)
- d. Temperature and pressure variation (temperature 30° – 100°C, and pressure up to 1750psig)
- e. Different chloride salt concentration (NaCl).

1.6 Aim and Objectives

Aim of Research -

The aim of the study is to investigate how different concentrations of a combination of nanoparticles (Silica Oxide) and polymer (Gum Arabic) influence the interfacial tension at different temperatures (30°C – 100°C) to enhance oil recovery (EOR).

Objectives -

- a. To prepare a solution of hydrophilic combination silica and polymer in brine with different concentrations.
- b. To measure IFT using the pendant drop system to measure the underlying mechanism behind the increased oil recovery.
- c. The interfacial measurements were performed at a few different temperature ranges to simulate the reservoir condition.
- d. To determine optimum silica polymer combinations at different temperatures (30°C to 100°C).

1.7 Structure of the dissertation

This dissertation comprises of five chapters and its structured is outlined as follows:

Chapter 1: This chapter begins with a brief introduction of the research background, including the aim and objectives and the research contribution.

Chapter 2: This chapter presents the literature reviews and the relevant theoretical background relating to the research study. The chapter also highlights the concepts of the interfacial prodigy, and fundamental theoretical equations are detailed.

Chapter 3: This chapter presents the materials used and the method adopted in carrying out the experimental trials, such as pH measurement for the liquid samples developed in this desertation and also the detail of all the apparatus used. The method of this research is primarily focused on experimentation.. The experiments involve the preparation of the solutions of the hydrophilic combination of silica and polymer in the presence of brine with different concentrations, liquid characteriztion and the measurement of the interfacial tension (IFT) using the pendent drop method. The IFT apparatus will be in measuring their IFT.

Chapter 4: This chapter presents the results obtained and the findings during the experiments. It presents the experimental results and discussions of the Fluid 3 Brine 5% (Silica 0.15wt% + Gum Arabic 0.4wt%), Fluid 5 Brine 10% (Silica 0.25wt% + Gum Arabic 0.2wt%) and Fluid 4 Brine 15% (Silica 0.2wt% + Gum Arabic 0.3wt%) at different temperature, the interfacial tension and pH values of the liquid solutions. The experimental investigations include the effect of temperature on the interfacial tension. Thus, analysis of the data obtained from the series of the experimental trials which relates to their interaction of different design and operational variables on ehancing oil recovery (EOR) are then be analyse appropriately.

Chapter 5: encompasses the conclusions and the recommendations in the research. It discusses the future direction in the research.

Chapter 2 Theoretical Background and Literature Review

2.1 Preface

In this Chapter, a review of background and studies on flow in the oil and gas industry is presented, showing the properties that affect the fluid flow characteristics, specifically interfacial tension and viscosity. This Chapter is also categorised into specific Sections as follows: 2.2 introduces the Chapter. 2.3. The fluid properties are given in Section 2.4, and an introduction to Nanotechnology for enhanced oil recovery in Section 2.5. Section 2.6 details the mechanism for increased recovery and polymers, and the effects of salinity, temperature and concentration are in Section 2.7. Finally, Section 2.8 is on mobility ratio.

2.2 Introduction

To understand the subsurface processes working in the reservoir, an understanding of basic reservoir engineering is important. The hydrocarbon system is complex and is driven by the interaction between the components present (rock, water, oil and/or gas). This Chapter explains the basic properties of oil and gas systems. However, the undiscovered conventional crude oil and natural gas evaluated in the Department of the Interior (DOI) resource assessment comprises a limited part of the total base of petroleum available for future production.

2.3 Reservoir Properties

2.3.1 Porosity

Porosity is defined as the rock's capacity to store fluids. The void part between rock grains and mineral cement is necessary to have hydrocarbons present in the rock, and the porosity is considered to be one of the most important parameters of a reservoir. The porosity can be expressed as the ratio of pore volume V_p over the total bulk volume V_b of the rock sample. Pore volume can be expressed as the grain volume, V_g subtracted from the bulk volume:

$$\phi = \frac{V_p}{V_B} = \frac{V_b - V_g}{V_b} \quad (2.1)$$

This is called the total porosity, where all the pore space is taken into account irrespective of whether or not the pores are interconnected. The effective porosity corresponds to the interconnected pores only, which permits fluid flow. Hence, it is a measure of the producible fluids in the reservoir.

2.3.2 Saturation

Saturation is defined as that fraction, or percent, of the pore volume occupied by a particular fluid (oil, gas, or water).

$$\text{fluid saturation} = (\text{total volume of the fluid})/(\text{pore volume})$$

$$S_o = (\text{volume of oil})/(\text{pore volume})$$

$$S_w = (\text{volume of water})/(\text{pore volume})$$

$$S_g = (\text{volume of gas})/(\text{pore volume})$$

Movable Oil Saturation (MOS) -

Movable oil saturation S_{om} is another saturation of parameter and is defined as the fraction of pore volume occupied by movable oil:

$$S_{om} = 1 - S_{wc} - S_{oc}$$

where -

$$S_{wc} = \text{connate water saturation}$$

$$S_{oc} = \text{critical oil saturation}$$

Residual Oil Saturation -

Saturation is denoted by the letter 'S', with subscript letters identifying the residual phase, e.g. 'o' and the displacing phase e.g. 'w'

Examples:

$$S_{orw} \text{ residual oil saturation to water displacement}$$

$$S_{org} \text{ residual oil saturation to gas displacement}$$

$$S_{grw} \text{ residual gas saturation to water displacement}$$

2.3.3 Surface and Interfacial Tension

Fluids have a natural tendency to minimise their surface area. To achieve this, droplets tend to form a spherical structure. This phenomenon occurs because molecules of the same fluid attract each other. At a surface or interface, the molecules have fewer neighbours of the same chemical compound, and they will try to minimise the number of broken bonds by minimising the surface area (Akiskal *et al.*, 1985).

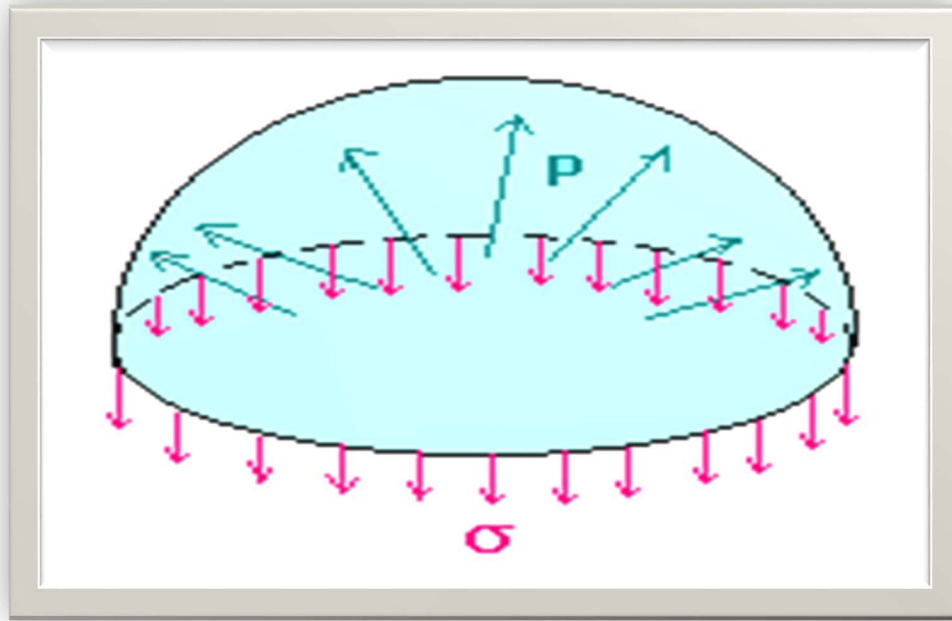


Figure 2.1: Droplet on the Surface (Hendraningrat, Shidong and Torsaeter, 2012).

Interfacial tension (IFT) is a force (per unit length) that is tangent to the interface between two immiscible fluids or at a fluid-solid interface. The surface forces act on the perimeter of droplets/bubbles, and work to make an equilibrium force balance in the horizontal direction. ‘Surface’ tension is defined as the interfacial tension between a liquid and a vapour. For a two-phase fluid system with constant mass, the interfacial tension under isothermal and isobaric condition can be formulated as follows:

$$\gamma = \frac{(\partial)G}{(\partial A)_{T,P,m}} \quad (2.2)$$

where -

G is Gibbs free energy (chemical potential)

A is the interface area. From the free energy term.

We can see that, for a high IFT, molecules are strongly attracted to the molecules of their own kind and, thereby, the two fluids are immiscible. A low IFT means that the molecules are more strongly attracted to molecules of the other fluids and, hence, dissolution occurs, resulting in a stable new mixture.

IFT is an important parameter, as the interaction between fluids and rock minerals affects reservoir properties like wettability, capillary pressure, relative permeability, viscosity, saturation distribution and displacement efficiency (Hocott, 1939; Batycky and McCaffery, 1978; Pedersen, Lund and Fredenslund, 1989).

Adding surfactants or nanoparticles to a fluid interface can significantly lower the interfacial tension, as the absorption at the interface between fluids lowers the repulsion between molecules of different fluids.

2.3.4 Wettability

A porous rock saturated with more than one fluid is a complex system of mutual static interactions between all the fluids present and between fluids and rock minerals. Wettability is defined as the tendency of one fluid to spread on to a solid's surface in the presence of another immiscible fluid. It is a result of interfacial tension between the fluid phases present and their individual adhesive attraction (electrostatic force) to the solid. The wettability of a rock's pore wall is dependent on the fluid's chemical composition and the rock's mineral composition (e.g. siliciclastic vs. carbonate) (Zolotukhin and Ursin, 2000).

Contact angle θ is a measurement of the degree of wetting by a particular fluid.

This can be described to Young's equation:

$$\cos \theta = \frac{\gamma_{SV} - \gamma}{\gamma_{LV}} \quad (2.3)$$

where –

θ is the contact angle, surface/interfacial tension

S , V and L denote solid, vapour and liquid respectively.

The contact angle can be measured at the fluid-fluid interface on the solid.

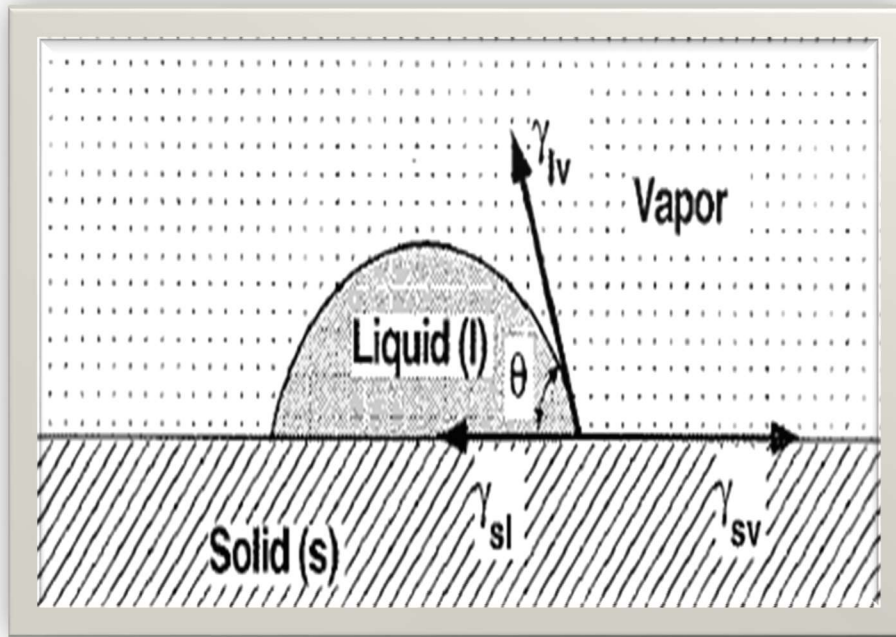


Figure 2.2: How the Interfacial Tensions Work on a Droplet/Bubble (Rajagopalan and Hiemenz, 1997).

For low contact angles ($\theta < 90^\circ$) the fluid is defined as the wetting phase, while for higher contact angles ($\theta > 90^\circ$), the fluid is non-wetting. A 90° angle indicates neutral wettability.

2.3.5 Permeability

Permeability, k , of a porous medium is defined as the medium's ability to transmit fluids through its interconnected pores. It is, together with porosity, considered the most important parameter of reservoirs. Permeability is a directional property, or a tensor, meaning it may vary by several magnitudes depending on the fluid's flow direction (Torsæter and Abtahi, 2000).

Darcy's law shows that a laminar, one phase, steady-state with a fluid flow rate, q , obeys the following relationship:

$$\frac{q}{A} = u = -\frac{k}{\mu} * \frac{dP}{dx} \quad (2.4)$$

where –

A is the cross-sectional area

K: is the permeability

μ: is the viscosity of the fluid

dP: is the pressure drop over the length dx .

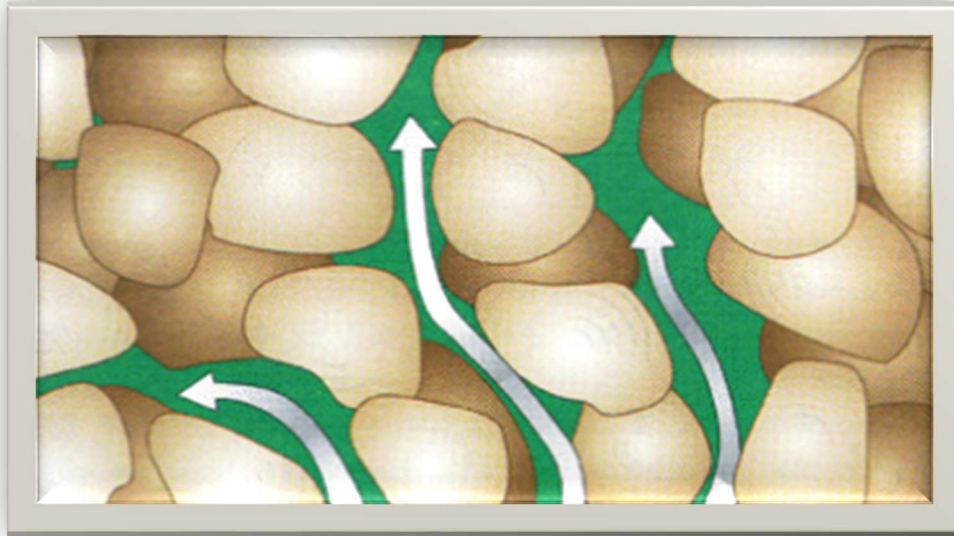


Figure 2.3: Connected Pores Give Permeability (MPG Petroleum, 2003)

Darcy's Law refers to a situation with 100 % saturation of one fluid; this is rarely the case for actual reservoirs. In order to generalise the equation, the concept of effective permeability, k_e , is introduced to describe the multiphase flow. The effective permeability is the ability of the porous medium to conduct a fluid with less than 100 % saturation of the pore space.

Relative permeability, k_{rj} , is a concept used to relate the absolute permeability (100% saturated with one fluid) to the effective permeability of a particular fluid in the system. It can be decomposed as shown below:

$$k_{ej} = k_{rj} * k \quad (2.5)$$

The relative permeability is a strong function of the saturation of the phase. Being a rock-fluid property, relative permeability is also a function of rock properties (e.g. pore size distribution), saturation history and wettability (Zolotukhin and Ursin, 2000). Relative permeability curves represent the dependence of saturation and saturation history on relative permeability. These curves show end-point saturations and end-point permeability for drainage and imbibition processes, giving valuable information about recoverable oil, as well as sweep efficiency (Torsæter and Abtahi, 2000)

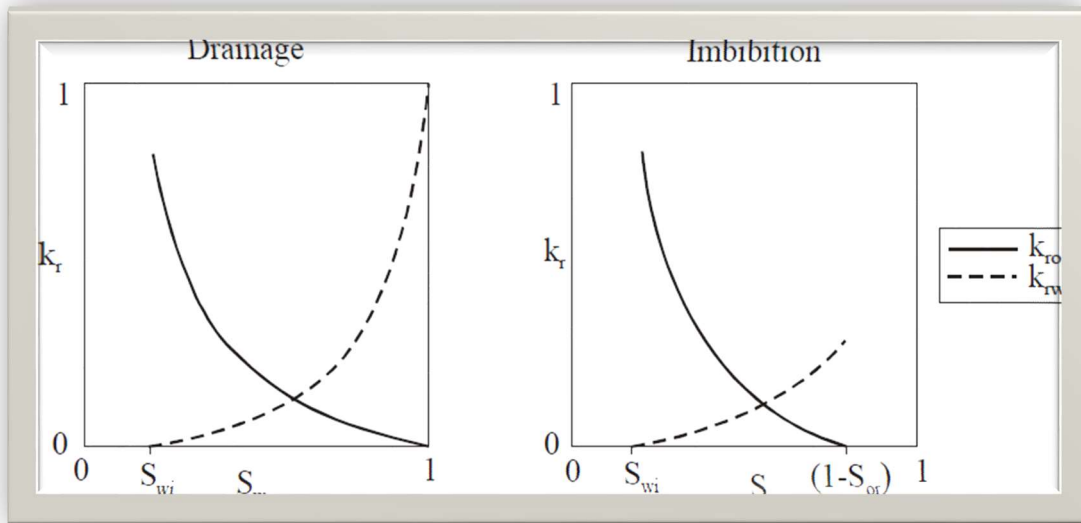


Figure 2.4: Typical Relative Permeability Curves for Water-Wet Sandstone (Zolotukhin and Ursin, 2000)

2.4 Fluid Properties

During production, the reservoir will undergo significant changes, both to temperature and to pressure, which affect the hydrocarbon mixture. Figure 2.5 illustrates how different types of depleting reservoirs vary. For the same hydrocarbon system, the type of reservoir is given by the initial pressure and temperature. Every composition of hydrocarbons has its own two-phase diagram. A given pressure and temperature will pinpoint a location in the diagram that will determine the type of reservoir fluid present (Whitson and Brule, 2000).

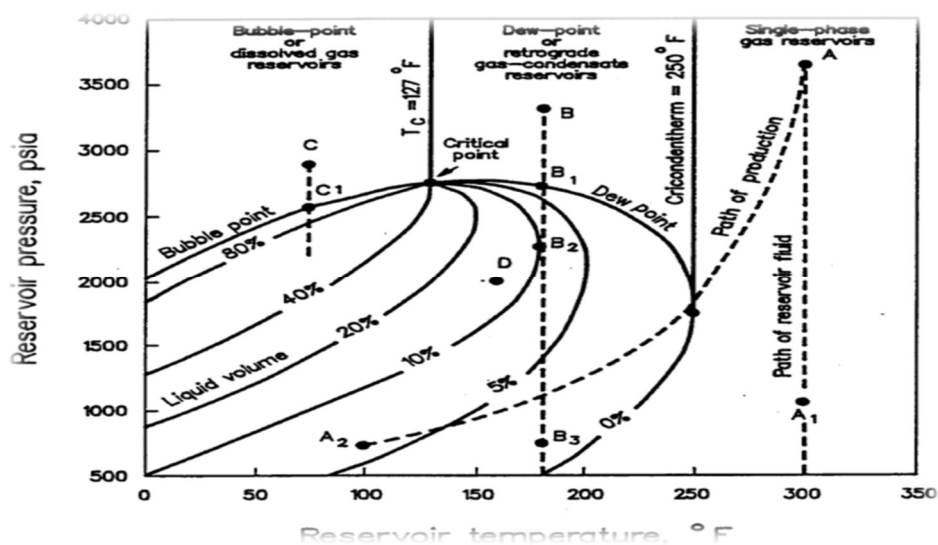


Figure 2.5: Two-Phase Diagram of Reservoir Fluids Showing how they will vary with Different Pressures and Temperatures (Whitson and Brule, 2000).

2.4.1 Density

Density is defined as the mass of a liquid, m , per unit of volume, v . As this property differs with pressure and temperature, it is important to report the density at a given reference point. Normally this is at 288 K and 1 atm (101 kPa) (Torsæter and Abtahi, 2000).

$$\rho = \frac{m}{v} \quad (2.6)$$

The term specific gravity, γ , is defined as the ratio volume of a given liquid to the volume of water at a given temperature, and water:

$$\gamma = \frac{\rho_{liquid}}{\rho_{water}} \quad (2.7)$$

2.4.2 Viscosity

Viscosity, μ , is defined as a fluid's resistance to shear angular deformation, or the internal resistance of a fluid to flow. The resistance to flow is caused by friction forces as a result of cohesion and momentum interchange between molecules.

2.5 Introduction to Nanotechnology for Enhanced Oil Recovery

Manipulating a matter on an atomic and molecular scale is called nanotechnology. This knowledge has developed very importantly in recent periods, and has spread to several different areas of industry like medicine, electronics and the energy sector. In terms of the oil and gas industry, nanofluids have been launched as a promising future technology for enhanced oil recovery (EOR). Nanoparticles (NP) have been engineered to fit a wide change of applications. New research has shown that it might also be applied as a method for EOR. Nanoparticles can activate trapped oil in the porous rock, or they can be used in combination with nanoparticles/polymers to enhance their effect and migration range.

2.5.1 Nanofluids

A nanofluid is a dispersion where small-sized solid particles are suspended in a carrying fluid, usually water. A nanoparticle is typically between 1nm and 100nm. Their size is much smaller than rock pore channels, meaning nanoparticles can easily penetrate through the reservoir rock without much retention (Li, Hendraningrat and Torsaeter, 2013).

Nanofluids can be designed with a wide variety of properties. Two of the main characteristics of nanoparticles are widely different from other EOR agents, and can change the properties

drastically; Firstly, their surface area to volume ratio is higher compared to similar material in a larger scale. Secondly, this can enhance strength and electrical properties, and can make materials more chemically reactive. The overall effect is that fewer nanoparticles are needed compared to other chemicals, like surfactants, to achieve the same functions. In addition, quantum effects can affect the optical, electrical and magnetic behaviour of the material. (Nanowerk)

2.5.2 Potential Nanoparticles

In many researches performed on nanofluids for EOR, an inorganic ceramic material composed of silica dioxide (SiO₂) is used as a nanoparticle. Some of the advantages with silica nanoparticles, apart from being cheap and easily accessible, are that they offer:

- a. Increased sedimentation stability as surface forces counter balance the gravity force;
- b. Thermal, stress-strain and rheological properties can be tailored for a certain purpose during production by changing size, shape and surface chemistry of the nanoparticles;
- c. The chemical properties of nanoparticles can easily be controlled by surface coating substances.

According to (Bera and Belhaj, 2016) Silica nanoparticles can be designed to be both hydrophilic and lipophobic (LHP), or hydrophobic and lipophilic (HLP), using surface treatment such as salinisation with a hydroxyl group or sulfonic acid. Moreover, as silica is found naturally as the main component in sandstone, it will be easy to extract and will also be environmentally friendly (Hendraningrat, Li and Torsæter, 2013). It is the most abundant mineral in the crust of the earth (Heiserman, 1991).

Other types of nanoparticles have also been studied as potential EOR agents. Among these are metal oxides of aluminium, zinc, magnesium, iron, zirconium, nickel and tin (Ogolo, Olafuyi and Onyekonwu, 2012; Zhang *et al.*, 2015). The results of these studies showed that only the aluminium and nickel oxides improved the recovery, where aluminium gave the best result. The increased recovery was explained by aluminium's ability to decrease oil viscosity, and nickels ability to increase the brine viscosity, both cases giving a favourable mobility factor (M). However, magnesium and zinc oxides caused severe permeability problems and decreased recovery (Ogolo, Olafuyi and Onyekonwu, 2012).

2.6 Mechanism for Increased Recovery

Several different EOR mechanisms for nanofluids are proposed and studied. Well-established concepts of wettability alteration and interfacial tension reduction are not sufficient to fully explain the increased recovery seen. An overview of the potential EOR mechanisms will be given here.

2.6.1 Structural Disjoining Pressure

One of the most prominent mechanisms is the disjoining pressure. Investigations performed by (Chengara *et al.*, 2004; Wasan, Nikolov and Kondiparty, 2011; McElfresh, Holcomb & Ector, 2012) have revealed that the nanoparticles present in the three-phase region between oil, water and rock tend to force themselves in between the discontinuous phase and the solid rock surface. The nanoparticles create a wedge-like structure, which works to separate the formation fluid (oil) from the pore wall and enhances the spreading behaviour of the nanofluid.

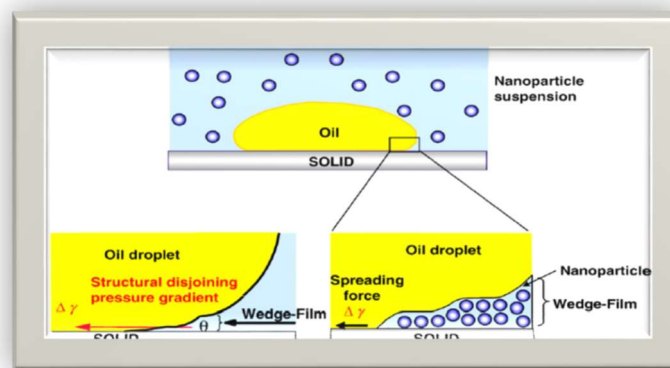


Figure 2.6: Nanoparticles Establishing a Wedge-Film, Resulting in a Structural Disjoining Pressure (Wasan, Nikolov and Kondiparty, 2011).

See Figure 3.1 for the ordering at the three-phase contact region. This assembly becomes more disordered and fluid-like towards the bulk phase. Studies have shown that the pressure arising from such an ordering in the confined region will enhance the spreading behaviour of nanofluids (Wasan and Nikolov, 2003; Zhang *et al.*, 2014). The particles that are present in the three-phase contact region will tend to form a wedge-like structure and force themselves in between the discontinuous phase and the solid rock surface. As reported by Mcelfresh *et al.*, 2012 in their study application of nanofluid technology to improve recovery in oil and gas wells that the particles present in the bulk fluid will apply a pressure that forces the particles in the

wedge structure forward. This applied force is called the structural disjoining pressure, or film tension gradient (McElfresh, Holcomb and Ector, 2012).

The driving forces behind this phenomenon are electrostatic repulsion (where equal charged particles repel each other), Brownian Motion (random movement) and van der Waals forces (attraction/repulsion between molecules due to dipoles) (McElfresh, Holcomb and Ector, 2012). The ordering of particles inside the wedge structure can occur because the overall entropy of the dispersion increases as the nanoparticles in the bulk liquid achieve greater freedom. The electrostatic repulsion between the particles will be higher for particles with a smaller size, giving a larger structural disjoining pressure. Also, when the number of particles increases, the force working on the wedge film will increase. Wasan and Nikolov, (2003) showed that the spreading behaviour increased when decreasing the film thickness, that is, the number of particle layers in the film. The force will be at maximum at the tip of the wedge as shown in Figure.2.7.

When the structural disjoining pressure works on the vertex of the discontinuous phase, displacement occurs as the system tries to regain equilibrium. This force is related to the nanofluid's ability to spread out on the surface of the rock due to the imbalance of the interfacial forces between oil phase, aqueous phase and solid. The magnitude of this pressure depends on parameters such as particle size, particle volume fraction, polydispersity, temperature, salinity and rock properties (Wasan and Nikolov, 2003; Zhang *et al.*, 2015). Adding more electrolytes to the aqueous nanofluid will lower the disjoining pressure, while increasing salt concentration will lower the repulsive forces between nanoparticles and, hence, reduce the pressure that drives the wedge film and due to this, an increase in salinity will have a negative effect on oil removal in the case of nanofluids (Wasan and Nikolov, 2003).

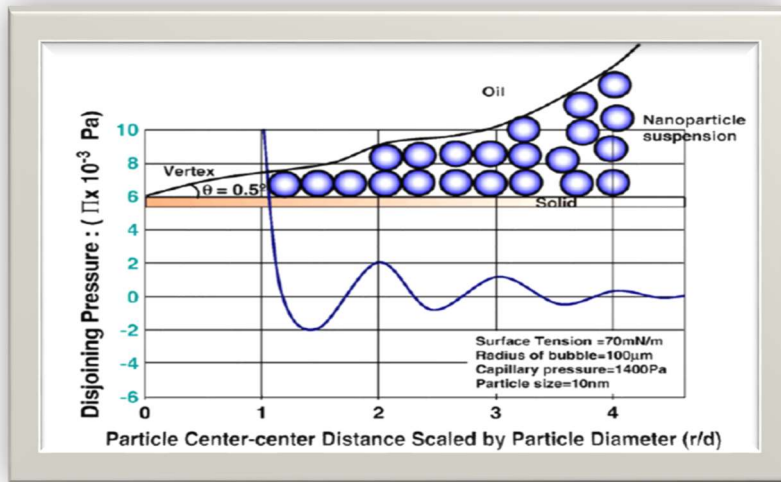


Figure 2.7: Disjoining Pressure in the Wedge Structure (Wasan and Nikolov, 2003).

2.6.2 Effect on Interfacial Tension

Oil and water are immiscible fluids, which means that the interfacial tension (IFT) between them is high. Introducing silica hydrophilic nanoparticles to the system has been observed to lower the IFT and, potentially, to produce more oil. The nanoparticles will structure themselves at the oil/brine interface, reducing the contact between the two phases. The layer of particles generates a lower IFT between the two phases, much like surfactants work. The IFT tension is sensitive to nanofluid concentration; as the concentration increases, IFT decreases (Li, Hendraningrat and Torsaeter, 2013; Dahle, 2014).

In this Thesis hydrophilic silica is used to reduce oil/water IFT, but also neutral wetting particles would have an effect. Frijters et al (2012) explained how the mechanisms behind the absorption of neutral wet particles work, and compare with surfactants. Surfactants absorb at the interface due to their hydrophilic head and hydrophobic tail, while neutral wetting nanoparticles absorb because maintaining a particle-fluid interface requires less energy. Neutral wetting nanoparticles were reported to change the interfacial free energy by taking away energetically expensive fluid-fluid interfaces and replacing them with a cheaper particle-fluid interface.

The reduction of the interfacial free energy requires either:

- a. Reduction of interfacial tension, which is achieved by adding surfactants.

- b. Reduction of the area of integration, which is the effect of absorbed particles. This shows that neutral wetting nanoparticles can reduce the overall interfacial free energy, not by reducing the IFT itself, but by removing parts of the energetically unfavourable fluid-fluid interface area. With emulsions, the assembly of particles on the oil droplet's surface is favourable because it blocks destabilisation by Ostwald ripening (larger droplets grow at the expense of small ones). It can also break up oil droplets (see Figure 2.8), making it easier for the emulsion to migrate through the porous media (Frijters, Günther and Harting, 2012).

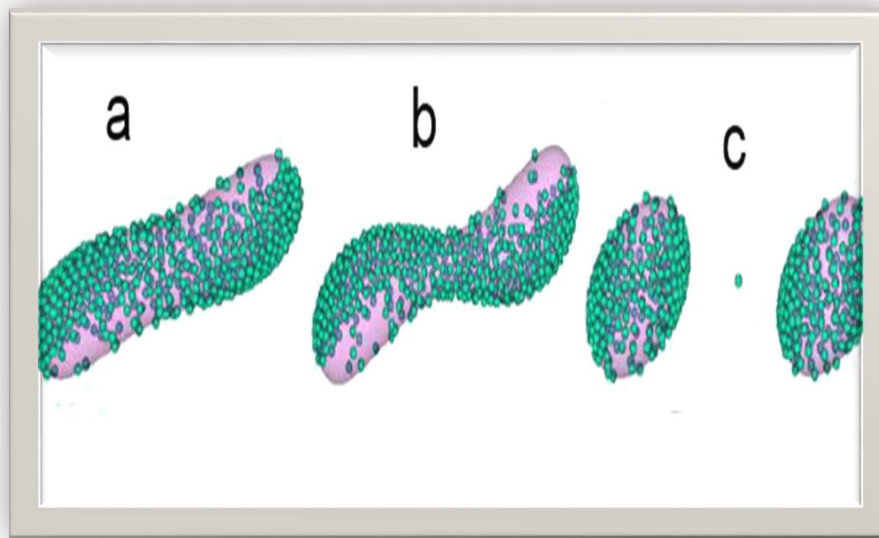


Figure 2.8: Breakup of Oil Droplets Due to Absorption of Nanoparticles (Frijters, Günther and Harting, 2012).

2.6.3 Effect on Wettability

The ideal wetting preference of rock for ultimate recovery is a much-debated topic. Owens and Archer (1971) reported that oil recovery increased with increasing water-wetness. However, Morrow (1990); Jadhunandan and Morrow (1995) reported increased recovery with decreasing water wetness. Even though there are conflicting reports, the wettability is, without doubt, an important factor when it comes to oil recovery. Li et al (2013) reported increased water wetness using an hydrophilic silica nanofluid, and increased oil wetness using hydrophobic silica in neutral wet sandstones. The result showed that the nanoparticles being driven by the aqueous bulk pressure spreading along the solid surface, decreasing the contact angle. A higher concentration of hydrophilic/hydrophobic nanoparticles will increase the wettability alteration

in the core. Contact angle is the most universal measurement of the surface's wettability. Vafaei *et al.*, (2006) showed that an increase in concentration of bismuth telluride nanoparticles increased the contact angle until it reached a peak, where it decreased again. Their experiments also showed that the contact angle as a function of concentration was also dependent on particle size. For the same mass concentration, smaller particles caused larger variations in contact angle. The experiments indicate that nanoparticles suspended in fluids can be effective at manipulating the contact angle and interfacial tension.

2.6.4 Effect on Viscosity

Experiments have shown that adding high concentrations of nanoparticles to water can increase the shear viscosity. Water molecules layered at the nanoparticle surface decreases the fraction of adjacent fluid molecules that are more mobile and, hence, increases the shear viscosity. The viscosity can be increased by either increasing the nanoparticle concentration, or by increasing the size of the particles (Balasubramaniam *et al.*, 2011). Another possibility is to mix polymers with nanoparticles, which will enhance the viscoelastic properties (Skauge, Spildo and Skauge, 2010). Increasing the viscosity of water will decrease the mobility factor, M . The mobility factor is defined as the mobility of the displacing fluid compared to the displaced fluid. It is favourable to have a low value of M ; the lower the value, the better displacement efficiency. Values of $M \approx 1$ give a stable displacement (piston like), while higher values give a low displacement efficiency. The mobility factor is a function of viscosity and relative permeability of the displacing fluid compared to the displaced fluid:

$$M = \frac{k_{rw}}{u_w} * \frac{\mu_o}{k_{ro}} \quad (2.8)$$

where

Kr: is the relative permeability

and

μ: is the viscosity of the respective fluids.

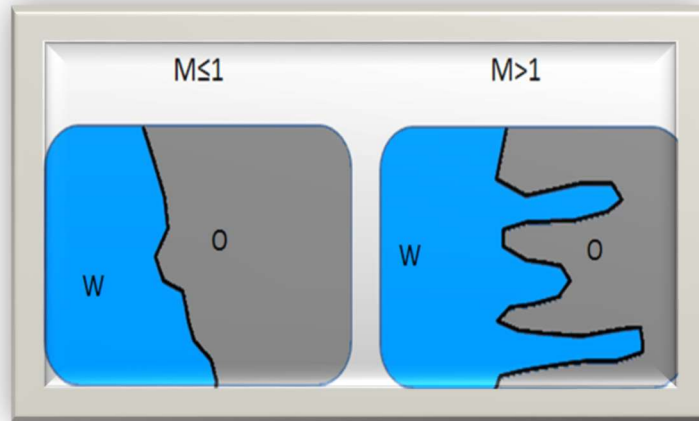


Figure 2.9 Effect of Viscosity and Relative Permeability on Displacement

Suleimanov et al., (2011) showed that, if a small number of a non-ferrous nanoparticles were added to surfactant solutions, the viscosity would increase significantly. Additionally, the nanoparticles enhanced the surfactants in terms of stability and IFT reduction. Skauge et al., (2010) reported that an increase in viscosity of the nanofluid with polymer additives, which could be useful for better sweep efficiency. This indicates that nanoparticles can be used to enhance polymers and surfactants and to increase stability, letting them migrate further into the reservoir.

2.7 Polymer (Gum Arabic)

2.7.1 Introduction

Gum Arabic is one of the oldest and best-known of all-natural gums. The use of Gum Arabic dates back to 5000 years ago, and Gum Arabic was considered to be a beneficial treatment for chronic kidney diseases in Middle Eastern countries. For its edibility, dynamic water solubility, generally familiar as safe (GRAS) status, lack of aftertaste, and other required characteristics, Gum Arabic has found provided wide benefits in the food industry. For its mixing, steadying, thickening and binding attributes, it is combined in food preparations ranging from ice creams, jellies, candies, soft drinks, beverages, syrups and chewing gums. The film-forming properties make it ideal for sweet coatings and glazes. The European Union has given its support to Gum Arabic for food applications. Codex Alimentarius, the collection of internationally recognised standards, codes of practice and guidelines has also recommended it. In pharmaceuticals and herbal medicines, it coats pills and lozenges. Also, it is used in cosmeceuticals for formulation of creams and lotions. Due to its excellent binding property, it is a key ingredient in traditional

lithography, printing and water colour paints. Gum Arabic has found use in the oil and gas industry for EOR.

2.7.2 Polymer Types

Most of the polymers used for EOR fall into two sets: synthetic polymers and biopolymers. The most commonly-used among them are synthetic (PAM), partially-hydrolysed polyacrylamide (HPAM), the biological polysaccharide, Xanthan, and some modified natural polymers, including HEC (hydroxyl ethyl cellulose), guar gum sodium carboxymethyl cellulose and carboxyethyl hydroxyethyl cellulose (Olajire, 2014) and for specific reservoir, every polymer has its own advantages and disadvantages.

- a. PAM (Polyacrylamide), with its high molecular weight ($> 1.0 \times 10^6$ g/mol) was the first thickening agent used for aqueous solutions. PAM is stable up to 90°C at normal salinity and up to 62°C at seawater salinity. Therefore, it is somewhat restricted to on-shore operations only (Olajire, 2014). High salinity can dramatically reduce the viscosity properties of this compound.
- b. Partially hydrolysed polyacrylamide (HPAM) is one of the most popular polymers used today. HPAM is obtained by partial hydrolysis of PAM, or by co-polymerisation of sodium acrylate with acrylamide. HPAM's advantages include its tolerance to high mechanical forces present during the flooding of a reservoir, its low cost, and its resistance to bacterial attack. This polymer can be used for temperatures up to 99°C depending on brine hardness. A few of its modifications, such as HPAMAMPS co-polymers and sulphonated polyacrylamide, can withstand temperatures of 104°C and 120°C respectively. The disadvantage of HPAM lies in its high sensitivity to the brine salinity, hardness and presence of surfactants or other chemicals. This makes it very ineffective in reservoirs containing salts (Olajire, 2014).
- c. Xanthan gum, a polysaccharide, is produced by different bacteria (one of which is *Xanthomonas campestris*) through fermentation of glucose or fructose. The molecule generally has a very high molecular weight ($2 - 50 \times 10^6$ g/mol) and very rigid polymer chains. This makes Xanthan gum relatively insensitive to high salinity and hardness. The polymer is compatible with most surfactants and other injection fluid additives used in tertiary oil recovery formulations. Xanthan gum is usually produced as broth in a concentrated form that can be easily diluted to working

concentrations without any complex mixing equipment. Xanthan is thermally stable in the range from 70°C to 90°C (Olajire, 2014). Nonetheless, this compound is very sensitive to bacterial degradation when injected into the field containing low-temperature regions in the reservoir. Furthermore, it has been reported that Xanthan can have some cellular debris that cause plugging (Abidin, Puspasari and Nugroho, 2012).

2.7.3 Effect of Salinity on Polymer Rheology

Moradi, (2011) illustrated that, at high salinity environments the cations present in dissolved salts cause the double layer of negative charges around the carboxylate group of polymer's backbones to collapse and screen. Thus, the repulsive forces are reduced, which results in decreasing the viscosity and poor performance due to the deterioration of the polymer solution. Ryles, (1988) investigated the effect of Ca^{2+} ion presence at concentration above 200 ppm and observed that the polymer lost one half of its viscosity at initial conditions. Also, Mg^{2+} gave a similar effect, but, somehow, less than with calcium ions. In addition, Litmann, (1989) stated that there is an inversely proportional relation between the salt concentration and viscofying efficiency of a polymer, as for every 10% increase in salt concentration, the viscosity in decreased by 10%.

Algharaib et al., (2011) conducted a study for several reservoirs where the water was too saline, and concluded that polymer flooding is not preferred when dissolved salt content is above 100,000 ppm. This study was applied using core samples saturated with oil of 10cp, brine of a high salt content at a temperature of 176°F, and injected polymer of 1cp dissolved in 30,000 ppm salinity water. The oil recovery was compared to a water flood, which reflects that the polymer failed to increase recovery as the viscosity of polymer degraded because it is in direct contact with high salinity water.

2.7.4 Effect of Temperature on Polymer Rheology

Knight, (1973) pointed out that, after studying the effect of temperature on the polymer's stability, high temperature may result in polymer degradation in two ways, and observed that at temperatures from 120°C - 150°C, which is equivalent to 250°F - 300°F, polymers may permanently lose their viscosity.

Additionally, high temperature accelerates oxygen free radical reactions, which causes the polymer to damage rapidly. Also, Knight, (1973) investigated the rate of polymer degradation

due to presence of oxygen at three different temperatures (140°F, 120°F and 73°F) and concluded that, at elevated temperatures, polymer deterioration takes place faster, but the total loss of viscosity is the same at all three temperatures. Furthermore, Cannella et al., (1988) observed the impact of elevated temperatures on flow behaviour of a polymer solution (Xanthan gum) and reported that the polymer started to behave as a Newtonian fluid at 80°C at a low shear rate.

2.7.5 Effect of Concentration on Polymer Rheology

Wang and Caudle, (1970) stated that, for efficient oil recovery, a concentrated polymer slug is required, and explained that increasing the polymer concentration reduces the volume of the required slug. Ferry, (1980) pointed out that increasing the polymer concentration causes the molecules to interact with each other (hydrodynamic interaction), which is a long-range effect, then form as actual contacts, aggregates and networks. He investigated the effect of increasing HPAM & Xanthan gum polymer's concentration on increasing the viscosity, thus improving oil recovery. An experiment was conducted using HPAM of (200, 600, 1500, 2000, and 2500) ppm and Xanthan gum of (840, 2250, 3440 and 4790) ppm. Results showed that the viscosity increases with increasing the concentration for the two types of polymers. Thus, the recovery was increased with 20% of OIIP.

2.7.6 Effect of Concentration on Polymer Absorption

As the polymer solution flows through porous media, its large molecules will adhere to the rock surface as it will not be able to pass through narrow pores. This behaviour is desired to a certain limit as, when polymer molecules attach to the surface, they stretch out and plug the path of water, thus its mobility is lowered. However, it is not favourable for polymers to absorb permanently or slowly, as this may result in excessive loss of the polymer or small flow resistance, which will affect the profitability of polymer flooding.

Omar, (1983) investigated the effect of absorption on polymer losses and concluded that, when polymer molecules adsorb on rock surfaces, the concentration of the solution leaving the pores is lower than the concentration of the initial polymer solution injected. This reduction in polymer concentration can be used as a measure of the absorption. Thus, polymer absorption results in an increase in the polymer resistance to flow and in loss of polymer.

2.7.7 Choosing the Best Polymer

Due to their different properties, polymers tend to work better or worse in different conditions. Thus, before application, one should take into account several factors before selecting the

optimal polymer to use. To determine the best molecular weight of the polymer, it is necessary to consider reservoir permeability and oil viscosity (Abidin, Puspasari and Nugroho, 2012). It is also important to consider the cloud point of the polymer solution, which reflects polymer thermal stability in high salt brine and high temperature. Incorrect measurement of this parameter can result in precipitations during injection or flow through the reservoir (Olajire, 2014). Another essential parameter is the polymer retention, which encompasses possible mechanisms responsible for the reduction of mean velocity of polymer molecules during their flow through porous media. Retention is commonly attributed to polymer absorption; however, some polymers can be mechanically entrapped in a porous medium or hydro dynamically trapped in stagnant zones (Olajire, 2014). Thus, it is important to know the rock composition and polymer adsorption level to determine the best antitonicity (degree of hydrolysis).

2.8 Mobility Ratio

After the second phase (water or gas injection) there is still a considerable amount of oil remaining, since it was not swept completely from the reservoir. One of the reasons for that phenomenon, outlined by Glatz, is the unfavourable mobility ratio. Mobility ratio is defined as the ratio of mobility (λ) of the displacing fluid (water) to the mobility of the displaced fluid (oil), where mobility is permeability (κ) divided by viscosity (μ).

$$M = \frac{\lambda_{water}}{\lambda_{oil}} = \frac{\frac{\kappa_{water}}{\mu_{water}}}{\frac{\kappa_{oil}}{\mu_{oil}}} \quad (2.9)$$

Thus, there is an inverse relation between the volumetric sweep efficiency and the mobility ratio. An M value greater than unity is unfavourable, since this will cause the instability of the displacement process and a so called ‘viscous fingering’ effect (Glatz, 2013). Under the condition of a large viscosity difference between the displacing (water, lower viscosity) and displaced (oil, higher viscosity) fluid, the mobility ratio will become larger than one and, thus, poor recovery will be reached (Figure 2.10).

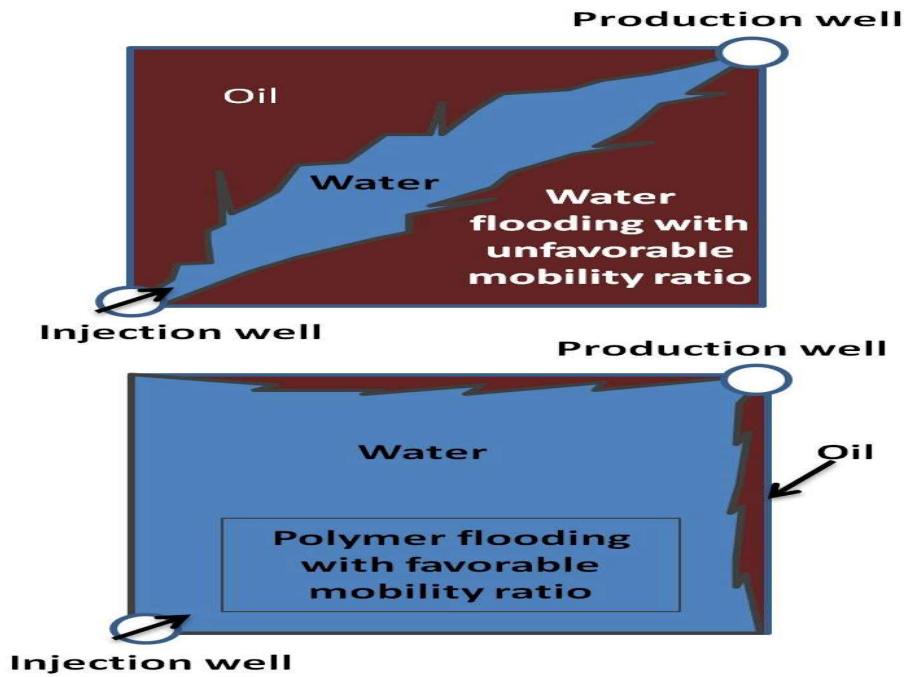


Figure 2.10: Fingering Effect Promoted by the Unfavourable Mobility Ratio (top), and Good Oil Recovery Facilitated by the use of Polymer Flooding (bottom) (G. Zerkalo)

The fingering effect is highly undesirable as it increasingly promotes itself and sharply reduces the production as soon as the finger reaches the production well site. In an endeavour to decrease the mobility ratio below one, the approach of using viscous fluid (polymer) to increase the viscosity of displacing fluid has been developed. This helps to promote the displacing fluid in a stable, uniform manner, and decreases the chance of a fingering effect, thus increasing the efficiency of oil recovery.

2.9 Chapter summary

In this chapter, relevant literature on reservoir properties, fluids properties, nanotechnology, and polymers used are detailed and examined with emphasis on nanotechnology and polymers in water and combination are outlined and their interactions. The effects of interfacial tension (IFT), wettability, and viscosity and as well as the effects of salinity on polymer rheology, temperature, concentrations are presented. Additionally, previous works including problems associated with the use of nanotechnology and biopolymers as additives in enhancing oil recovery (EOR) are reviewed.

Chapter 3 Experimental, Materials & Methods of IFT

3.1 Introduction

This chapter highlights the equipments/appartus, materials (additives), procedures and techniques employed in carrying out this research work. The experimental and sample preparation procedures needed to obtain precise and accurate results are presented in this chapter.

3.2 Materials used

3.2.1 Brine

Sodium chloride (NaCl) was the type of salt used in the preparation of brine in this present research study. This is because sodium chloride (NaCl) has a high percentage in produced water. In this investigation, the salt-water was prepared at different concentrations of NaCl as tabulated in Table 3.1.

Table 3.1: Types and salt properties used

Component	Chemical Formula	Molecular Mass (g/mol)	Percentage Purity	Supplier
Sodium Chloride	NaCl	58.45	99.99	Fisher Scientific

3.2.2 Distilled Water

Distilled water is water that has had many of its contaminants removed by the process of boiling the water and condensing the steam into a clean reservoir (container). Thus, distilled water was prepared and used to conduct the present study. Distilled water is used to avoid having any components that may be present in the water, which may affect the results of the experiment, and will prevent any mineral build-up in the equipment. Other uses of distilled water during the research were in the cleaning and maintenance of the apparatus used.

3.2.3 Polymer (Gum Arabic)

Gum Arabic from Acacia trees is extracted from the branches of Acacia Senegal and Acacia Seyal trees. It is an edible, dried, gummy exudate. Gum Arabic has high solubility and is used in the food industry as a stabiliser, emulsifier, flavouring agent, thickener and surface-finishing

agent. It initiates turbidity or hinders sugar crystallisation. Gum Arabic inhibits colour pigmentation and protein precipitation in wine production.

3.2.4 Nano Particles (Silica)

This is a good hydrophilic, suitable for oil systems, and is widely used in plastics, coatings, composite materials, rubber, ceramics and so on.

Table 3.2: Types of Nanoparticles (Silica) used

Name	Appearance	Average particles size	Purity	SSA
KH570 processing Nano silicon dioxide powder	White powder	20nm	99%	140.21m ² /g

3.3 Sample preparation

3.3.1 Preparation of Salt Water (Brine)

The brine solution used in carrying out the present investigations was prepared in the petroleum and gas laboratory. The apparatus used during brine preparation includes; an electronic weighing balance, different salt sample containers and a magnetic stirrer shown pictorially in Figure 3.1. For optimal brine solution, the amount in grams (g) of salt required to make an intended concentration in 1000ml of distilled water are calculated using mass-volume.

3.3.1.1 Brine Preparation Procedure

All the equipment required is collected and set ready for use. The general procedure followed for the preparation of the brine solution in the present study are described as follows:

- a. The weighing balance was plugged-in to the power sources, and the ‘Start’ button was turned on, making it ready to be used
- b. 5, 10 and 15g of NaCl were weighed out and put into a Petri dish.
- c. Each of the measured amounts of NaCl was carefully poured into a container of 1000ml-of distilled water.
- d. Each container was then filled to the graduation mark and stirred with a magnetic hotplate stirrer at 400 rpm for 30 minutes at room temperature.



A

B

C

Figure 3.1: Materials and Equipment used for Salt-Water; (a) Sodium Chloride, (b) Magnetic Stirrer with Brine Contained (c) Tared Mass Balance with Petri Dish

3.3.2 Combination (Silica and Gum Arabic) Preparation Procedure

Two phases of fluids were prepared:

3.3.2.1 Brine Phase -

- a. Added the calculated weight of the combination of silica and Gum Arabic to the brine to prepare a few different concentrations of combinations. (See Table 3.3 and Figure 3.2)
- b. Stirred the mixture with the magnetic stirrer as shown in Figure (3.12 B) for 60 minutes.
- c. Measured the PH.

Table 3.3: Different Concentrations of Combinations used for the Investigations

Fluid no	Combination	Total wt.%
3	(Silica 0.15wt% + Gum Arabic 0.4wt%)	0.55
4	(Silica 0.2wt% + Gum Arabic 0.3wt%)	0.5
5	(Silica 0.25wt% + Gum Arabic 0.2wt%)	0.45

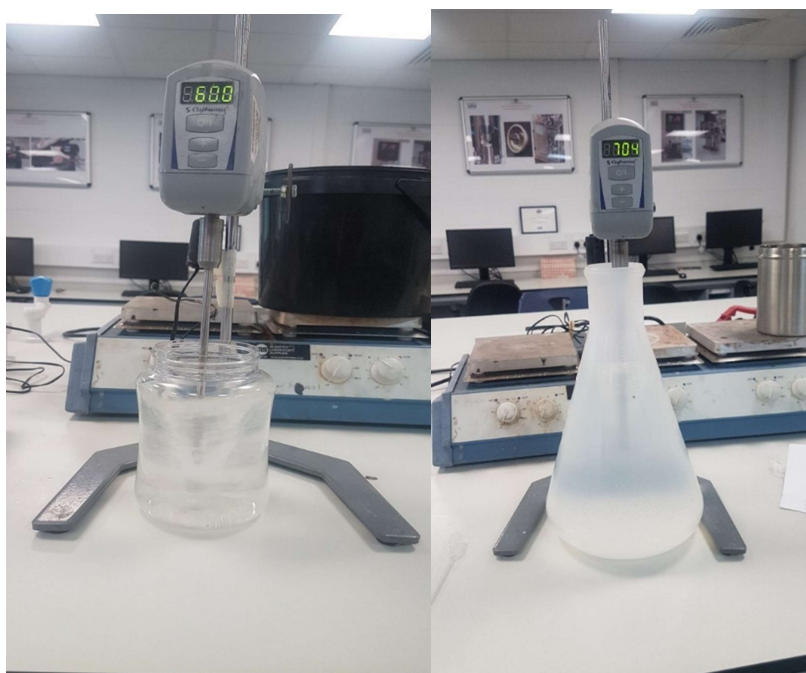


Figure 3.2: Brine Preparation using a Mixer

3.3.2.2 Distilled Water Phase -

- a. Added the same calculated weight of combinations to 1000ml of distilled water to prepare the same different concentrations of brine (see Figure 3.2).
- b. Stirred the mixture with the magnetic stirrer for 30 minutes.
- c. Measured the pH.

3.3.3 Cleaning of Equipment used for brine preparation

The apparatus used during the preparation of brine were thoroughly cleaned Immediately after use and were placed in their appropriate position safely so that another student can use them. If these equipment are not properly clean, it cause hazards within the laboratory and also stop other students from using them. To ensure the apparatus are kept after use, the following clean procedure were employed:

- i. The petri dish and the volumetric flask wer washed and rinse out with tap water as soon as the experiment carried out and were dried in the basket.
- ii. When these apparatus are dried, it is ensure that the apparatus are placed back in the cabinet for good protection from human error (breakage) as well as prevent dust from entering.

3.4 Liquid Characterisation

3.4.1 pH Measurement

pH is a measure of the acidity or alkalinity of a given solution. The acidity or alkalinity of a solution is controlled by the relative number of hydrogen particles (H^+) or hydroxyl particles (OH^-) present in the solution. Any liquid solution that has a higher relative number of hydrogen ions is an acid solution, while an alkaline solution has a higher relative number of hydroxyl ions. Acids are substances that either separate to discharge hydrogen ions or that react with water to form hydrogen ions. Bases are the substances that separates to release hydroxyl particles or to react with water to form hydroxyl ions, and is equivalent to a dissociation constant (K_W). Hence, knowing the value of (K_W) and the concentration of (H^+) makes it possible to calculate the concentration of (OH^-) and vice versa. However, the product of an hydroxyl ion is always equal to (K_W), and has a value of (10^{-14}). See the equation below (3.3):

$$(H^+)(OH^-) = 10^{-14}(Mol/L)^2 = K_W \quad (3.1)$$

It is essential to understand the acidity or alkalinity of a given liquid sample, hence the importance of pH in the solution of inhibitors in brine.

3.4.2 Equipment Description

The pH meter as shown in Figure 3.3 was the apparatus used in measuring the pH value of all the solutions prepared for the present investigation. The apparatus calibration, procedure, and cleaning are detailed in the following subsection.



Figure 3.3: pH Measuring Device

3.4.3 pH Calibration Procedure

The pH tester was usually calibrated a few times, and it can be calibrated up to three points using either of the Standards. For this study, the USA Standard was used to calibrate the meter using the following steps:

- a. The pH meter was switched on by pressing the 'ON/OFF' button.
- b. The electrode was dipped into the PH standard buffer solution to a depth of approximately 3 cm.
- c. The 'CAL' button was pressed to enter Calibration Mode. The 'CAL' indicator was displayed, and upper display showed the measured reading based on the last calibration, while the lowered displayed the value of the PH standard buffer solution.
- d. The PH reading stabilised and the calibration point was confirmed by pressing the 'HOLD/ENT' button. The upper value displayed was calibrated to the PH standard buffer solution, and the lower value was toggling in between reading of the next PH standard solution.
- e. All steps above were repeated with other buffer solutions, and the electrode was rinsed using distilled water before dipping into the next standard solution.

3.5 Interfacial tension (IFT) Equipment description and principles

Because of its important role in many technical areas, many tensiometers have been established for the experimental study of IFT between fluid phases interaction. Amid all the several techniques reviewed by Dorsey (1929), only a few are still being utilised for interfacial tension measurements in fluid–liquid interfaces. The most general techniques used today were briefly studied by (Drelich, Fang and White, 2002).

They are also designated in detail in (Rusanov and Prokhorov, 1996). More valuable sources of information on experimental measurement techniques of interfacial tension include (Harkins and Jordan, 1930; Cheng *et al.*, 1990; Del Rio and Neumann, 1997; Arashiro and Demarquette, 1999; Lee, Kim and Needham, 2001). The Pendant Drop (PD) is possibly the most generally used method for measuring the IFT at liquids phase system, due to its simplicity and ease of implementation at a gas-liquid interface under a wider range of pressure and temperature conditions. In the context of the PD technique, a drop of a denser fluid is

formed at the tip of a capillary tube and kept in equilibrium with a surrounding less dense fluid (vapour or liquid), and the shape of the drop is subsequently analysed.

Once the profile of the drop or the height of the liquid column is determined, they are combined with pertinent phase density data to obtain interfacial tension values. In essence, the estimation of the IFT with the other technique relies on the balance between capillary and gravity forces, which were recently described and improved by (Berry et al., 2015). In the PD the effect of gravity on the shape of a drop of the fixed volume is analysed (Drelich, Fang and White, 2002). In this section, a brief historical and technical discussion of the theoretical background of these techniques are presented, along with a detailed description of the apparatus used in this work to measure the interfacial tension of reservoir fluids over a broad range of experimental conditions.

3.5.1 Measuring Principle

At the tip of a needle, a suspended drop of a specifically heavier liquid generated within a specifically lighter phase is shown in Figure. 3.1 A. The lighter phase is either air (surface tension measurement) or another liquid (interfacial tension measurement).

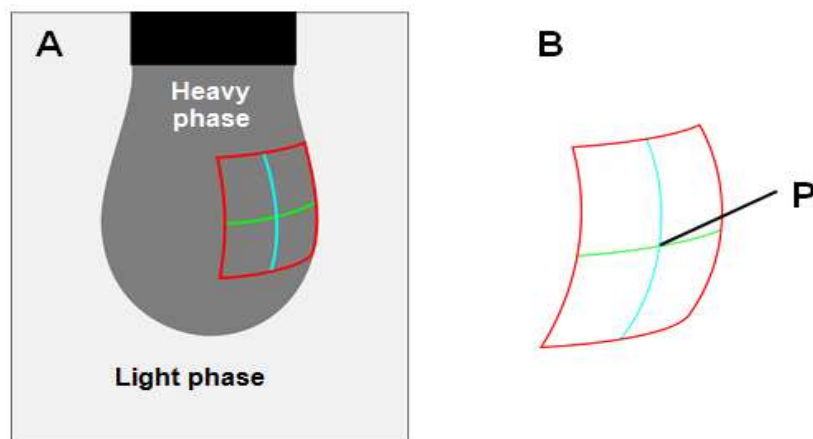


Figure 3.4: Pendant Drop (A); Curved Surface Segment (B), the Radii of the Horizontal (green) and Vertical (blue) Circles of Curvature Defines the Surface Curvature at Point P

Alternatively, the interfacial tension can be measured on an ascending drop, if the lighter phase is generated within a heavier one.

The interfacial tension between the inner and outer phases results in increased pressure inside the drop. The relationship between the difference in pressure Δp and the interfacial tension is described by the Laplace equation (Eq. 3.1):

$$\Delta p = \sigma \cdot \left(\frac{1}{R_1} + \frac{1}{R_2} \right) \quad (3.1)$$

where -

Δp = *p_{inner} – p_{outer} = Laplace pressure*

σ = *interfacial tension*

R_1, R_2 = *radii of horizontal and vertical circles of curvature.*

Surface tension results in the drops assuming the smallest possible surface area; this means that, without other forces acting upon them, drops will be spherical. The effect of gravity deforms the drops because their weight generates a hydrostatic pressure within the drop (Eq. 3.2), which makes a contribution to the inner pressure and, therefore, in accordance with Eq. 5.2, influences the primary radii of curvature R_1 and R_2 .

$$\Delta p_{Hyd} = \Delta \rho \cdot g \cdot l \quad (3.2)$$

where -

Δp_{Hyd} = *Hydrostatic pressure*

$\Delta \rho$ = *Difference in density between heavier and lighter phase*

g = *Gravitational acceleration*

l = *Vertical distance between the measuring point and needle opening.*

As the hydrostatic pressure is height-dependent – it is minimal directly below the needle opening and increases in a vertical direction as the distance from the needle increases – the curvature of the drop surface also alters in a vertical direction. This results in the characteristic ‘pear shape’ of a pendant drop.

The degree of variation from a spherical shape gives the relationship between the weight of the drop and its surface tension. If the difference in densities between the phases is known, then the surface tension can be calculated from the drop shape. The shape is not freely saleable; the actual dimensions of the drop are used in the calculation. During a measurement, the magnification of the video image is first determined in order to be able to access the actual

drop dimensions. The drop shape is then determined from the video image of the generated drop by grey level analysis. A numerical method is then used to vary a shape parameter known as 'B' until the calculated drop shape coincides with the actual drop shape.

3.5.2 Making a Measurement

A pendant drop measurement is carried out simply and quickly. The following Section describes the procedure and mentions some easily avoidable obstructions on the way to a reliable result.

3.5.2.1 Preparing for the Measurement

Instrument Location -

Bright radiant light and vibrations that could cause the pendant drop to oscillate make drop shape analysis difficult, or could lead to unwanted drop break-off from the needle. This means that the location should be as vibration-free as possible and that sunlight or bright room illumination should be screened off.

3.5.2.2 Choice of Needle Diameter

Deformation of the drop that is adequate for the measurement is only achieved when the drop is sufficiently large. This is why a large needle diameter should be selected in order to be able to generate correspondingly large drops. The KRÜSS standard needles for pendant drops have a diameter of about 1.8mm and are suitable for most measurements. Narrower needles should only be used when, because of low surface tension and/or a large difference in density, drop break-off from the standard needle occurs quickly.

3.5.2.3 Determining the Image Magnification

As the actual weight of the drop itself plays a major role in the calculation, in addition to the density and acceleration due to gravity (see Figure 3.2), the absolute size of the drop must also be known. This is determined from the image and, therefore, the magnification of the image must be determined using an object which dimensions are known before the measurement itself can be made. The magnification is a sensitive parameter which determination should be carried out with the greatest of care.

The outer diameter of the needle seen on the screen is normally used as the reference size. This diameter should be determined with an accuracy of at least 10 μ m, with the lower section of the needle being used for determining the magnification in order to eliminate any possible height-dependent diameter variations. The tool used, for example, an external micrometer, should be

positioned so that the diameter is measured at right angles to the optical axis. In this way, errors due to possible variation of the needle profile from a true circle can be eliminated.

The capillary tip must be located vertically on the screen and must not be tilted. Figure. 3.2 clearly shows that a needle tilted on the screen results in a considerable error in the magnification factor and therefore represents a significant source of error for the results.

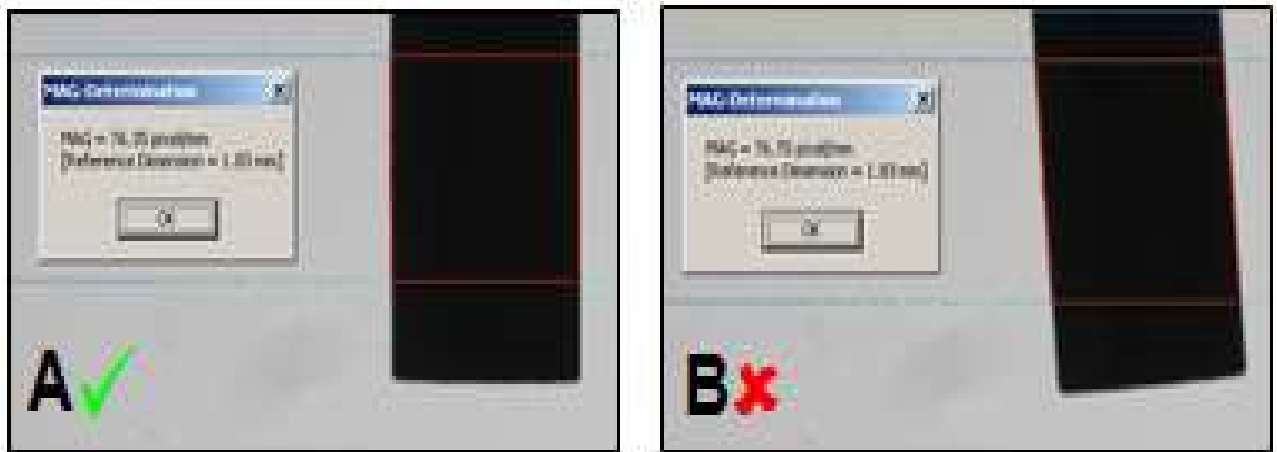


Figure 3.5: Influence of Tilted Needle on the Magnification Factor.
(A) The Correct Factor is Measured; and (B) The Result Varies by 0.5%

The outline of the needle should be readily visible, and the image should be sharp. For determining the magnification factor, a rule of thumb states that the width of the needle outline should occupy at least 10% of the whole screen width. Otherwise, the scale will be too small and the size resolution for the measurement will be poorer.

The maximum width of the needle image is limited by the fact that the whole of the generated drop must also be visible on the screen.

The two measuring lines for determining the magnification should be at a distance of at least 20 pixels from one another (Figure.3.3) and should also be at the height at which the diameter was determined.

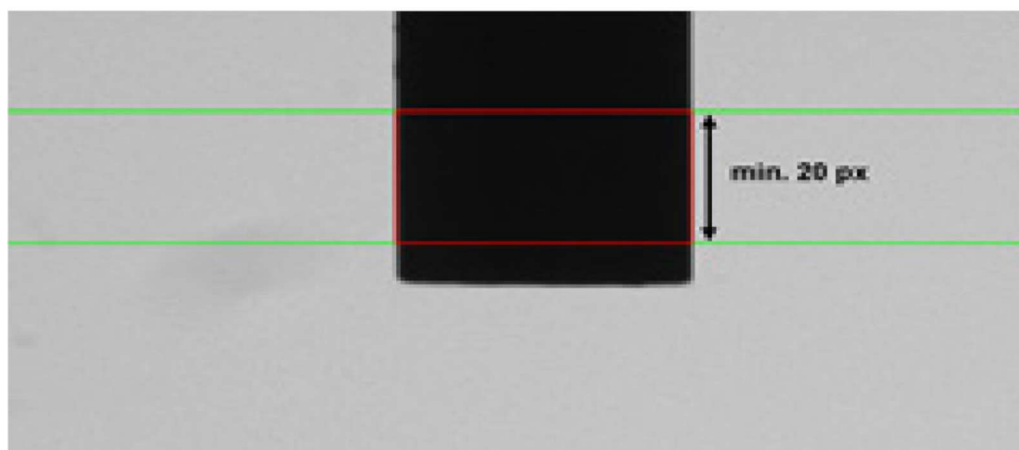


Figure 3.6: Proper Distance Between the Two Measuring Lines for Determining the Magnification

As the optimal needle width on the screen and the suitable image settings are frequently only known after drop generation, the determination of the magnification factor is often carried out after drop generation and image adjustment, directly before the measurement itself. In any case, each alteration to the image adjustment described below means that a new determination of the magnification factor is absolutely essential.

3.5.2.4 Generating the Pendant Drop and Drop Image Optimisation

For PD, the force of gravity must significantly deform analysis of the drop; the drop shape must differ considerably from that of a true sphere. Normally, the most favourable deformation is obtained when the drop is just before the point of break-off from the needle tip. In order to avoid premature drop break-off, the drop should be generated as slowly and vibration-free as possible. Figure. 3.4 shows a drop with a suitable deformation and one with an inadequate one.

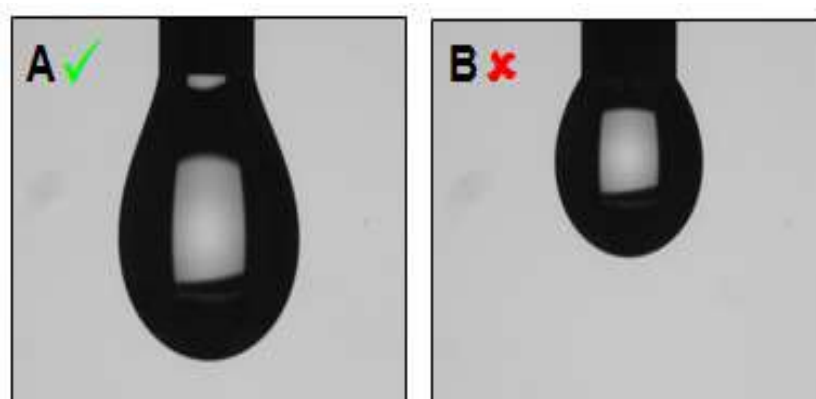


Figure 3.7: Adequately (A) and Inadequately (B) Deformed Pendant Drops

In a similar way to the needle width on the screen, a sufficiently large drop image is required for accurate measurements because, as the magnification of the drop shape increases, the

number of pixels available for the analysis also increases. This is why the drop and needle together should occupy as much of the screen in a vertical direction as possible (Figure. 3.5).

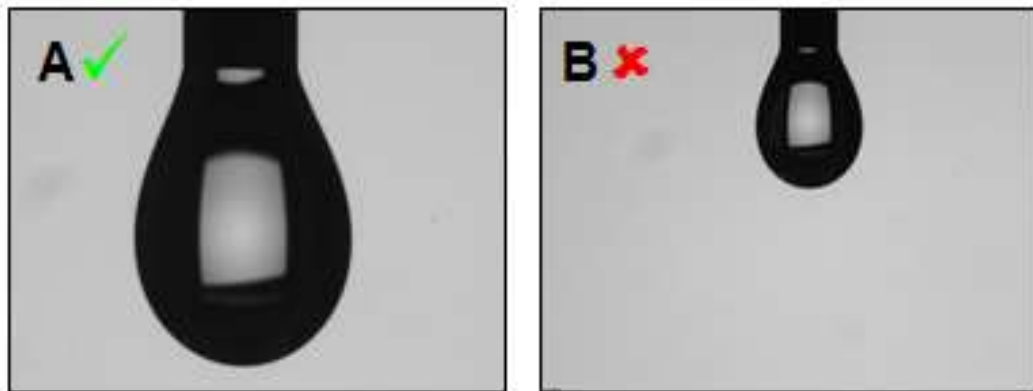


Figure 3.8: Drops with Correct (A) and Too Low (B) Magnification

After the magnification, the sharpness of the image should be optimised, as fuzziness results in less accurate profile recognition by the software. Figure.3.6 shows a correctly focused image and a fuzzy one.

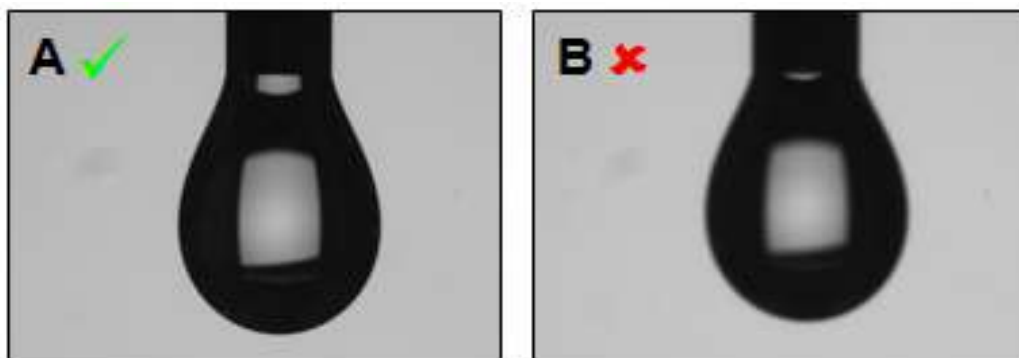


Figure 3.9: Correct (A) and Incorrect (B) Focus Setting

The brightness of the background illumination should also be optimised. If the light intensity is too dark, then the contrast between the background and the drop will also be too weak; this means that profile recognition by the software will be incorrect or even impossible. In contrast, too bright a background illumination can lead to over-illumination of the drop, which then appears narrower than it actually is. Figure. 3.7 shows the influence of the illumination on the contrast between the drop and the background.



Figure 3.10: Drop Image with Suitable (A), Too Dark (B) and Too Bright (C) Background Illumination

As a suitable guideline for the illumination intensity, the grey level value of the dark part of the drop should have a maximum of 40 and the surrounding phase should have 170-200 (Figure. 3.8).

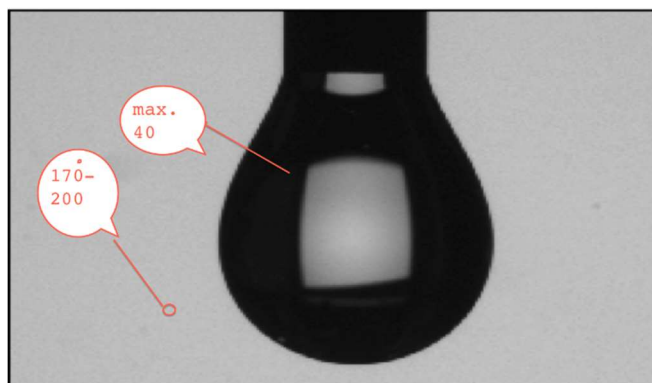


Figure 3.11: Grey Level Values of the Drop and Surrounding Phase Under Optimal Illumination

3.5.2.5 Excluding Evaporation Effects

Preventative measures against evaporation should be taken with volatile liquids or sample components, as otherwise the drops will be reduced in volume and may also lose their optimally-deformed shape. In addition, with solutions of surface-active substances their surface concentration and, therefore, their surface tension can alter so that constant measured value cannot be obtained.

Carrying out the measurement in a covered glass cuvette is beneficial, on which base several drops of the liquid to be analysed is placed. As the vapour pressure in the filled cuvette corresponds approximately to that of the drop surroundings, evaporation is reduced. Measurement in a cuvette also protects the drop against vibrations caused by air movements and can therefore also be a good idea for non-volatile samples.

3.5.2.6 Recording the Stationary Value

The variation of surface tension with the time mentioned above can also occur without evaporation for surfactants, which only migrate slowly to the boundary. The slow flow rate of high-viscosity liquids means that the formation of the final drop shape can take some time. In such cases, we recommend that the interfacial or surface tension is measured as a function of time and that the stationary value is regarded as being the result.

3.5.3 Carrying out the Drop Shape Analysis

Measurement irregularities can also result from incorrect software settings or occur when carrying out the drop shape analysis itself. The following Sections show where the sources of error are to be found when making a measurement.

3.5.3.1 Required System Parameters

In order to be able to make a PD measurement, the densities of the heavy and light phases, as well as the value of the acceleration due to gravity, must be entered in the software. The values at the particular measuring temperature must be used for the densities of the participating phases. For surface tension measurements, the density of the surrounding air that, despite its low value still has an influence on the result, should also be entered.

For the acceleration, due to gravity, the international standard value of 9.80665 m/s² is entered in the software as the default value. This should be replaced by the local value at your location; this can normally be obtained from your national physical institute.

3.5.3.2 The Sensibility of Profile Recognition in the Analysis Software

The sensitivity of the profile recognition is expressed by the determined difference in grey levels that are considered as the transition between the drop and the surrounding phase. For sharp drop images with a good contrast, a value of around 30 is recommended – this is the default setting for ‘profile detection’ in the KRÜSS software. With poorly recognisable phase transitions, the value can be reduced. If the sensitivity is set incorrectly, then the software cannot determine the drop profile or cannot determine it correctly (Figure. 3.9). If this is the case, then the value in the software must be adapted until the drop profile is recognised correctly.

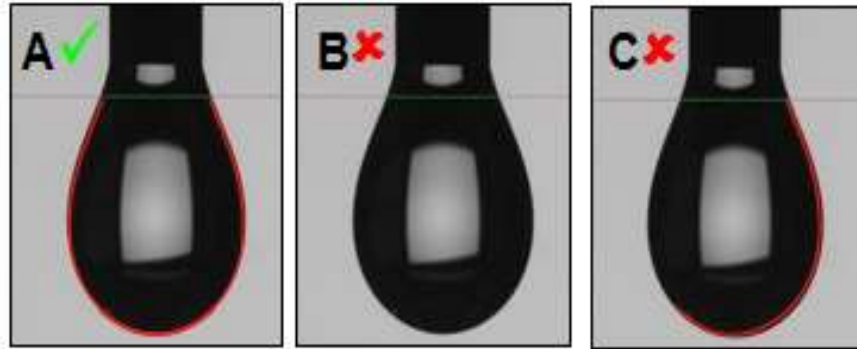


Figure 3.12: Influence of the 'Profile Detection' Value on Profile Recognition:
 (A) Correct Value - Profile Found Completely; (B) Value Too Low - No Profile Found; (C)
 Value Too High - Profile Only Partly Found

3.5.3.3 Setting the Baseline for the Analysis

The baseline is used to define which part of the drop profile will be used for the drop shape analysis. This means that a reliable result can only be obtained when this line is applied to the drop profile at the correct height. In principle, the baseline should be placed as near as possible to the needle tip, but far enough away from it so that it excludes that part of the drop profile which shape is influenced by contact with the needle.

Whether the baseline has been applied correctly can be evaluated by seeing if the line generated by the software corresponds exactly to the profile of the whole drop (Figure 3.10A). If this is the case, then it can be assumed that the profile analysis will be reliable.

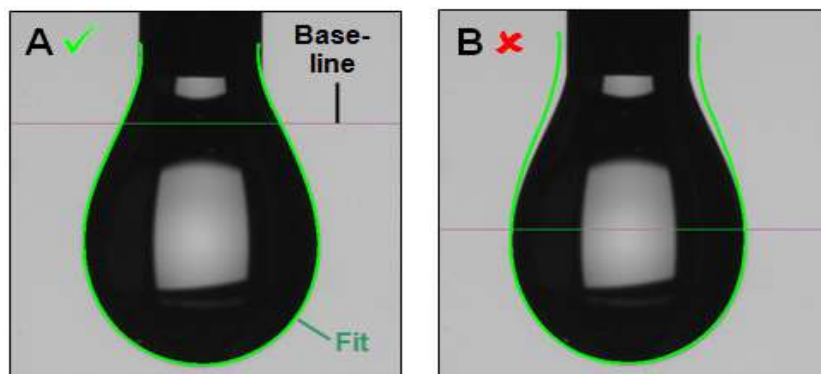


Figure 3.13: (A) Fit Depicts Drop Profile Correctly and Provides an Accurate Result;
 (B) Fit Clearly Varies from Drop Profile and Provides an Inaccurate Result

If there are significant variations between the fit and the drop profile (Figure 3.10B) the position of the baseline should be altered until the variations disappear. In order to assure reproducibility, it is recommended that all quantities influencing the result are included in the measurement report: the gravitational acceleration, the density values of the two phases, the needle diameter and the magnification.

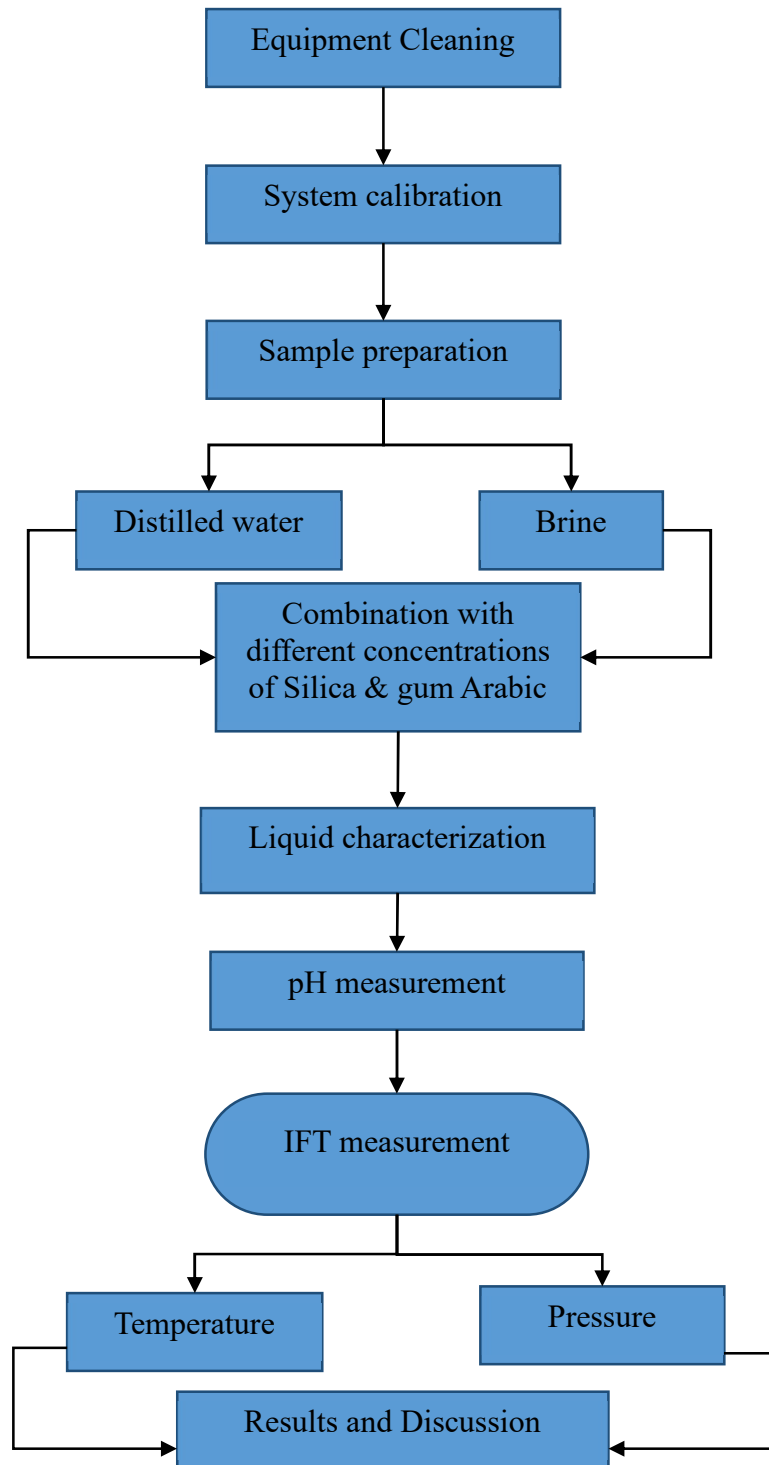


Figure 3.14: Schematic presentation of the experimental validation stage

Chapter 4 Results and Discussion

4.1 Introduction

This Chapter presents the obtained results and discussion of the research. According to the aims and objectives of this study, the original technique to produce the effect of operating conditions representative of surface facilities on the combination of nanoparticles and polymer Interfacial Tension (IFT) at the liquid phase system in the presence of NaCl was used. The characterisation of the fluid sample was conducted in terms of pH, temperature and pressure of the brine and distilled water, both before and throughout the IFT measurement trials.

4.2 Combination of Silica and Gum Arabic Results

Table 4.1: Results for all Fluids with 15% Brine used for Investigations

Fluid no	Combination	Total wt%
3	(Silica 0.15wt% + Gum Arabic 0.4wt%)	0.55
4	(Silica 0.2wt% + Gum Arabic 0.3wt%)	0.5
5	(Silica 0.25wt% + Gum Arabic 0.2wt%)	0.45

4.3 Results Presentation

4.3.1 pH Measurement

Figure 4.13 and Table 4.2 indicates the variation of pH value at different concentration of NaCl 0%, 0.5%, 10% and 15%. As tabulated in the Table 4.2, the pH value initially measured for the water without the addition of the NaCl shows a different values of 6.4, 6.8 and 7.1 for the three fluids scenarios (fluids 3, 4, and 5). Nonetheless, the addition of NaCl to the system was seen to influence the pH values. The pH value decreased from 7.1 to 5.8, 6.1 and 6.3 at 15%, 6.0, 6.2, and 6.4 at 10% and 6.2, 6.3, and 6.4 at 5% respectively. These decrease in pH value resulted from basicity nature of the NaCl, and as well as the chemical nature of the water. The reason is that the ionic solution of the NaCl pushes the surfactant to oil-water interface. In other words, the base characteristic of the NaCl tend to push the H^+ concentration towards the centre value if the concentration is low. However, due to the high concentration of H^+ , the NaCl then pushed it down near the neutral value. This behaviour similarly reported by (Jiravivitpanya et al., (2017; Yahaya, 2018).

Table 4.2: Results for pH for Fluids 3, 4 and 5 at Brine and Distilled Water Combinations

Brine%	Fluid 3	Fluid 4	Fluid 5
15%	5.8	6.1	6.3
10%	6.0	6.2	6.4
5%	6.2	6.3	6.4
0%	6.4	6.8	7.1

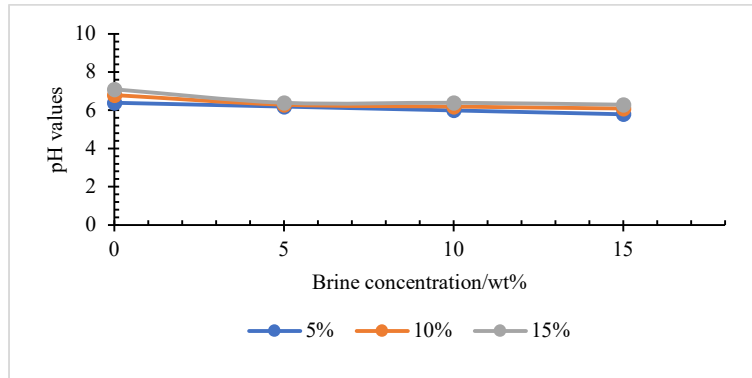


Figure 4.13: pH value of the liquid sample at different Brine concentrations

4.3.2 Interfacial Tension Results

The interfacial tension (IFT) between crude oil and nanopolymer fluids with different concentrations was measured using the pendant drop method. All tests were conducted at ambient conditions until a stable value of IFT was reached. It was observed that the tension between crude oil and brine was decreased in the presence of polymer-silica nanoparticles. The IFT between crude oil and brine was 22.5mN/m, 12.61mN/m and 19.87mN/m; this value was decreased to 7.43mN/m, 5.11mN/m and 8mN/m respectively as showed in Figures 4.1, 4.2 and 4.3 with nanopolymer fluid for Fluids 3, 5 and 4, with 5% of brine. These may be due to the ionic solution that pushes the surfactant to oil-water interface similarl reported by (Jiravitpanya et al., 2017). A combination of 15% brine reduced the IFT from 17.48mN/m, 8.4mN/m and 12.28mN/m (Figures 4.4, 4.5 and 4.6) to 5.74mN/m, 3.24mN/m and 5.06mN/m respectively. Fluids 3, 4 and 5 with brine 10% decreased the IFT from 16.64mN/m, 37.35mN/m and 74.4mN/m to 5.31mN/m, 15.40mN/m and 42.2mN/m respectively (Figures 4.7, 4.8 and 4.9). Fluids 3, 4 and 5 with distilled water-reduced the IFT from 18.1, 31.62 and 20.6 to 11.75, 9.52 and 14.09 (Figures 4.10, 4.11 and 4.12). The lowest declining IFT value was observed with Fluid 3 with 10% of brine, reducing by almost 68%.

4.3.2.1 Fluid 3 Brine 5% (Silica 0.15wt% + Gum Arabic 0.4wt%)

Figure 4.1 showed how the IFT of Fluid 3 (Silica 0.15wt% + Gum Arabic 0.4wt%) decrease down at different temperature from 30°C to 100°C respectively. From the initial value of 22.51mN/m at

30°C reduces to 19.77mN/m as the temperature increases to 50°C, 16.15mN/m at 70°C, 11.13mN/m at 90°C, and further decreases to 7.43mN/m as the temperature increases to 100°C. The IFT reduced from 22.51mN/m to 7.43mN/m, at temperatures of 30°C to 100°C, resulting in a reduction of almost 67%.

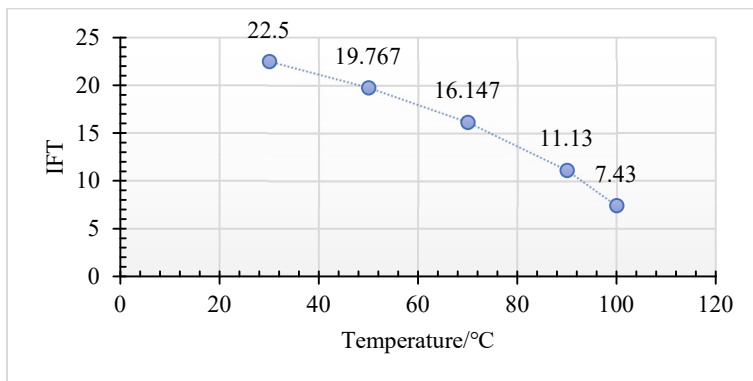


Figure 4.1: Fluid 3 IFT -Brine 5% - Oil Details at Five Temperature Ranges (30°C, 50°C, 70°C, 90°C and 100°C)

4.3.2.2 Fluid 5 Brine 5% (Silica 0.25wt% + Gum Arabic 0.2wt%)

Figure 4.2 presents the plot of fluid 5 with same brine (5%) content but increases the silica content (0.25wt%) and reduces gum-Arabic content (0.2wt%). The results indicates a similar trends of reduction of IFT value from 12.61mN/m at 30°C, to 11.77mN/m at 50°C, to 9.66mN/m at 70°C, and to 6.05mN/m and 5.11mN/m at 90°C and 100°C respectively. The IFT reduced from 12.61mN/m to 5.11mN/m, at temperatures of 30°C to 100°C, resulting in a reduction of almost 59.48%.

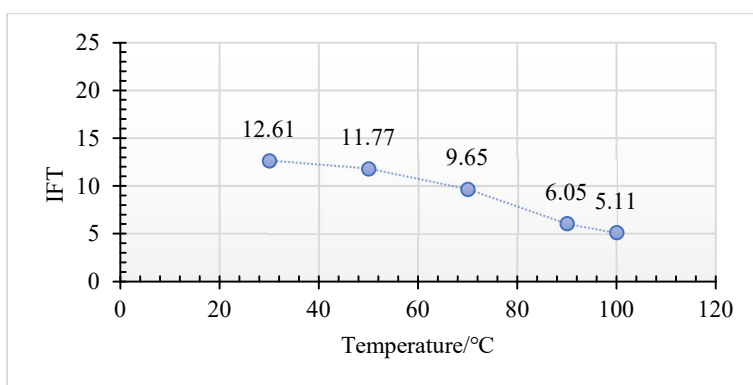


Figure 4.2: Fluid 5 IFT - Brine 5% - Oil Details at Five Temperature ranges (30°C, 50°C, 70°C, 90°C and 100°C)

4.3.2.3 Fluid 4 Brine 5% (Silica 0.2wt% + Gum Arabic 0.3wt%)

Figure 4.3 present the results obtained with Fluid 4. Similar to Figure 4.1, the IFT value reduces from 19.87mN/m at 30°C, to 16,72mN/m at 50°C, to 14.86mN/m at 70°C, and then to 8.53mN/m and 8.40mN/m at 90°C and 100°C respectively. It is observed that almost a stable value between the

IFT value at 90°C and 100°C are reached. The IFT reduced from 19,87mN/m to 8.40mN/m, at temperatures from 30°C to 100°C, resulting in a reduction of almost 57.73%.

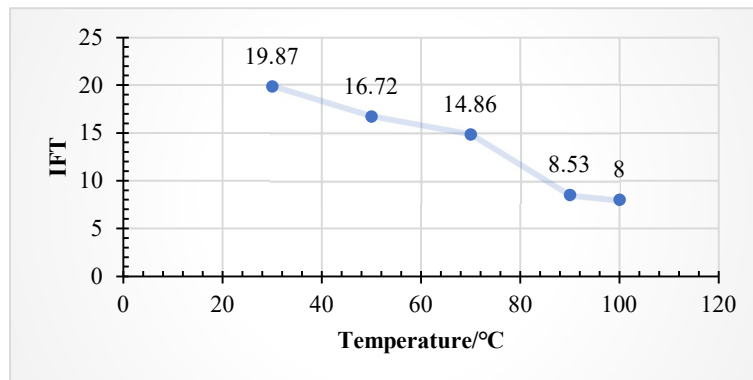


Figure 4.3: Fluid 4 IFT - Brine 5% - Oil Details at Five Temperature Ranges (30°C, 50°C, 70°C, 90°C and 100°C)

This declining trends in IFT values observed from Figures 4.1, 4.2, and 4.3 agrees well with the observation made by (Ruckenstein and Rao, 1987; Tang and Morrow, 1999; Al-Sahhaf *et al.*, 2005; Okasha and Alshiwaish, 2009). It is also observed that the brine has significant effect at low concentration of nanoparticles (silica + gum Arabic).

4.3.2.4 Fluid 3 Brine 10% (Silica 0.15wt% + Gum Arabic 0.4wt%)

Figure 4.4 present the obtained results with Fluid 3 (brine 10%). As the concentration of brine increases to 10%, similar results of declining IFT values at different temperature were observed. The IFT values decline from 16.64mN/m at 30°C to 11.88mN/m, 9.54mN/m, 7.73mN/m and 5.31mN/m at 50°C, 70°C, 90°C and 100°C respectively. The IFT was reduced from 16.64mN/m to 5.31mN/m, at temperatures of 30°C to 100°C, resulting in a reduction of almost 68%.

4.3.2.5 Fluid 5 Brine10% (Silica 0.25wt% + Gum Arabic 0.2wt%)

Moreover, Figure 4.5 indicates a plot of fluid 5 with same brine concentration of 10% but increased silica concentration by 0.10wt% and reduced gumArabic concentration by 0.2wt%. The results shows that the IFT values continue to decline in the same manner as in Figure 4.4. The IFT decreases from 37.35mN/m at 30°C to 35.35mN/m, at 50°C, and then to 24.82mN/m, 19.96mN/m and 15.40mN/m at 70°C, 90°C, 100°C. The IFT reduced from 37.35mN/m to 15.40mN/m, at temperatures from 30°C to 100°C, with a reduction of almost 58.77%.

4.3.2.6 Fluid 4 Brine10% (Silica 0.2wt% + Gum Arabic 0.3wt%)

Additionally, Figure 4.6 presents the results obtained with Fluid 4. Similarly, the IFT values exhibits same declining character from 74.4mN/m at 30°C to 66.96mN/m at 50°C and then to 61.68mN/m,

54.49mN/m and 42.20mN/m at 70°C, 90 °C and 100°C respectively. The IFT reduced from 74.4mN/m to 42.20mN/m, at temperatures from 30°C to 100°C, with a reduction of almost 43.28%.

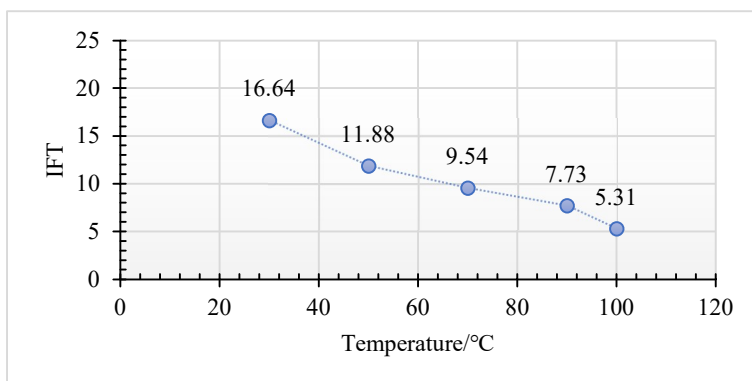


Figure 4.4: Fluid 3 IFT - Brine 10% - Oil Details at Five Temperature Ranges (30°C, 50°C, 70°C, 90°C and 100°C)

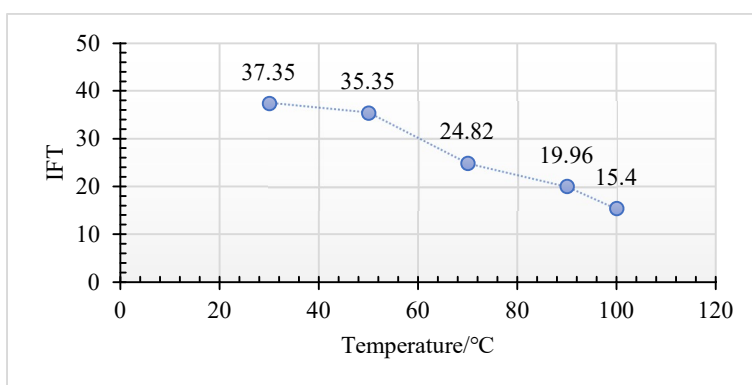


Figure 4.5: Fluid 5 IFT - Brine 10% - Oil Details at Five Temperature Ranges (30°C, 50°C, 70°C, 90°C and 100°C)

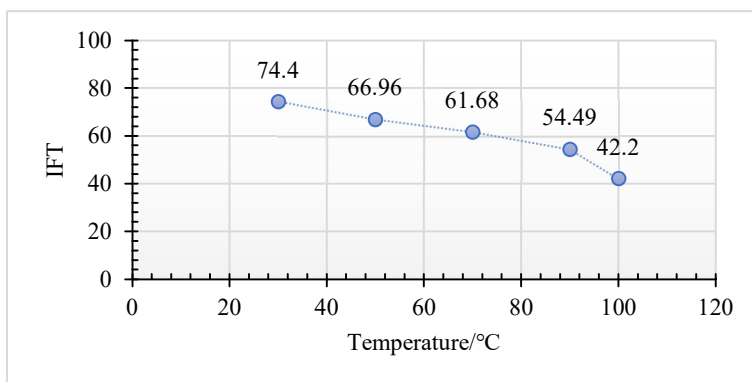


Figure 4.6: Fluid 4 IFT - Brine 10% - Oil Details at Five Temperature Ranges (30°C, 50°C, 70°C, 90°C and 100°C)

4.3.2.7 Fluid 3 Brine 15% (Silica 0.15wt% + Gum Arabic 0.4wt%)

The IFT between oil and 1.5wt% brine-based combinations (silica + Gum Arabic) particles was 17.48mN/m at 30°C; it then decreased to 12.58mN/m at 50°C and to 5.75mN/m and 5.74mN/m at 90°C and 100°C respectively. The best results were shown at the lower temperature of 30°C and at the higher temperature of 100°C, where interfacial tension reduced from 17.48mN/m to 5.74mN/m, with a reduction almost 67.17%.

4.3.2.8 Fluid 5 Brine 15% (Silica 0.25wt% + Gum Arabic 0.2wt%)

The IFT between oil and combination for Fluid 5 was 8.4mN/m at 30°C, to 8.18mN/m at 50°C, with a slight reduction to 7.1mN/m at 70°C, to 4.26mN/m at 90c, and then to 3.24mN/m at 100°C. The IFT reduced from 8.4mN/m to 3.24mN/m, at temperatures from 30°C to 100°C, with a reduction of almost 61%.

4.3.2.9 Fluid 4 Brine 15% (Silica 0.2wt% + Gum Arabic 0.3wt%)

The IFT between oil and combination Fluid 4 was 12.28mN/m at 30°C, decreasing to 7.54mN/m at 50°C, and to 6.22mN/m, 5.22mN/m and 5.06mN/m at 70°C, 90°C and 100°C respectively. The IFT reduced from 12.28mN/m to 5.06mN/m, at temperatures from 30°C to 100°C, with a reduction of almost 58.8%.

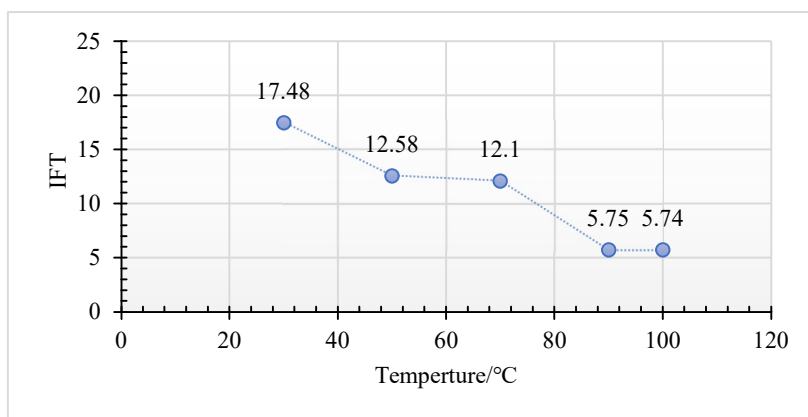


Figure 4.7: Fluid 3 IFT - Brine 15% - Oil Details at Five Temperature Ranges (30°C, 50°C, 70°C, 90°C and 100°C)

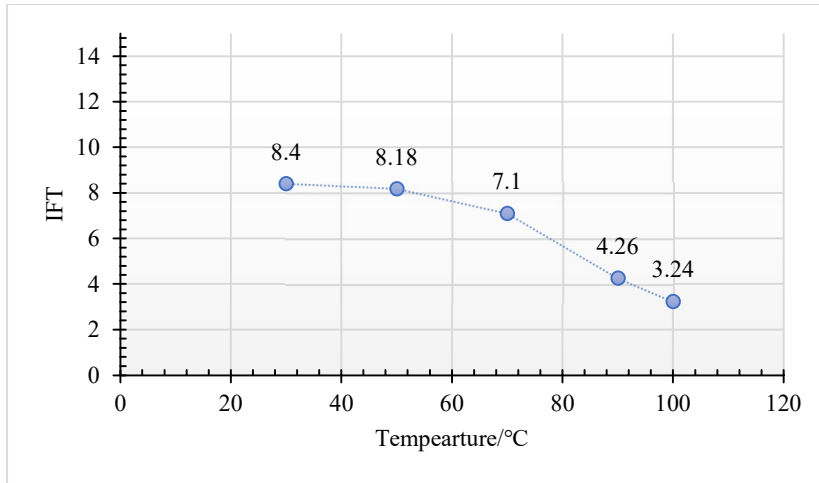


Figure 4.8: Fluid 5 IFT - Brine 15% - Oil Details at Five Temperature Ranges (30°C, 50°C, 70°C, 90°C and 100°C)

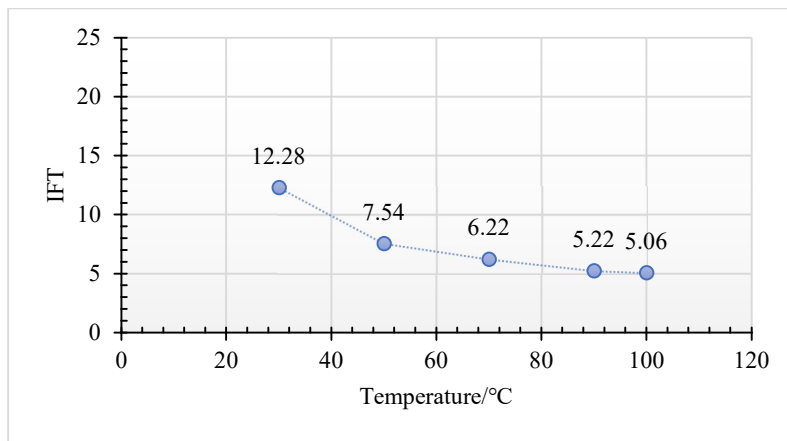


Figure 4.9: Fluid 4 IFT - Brine 15% - Oil Details at Five Temperature Ranges (30°C, 50°C, 70°C, 90°C and 100°C)

4.3.2.10 Fluid 4 Distilled Water (Silica 0.2wt% + Gum Arabic 0.3wt%)

For Fluid 4, the IFT decreased from 13.62mN/m at 30°C, to 12.64mN/m at 50°C, and then gradually decreased to 11.63mN/m, 10.61mN/m and 9.51mN/m at 70°C, 90°C and 100°C respectively. The IFT reduced from 13.62mN/m to 9.51mN/m, at temperatures from 30°C to 100°C, with a reduction of almost 30.18%.

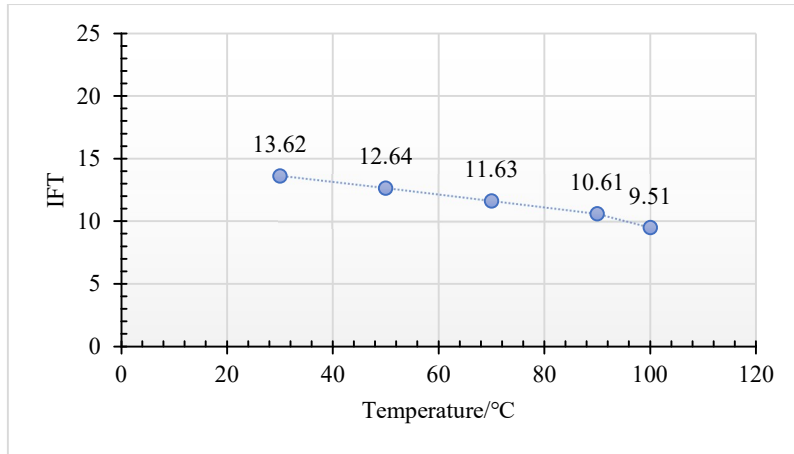


Figure 4.10: Fluid 4 IFT - Distilled Water - Oil Details at Five Temperature Ranges (30°C, 50°C, 70°C, 90°C and 100°C)

4.3.2.11 Fluid 3 Distilled Water (Silica 0.15wt% + Gum Arabic 0.4wt%)

The IFT for Fluid 5 was 18.10mN/m at 30°C, and decreased to 15.08mN/m at 50°C, and then to 13.65mN/m, 11.92mN/m and 11.75mN/m at 70°C, 90°C and 100°C respectively. The IFT reduced from 18.10mN/m to 11.75mN/m, at temperatures from 30°C to 100°C, with a reduction of almost 35.08%.

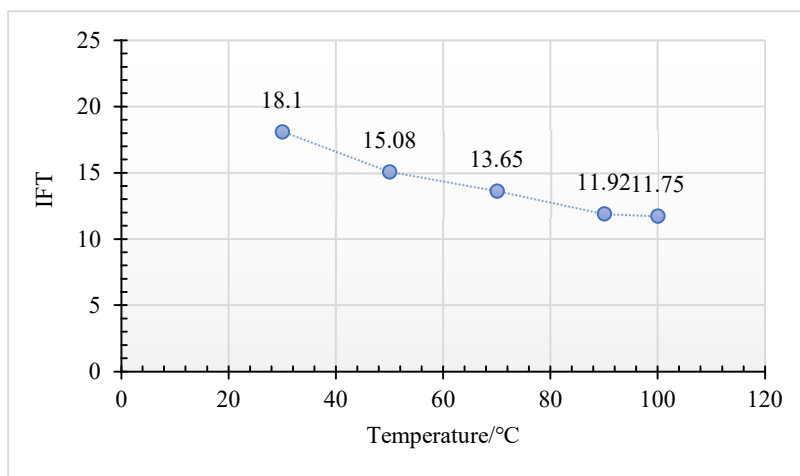


Figure 4.11: Fluid 3 IFT - Distilled Water - Oil Details at Five Temperature Ranges (30°C, 50°C, 70°C, 90°C and 100°C)

4.3.2.12 Fluid 5 Distilled Water (Silica 0.25wt% + Gum Arabic 0.2wt%)

The IFT for Fluid 5 with distilled water decreased from 20.60mN/m at 30°C, and then gradually to 19.67mN/m, 18.79mN/m, 17.40mN/m, and 14.09mN/m at 50°C, 70°C, 90°C and 100c respectively. The IFT reduced from 20.60mN/m to 14.09mN/m, at temperatures from 30°C to 100°C, with a reduction of almost 31.60%.

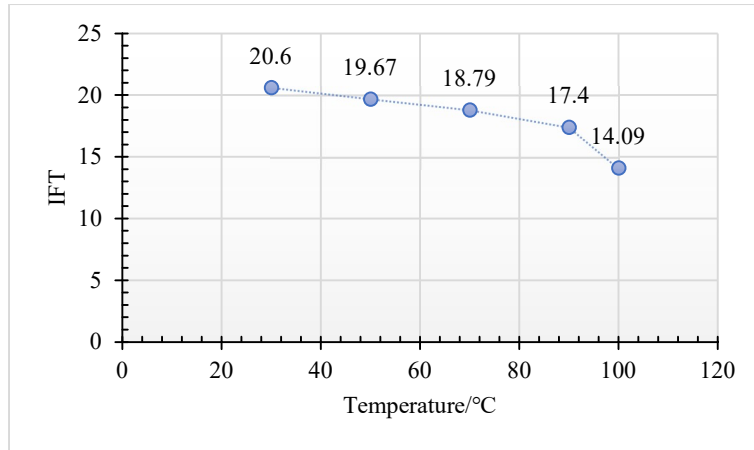


Figure 4.12: Fluid 5 IFT - Distilled Water -Oil Details at Five Temperature Ranges (30°C, 50°C, 70°C, 90°C and 100°C)

4.3.3 The Effect of Pressure and Temperature on IFT

The pressure range used was between 1750psig and 2000psig, at different temperatures of 30°C, 50°C, 70°C, 90°C and 100°C. Generally, as discussed earlier in figures 4.1 to 4.12, it was clearly observed that as the temperature increases, the values of the IFT decreases at different concentrations of brine+silica+gum-Arabic respectively. However, in some of the concentrations, a significant effects were seen. This decrease in the IFT values with increase in temperature may be attributed to the weakening of the molecular forces at the oil/nanopticles solution interface. This trnds of reduction in IFT values with increasing temperature is also investigated by (Aoudia *et al.*, 2006). the IFT values observed to be decreasing as the temperature increases but for pressure, we can see more clearly the slight decrease from 2000psig to 6000psig as Figure 4.14 shows. We can say that the temperature has more effect on IFT than does the pressure on liquid phase, the reason being that inter molecules force it up higher for the liquid phase than for the gas phase.

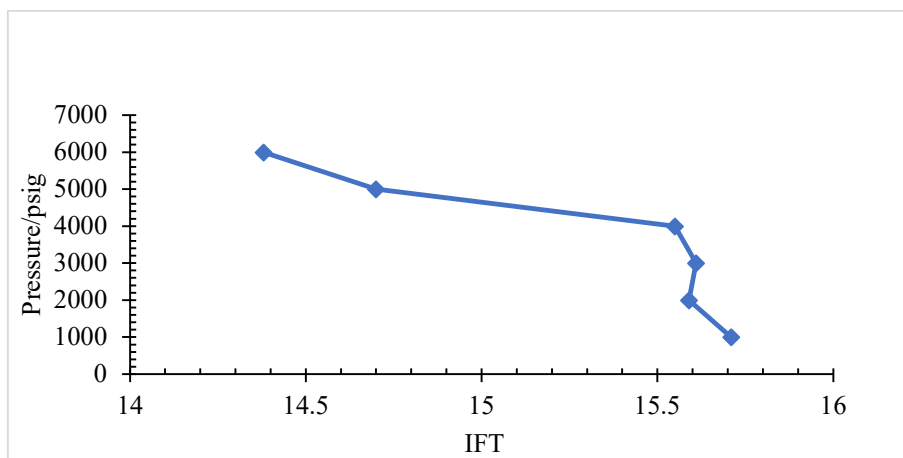


Figure 4.14: Showing the Results Between IFT and Pressure

4.3.4 The Effect of Salinity on IFT Reduction

The effect of salinity on a combination (silica-gum Arabic) was investigated by first evaluating the presence of NaCl at different concentrations. From the comber, the combination of brine with distilled water it shows that the IFT of the NaCl solution has clear addiction on the salinity of brine and plays an important role in the reduction in IFT. The values obtained for Fluids 3, 5 and 4 with brine reduced the IFT to 67.17%, 61% and 58.8% respectively. For Fluids 3, 5 and 4 with distilled water reduced the IFT 35.08%, 31.60% and 30.18% respectively. (See Figure 4.14). This reduction is due to the same electric charge of the divalent cations, which increase the electric charge of the cationic surfactant to compress the interfacial double layer. Thus, by increasing the repulsion between surfactant molecules with the same charge in the micelle, more surfactant molecules could enter the micelle to enlarge the radius of the micelle particle, resulting in a decrease of IFT.

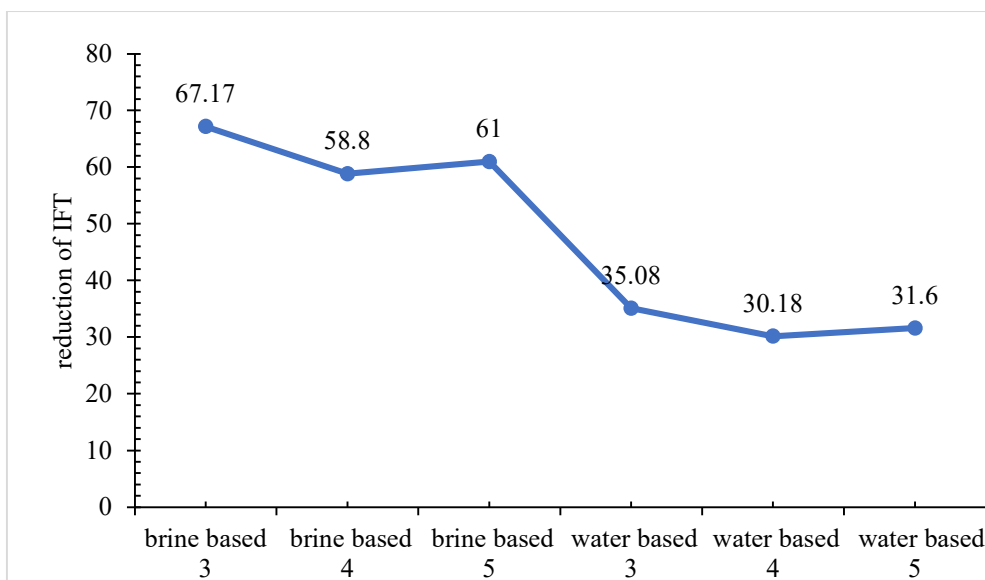


Figure 4.14: Influence of NaCl Concentration

Chapter 5 Conclusion and Recommendations

5.1 Introduction

In this dissertation, the interfacial tension of two-phase fluid system were experimentally investigated. The experiments carried out involves the characterisation of the liquid samples and the interfacial tension of liquid interfaces at various conditions ranging from (30°C to 100°C and 1750psig). The investigation includes binary synthetic mixtures including water, salts, nanoparticles (silica) and polymer (Gum Arabic). Interfacial tensions were observed to span from near-complete miscibility (low IFT values) to immiscible (high IFT values) at two-phase equilibria conditions. More specific details on the experimental achievements and results of this desertation are concluded as follows as well as advice and future investigations.

5.2 Conclusions

The research study was aimed at investigating how different concentrations of a combination of nanoparticles (Silica Oxide) and polymer (Gum Arabic) influence the interfacial tension at different temperatures (30°C – 100°C) to enhance oil recovery (EOR). That is the effect of the IFT on silica nanoparticles and gum Arabic polymer at different temperatures to enhanced oil recovery. Brine-based nanoparticles with a few different concentrations, and distilled water-based nanoparticles with different concentrations were used during the experiment. The IFT was measured to explain the mechanism that leads to an increase in the recovery of oil. The IFT equipment was based on the Pendant Drop method and the Axisymmetric Drop Shape Analysis technique. Based on the obtained results and observations, the following conclusions were drawn:

- a. The preparation of the solution of hydrophilic combination of silica nanoparticles and gum Arabic polymer in brine with different concentrations were achieved successfully.
- b. The IFT tends to decrease significantly even with increasing and decreasing the combination of silica nanoparticles and gum Arabic polymer concentration. Although, fluid 5 with 15% brine shows more efficient in lowering IFT compared with the other combinations, fluid 5 solutions were able to reduce IFT the most at 100°C, thus, fluid 5 solution also gives the lowest IFT values at 30°C temperature.
- c. The IFT between oil and 1.5wt.% brine-based combinations (silica (0.15wt%) + Gum Arabic (0.4wt%) particles was 17.48mN/m at 30°C. It then decreased to 12.58mN/m at 50°C and to 5.75mN/m and 5.74mN/m at 90°C and 100°C respectively, demonstrating that the best results are at the lower temperature 30°C and at the higher temperature of

- 100°C, where interfacial tension reduced from 17.48mN/m to 5.74mN/m, with a reduction of almost 67.17%.
- d. The results obtained for brine 0.5 wt.% and oil at different temperatures, (silica 0.15wt% + Gum Arabic 0.4wt%) demonstrate that the IFT reduces from 22.51mN/m at 30°C, to 19.77mN/m at 50°C, then to 16.15mN/m, 11.13mN/m, 7.43mN/m at 70°C, 90°C and 100°C respectively.
 - e. For silica 0.25wt% + Gum Arabic 0.2wt%, the IFT reduces from 12.61mN/m at 30°C then to 11.77mN/m at 50°C, to 9.66mN/m at 70°C, and to 6.05mN/m and 5.11mN/m at 90°C and 100°C respectively. For silica 0.2wt% + Gum Arabic 0.3wt%, the IFT reduces from 19.87mN/m at 30°C, to 16.72mN/m at 50°C, to 14.86mN/m at 70°C, and then to 8.53mN/m and 8.40mN/m at 90°C and 100°C respectively.
 - f. However, the result obtained for the interfacial tension between distilled water and oil decreases from 20.60mN/m at 30°C; it then decreased gradually to 19.67mN/m, 18.79mN/m, 17.40mN/m and 14.09mN/m at 50°C, 70°C, 90°C and 100°C respectively.
 - g. The pressure range was between 1750psig and 2000psig at 30°C, 50°C, 70°C, 90°C and 100°C. In general, the IFT was observed to decrease as the temperature increases but, for pressure, we can see it slightly decrease from 2000psig to 6000psig. We can say that the temperature has more effect than pressure on the IFT in the liquid phase, due to the inter molecular force for the liquid phase being higher than in the gas phase.
 - h. Results on interfacial tension involving nanosilica and Gum Arabic demonstrates that the IFT is a function of pressure, temperature, salinity and silica+polymer. Increase in pressure and temperature both decrease the IFT. The presence of 5, 10 and 15wt% NaCl resulted in an average reduction of between 55 – 60% in the IFT .
 - i. The effect of the pressure is negligible on IFT.
 - j. Based on the results obtained for different fluid scenarios, fluids 5 with 15% brine and Silica 0.25wt% + Gum Arabic 0.2wt% indicates more effects on oil recovery. The IFT results indicate that at high temperature 100°C of the combination decreases the IFT value to 3.24m/Nm.
 - k. The optimum distilled water-based nanoparticle fluid concentration decreased the IFT at most temperature.
 - l. Based on the obtained results, brine-based nanoparticle fluid showed efficient results by reducing the IFT more than when using the distilled water-based nanoparticle fluid.

- m. The obtained result of the IFT that is measured using a Pendant Drop system is more accurate than other devices because of the ability of the system to simulate the reservoir conditions.

5.3 Recommendations

- a. The system must be cleaned periodically to remove any contamination or any heavy fluid build-up.
- b. It is recommended to place a shield at each end of the window axis especially if the cell is left unattended.
- c. Avoiding direct contact with the surface of the IFT cell because it can be very hot.
- d. It is necessary to change the associated fluid densities and oil densities in the software at different temperature.
- e. The IFT cell should not be observed closely unless protective eyewear is used in case of sudden glass failure.
- f. The IFT cell is a high temperature to obtain accurate results. Therefore, it must be used and observed carefully.
- g. Another scenario of IFT measurement can be conducted by changing the dispersion fluid to a low brine concentration, such as 1wt%.
- h. Another investigation could be done to investigate the effect of nanoparticles on the contact angle, which is another essential parameter to produce more oil from the reservoir.
- i. Pressure does not have any effect on IFT.

References

- Abidin, A. Z., Puspasari, T. and Nugroho, W. A. (2012) 'Polymers for enhanced oil recovery technology', *Procedia Chemistry*. Elsevier, 4, pp. 11–16.
- Abubakar, A. *et al.* (2015) 'Effect of low interfacial tension on flow patterns, pressure gradients and holdups of medium-viscosity oil/water flow in horizontal pipe', *Experimental Thermal and Fluid Science*. Elsevier, 68, pp. 58–67.
- Akiskal, H. S. *et al.* (1985) 'Affective disorders in referred children and younger siblings of manic-depressives: mode of onset and prospective course', *Archives of General Psychiatry*. American Medical Association, 42(10), pp. 996–1003.
- Al-Sahhaf, T. *et al.* (2005) 'The influence of temperature, pressure, salinity, and surfactant concentration on the interfacial tension of the n-octane-water system', *Chemical Engineering Communications*. Taylor & Francis, 192(5), pp. 667–684.
- Algharaib, M., Alajmi, A. and Gharbi, R. (2011) 'Investigation of polymer flood performance in high salinity oil reservoirs', in *SPE/DGS Saudi Arabia Section Technical Symposium and Exhibition*. Society of Petroleum Engineers.
- Amani, P. *et al.* (2017) 'Two-phase pressure drop and flooding characteristics in a horizontal-vertical pulsed sieve-plate column', *International Journal of Heat and Fluid Flow*. Elsevier, 65, pp. 266–276.
- Aoudia, M. *et al.* (2006) 'Novel surfactants for ultralow interfacial tension in a wide range of surfactant concentration and temperature', *Journal of surfactants and detergents*. Wiley Online Library, 9(3), pp. 287–293.
- Arabloo, M., Ghazanfari, M. H. and Rashtchian, D. (2016) 'Wettability modification, interfacial tension and adsorption characteristics of a new surfactant: Implications for enhanced oil recovery', *Fuel*. Elsevier, 185, pp. 199–210.
- Arashiro, E. Y. and Demarquette, N. R. (1999) 'Use of the pendant drop method to measure interfacial tension between molten polymers', *Materials Research*. SciELO Brasil, 2(1), pp. 23–32.
- Asadollahzadeh, M. *et al.* (2016) 'Experimental investigation of dispersed phase holdup and flooding characteristics in a multistage column extractor', *Chemical Engineering Research and Design*. Elsevier, 105, pp. 177–187.

- Balasubramaniam, S. *et al.* (2011) ‘Poly (N-isopropylacrylamide)-coated superparamagnetic iron oxide nanoparticles: relaxometric and fluorescence behavior correlate to temperature-dependent aggregation’, *Chemistry of Materials*. ACS Publications, 23(14), pp. 3348–3356.
- Batychy, J. P. and McCaffery, F. G. (1978) ‘Low interfacial tension displacement studies’, in *Annual Technical Meeting*. Petroleum Society of Canada.
- Bera, A. and Belhaj, H. (2016) ‘Application of nanotechnology by means of nanoparticles and nanodispersions in oil recovery-A comprehensive review’, *Journal of Natural Gas Science and Engineering*. Elsevier, 34, pp. 1284–1309.
- Cannella, W. J., Huh, C. and Seright, R. S. (1988) ‘Prediction of xanthan rheology in porous media’, in *SPE annual technical conference and exhibition*. Society of Petroleum Engineers.
- Cheng, P. *et al.* (1990) ‘Automation of axisymmetric drop shape analysis for measurements of interfacial tensions and contact angles’, *Colloids and Surfaces*. Elsevier, 43(2), pp. 151–167.
- Chengara, A. *et al.* (2004) ‘Spreading of nanofluids driven by the structural disjoining pressure gradient’, *Journal of colloid and interface science*. Elsevier, 280(1), pp. 192–201.
- Ciriminna, R. *et al.* (2013) ‘The sol–gel route to advanced silica-based materials and recent applications’, *Chemical reviews*. ACS Publications, 113(8), pp. 6592–6620.
- Dahle, G. S. (2014) *Investigation of how Hydrophilic Silica Nanoparticles Affect Oil Recovery in Berea Sandstone*.
- Drelich, J., Fang, C. and White, C. L. (2002) ‘Measurement of interfacial tension in fluid-fluid systems’, *Encyclopedia of surface and colloid science*. Marcel Dekker: New York, 3, pp. 3158–3163.
- Ferry, J. D. (1980) *Viscoelastic properties of polymers*. John Wiley & Sons.
- Frijters, S., Günther, F. and Harting, J. (2012) ‘Effects of nanoparticles and surfactant on droplets in shear flow’, *Soft Matter*. Royal Society of Chemistry, 8(24), pp. 6542–6556.
- Goolsby, J. L. (1967) *Relation of geology to fluid injection in Permian carbonate reservoirs in west Texas*. Gulf Oil Corp.
- Harkins, W. D. and Jordan, H. F. (1930) ‘A method for the determination of surface and interfacial tension from the maximum pull on a ring’, *Journal of the American Chemical Society*. ACS Publications, 52(5), pp. 1751–1772.

- Heiserman, D. (1991) *Exploring chemical elements and their compounds*. McGraw-Hill.
- Hendraningrat, L., Li, S. and Torsæter, O. (2013) ‘A coreflood investigation of nanofluid enhanced oil recovery’, *Journal of Petroleum Science and Engineering*. Elsevier, 111, pp. 128–138.
- Hendraningrat, L., Shidong, L. and Torsaeter, O. (2012) ‘A glass micromodel experimental study of hydrophilic nanoparticles retention for EOR project’, in *SPE Russian Oil and Gas Exploration and Production Technical Conference and Exhibition*. Society of Petroleum Engineers.
- Hocott, C. R. (1939) ‘Interfacial tension between water and oil under reservoir conditions’, *Transactions of the AIME*. Society of Petroleum Engineers, 132(01), pp. 184–190.
- Jadhunandan, P. P. and Morrow, N. R. (1995) ‘Effect of wettability on waterflood recovery for crude-oil/brine/rock systems’, *SPE reservoir engineering*. Society of Petroleum Engineers, 10(01), pp. 40–46.
- Jiravitpanya, J., Maneeintr, K. and Boonpramote, T. (2017) ‘Experiment on measurement of interfacial tension for subsurface conditions of light oil from thailand’, in *MATEC Web of Conferences*. EDP Sciences, p. 18007.
- Knight, B. L. (1973) ‘Reservoir stability of polymer solutions’, *Journal of Petroleum Technology*. Society of Petroleum Engineers, 25(05), pp. 618–626.
- Lee, S., Kim, D. H. and Needham, D. (2001) ‘Equilibrium and dynamic interfacial tension measurements at microscopic interfaces using a micropipet technique. 2. Dynamics of phospholipid monolayer formation and equilibrium tensions at the water– air interface’, *Langmuir*. ACS Publications, 17(18), pp. 5544–5550.
- Li, S., Hendraningrat, L. and Torsaeter, O. (2013) ‘Improved oil recovery by hydrophilic silica nanoparticles suspension: 2 phase flow experimental studies’, in *IPTC 2013: International Petroleum Technology Conference*. European Association of Geoscientists & Engineers, p. cp-350.
- Liang, T. *et al.* (2017) ‘Evaluation of wettability alteration and IFT reduction on mitigating water blocking for low-permeability oil-wet rocks after hydraulic fracturing’, *Fuel*. Elsevier, 209, pp. 650–660.
- McElfresh, P. M., Holcomb, D. L. and Ector, D. (2012) ‘Application of nanofluid technology to improve recovery in oil and gas wells’, in *SPE international oilfield nanotechnology conference and exhibition*. Society of Petroleum Engineers.

- Moradi, O. (2011) 'Thermodynamics of interfaces', in *Thermodynamics-Interaction Studies-Solids, Liquids and Gases*. IntechOpen.
- Morrow, N. R. (1990) 'Wettability and its effect on oil recovery', *Journal of petroleum technology*. Society of Petroleum Engineers, 42(12), pp. 1–476.
- Ogolo, N. A., Olafuyi, O. A. and Onyekonwu, M. O. (2012) 'Enhanced Oil Recovery Using Nanoparticles. 2012'. SPE.
- Okasha, T. M. and Alshiwaiash, A. (2009) 'Effect of brine salinity on interfacial tension in Arab-D carbonate reservoir, Saudi Arabia', in *SPE Middle East Oil and Gas Show and Conference*. Society of Petroleum Engineers.
- Olajire, A. A. (2014) 'Review of ASP EOR (alkaline surfactant polymer enhanced oil recovery) technology in the petroleum industry: Prospects and challenges', *Energy*. Elsevier, 77, pp. 963–982.
- Owens, W. W. and Archer, D.I. (1971) 'The effect of rock wettability on oil-water relative permeability relationships', *Journal of Petroleum Technology*. Society of Petroleum Engineers, 23(07), pp. 873–878.
- Pedersen, K. S., Lund, T. and Fredenslund, A. (1989) 'Surface tension of petroleum mixtures', *Journal of Canadian Petroleum Technology*. Petroleum Society of Canada, 28(02).
- Rajagopalan, R. and Hiemenz, P. C. (1997) 'Principles of colloid and surface chemistry', *Marcel Dekker, New-York*, 8247, p. 8.
- Del Rio, O. I. and Neumann, A. W. (1997) 'Axisymmetric drop shape analysis: computational methods for the measurement of interfacial properties from the shape and dimensions of pendant and sessile drops', *Journal of colloid and interface science*. Elsevier, 196(2), pp. 136–147.
- Ruckenstein, E. and Rao, I. V (1987) 'Interfacial tension of oil—brine systems in the presence of surfactant and cosurfactant', *Journal of colloid and interface science*. Elsevier, 117(1), pp. 104–119.
- Rusanov, A. I. and Prokhorov, V. A. (1996) *Interfacial tensiometry*. Elsevier.
- Ryles, R. G. (1988) 'Chemical stability limits of water-soluble polymers used in oil recovery processes', *SPE reservoir engineering*. Society of Petroleum Engineers, 3(01), pp. 23–34.
- Sattari-Najafabadi, M. *et al.* (2018) 'Mass transfer between phases in microchannels: A review', *Chemical Engineering and Processing-Process Intensification*. Elsevier, 127, pp. 213–237.

- Skauge, T., Spildo, K. and Skauge, A. (2010) ‘Nano-sized particles for EOR’, in *SPE improved oil recovery symposium*. Society of Petroleum Engineers.
- Suleimanov, B. A., Ismailov, F. S. and Veliyev, E. F. (2011) ‘Nanofluid for enhanced oil recovery’, *Journal of Petroleum Science and Engineering*. Elsevier, 78(2), pp. 431–437.
- Tang, G.-Q. and Morrow, N. R. (1999) ‘Influence of brine composition and fines migration on crude oil/brine/rock interactions and oil recovery’, *Journal of Petroleum Science and Engineering*. Elsevier, 24(2–4), pp. 99–111.
- Vafaei, S. *et al.* (2006) ‘Effect of nanoparticles on sessile droplet contact angle’, *Nanotechnology*. IOP Publishing, 17(10), p. 2523.
- Wang, G. C. and Caudle, B. H. (1970) ‘Effects of polymer concentrations, slug size and permeability stratification in viscous waterfloods’, in *Fall Meeting of the Society of Petroleum Engineers of AIME*. Society of Petroleum Engineers.
- Wasan, D., Nikolov, A. and Kondiparty, K. (2011) ‘The wetting and spreading of nanofluids on solids: Role of the structural disjoining pressure’, *Current Opinion in Colloid & Interface Science*. Elsevier, 16(4), pp. 344–349.
- Wasan, D. T. and Nikolov, A. D. (2003) ‘Spreading of nanofluids on solids’, *Nature*. Nature Publishing Group, 423(6936), pp. 156–159.
- Whitson, C. H. and Brule, M. R. (2000) ‘Gas and Oil Properties and Correlations’, *Phase Behavior*. SPE Monograph, SPE Richardson, TX, 20, pp. 18–46.
- Yahaya, A. A. (2018) ‘Experimental investigation of interfacial tension in two-phase system involving methane and water’. University of Salford.
- Zhang, T. *et al.* (2015) ‘Investigation of nanoparticle adsorption during transport in porous media’, *SPE Journal*. Society of Petroleum Engineers, 20(04), pp. 667–677.
- Zolotukhin, A. B. and Ursin, J.-R. (2000) *Introduction to petroleum reservoir engineering*. Norwegian Academic Press (HóyskoleForlaget).
- Caenn, R., Burneit, & chilingauruan. (1985). Polymer flooding. In E. Donaldson, & Donaldson (Ed.), *Enhanced oil recovery II processes and operations* (Vol. 17 B, pp. 157-168). New york: ELseiver.

Dorsey, W. E. (1929). The investigation of surface tension and associated phenomena. Bull. Nat. Res. Conn, (69), 56–118.<http://books.google.no/books?id=QphRAAAAMAAJ>.

Dorsey, W. E. (1929). The investigation of surface tension and associated phenomena. Bull. Nat. Res. Conn, (69), 56–118.

Einstein, M. and Civan, F., 1992.Characterization Of Formation Damage By Particulate Processes. Journal of Canadian Petroleum Technology, 31(03).

Google Docs. 2020 Fluid Mechanics With Engineering Applications By Franzini 10Th. Edition. Pdf.[online] Available at: <<https://docs.google.com/file/d/0B9LJy8vattSMV19QcGtTeV9Cd0U/edit>> [Accessed 21 March 2020].

Salarizadeh, P., Abdollahi, M. and Javanbakht, M., 2012. Modification of silica nanoparticles with hydrophilic sulfonated polymers by using surface-initiated redox polymerization. Iranian Polymer Journal, 21(10), pp.661-668.

Habermann, B., 1960. The Efficiency of Miscible Displacement as a Function of Mobility Ratio. Transactions of the AIME, 219(01), pp.264-272.

Hansen, F. K., & Rodsrud, G. (1991).Surface Tension by Pendant Drop I. A Fast Standard Instrument Using Computer Image Analysis. Journal of Colloid and Interface Science,141(I).

Hiemenz, P. and Rajagopalan,1997 Principles of Colloid and Surface Chemistry, Third Edition, Revised and Expanded. Taylor and Francis,. ISBN 9781420001297. URL <http://books.google.no/books?id=CBvrS8rfPIYC>.(accssses 20/20/2019).

Improved Oil and Gas Recovery, 2018.Incorporation of Homogenizer in Nanoemulsion Injection Scheme for Enhanced Oil Recovery.

Nanowerk.IntroductiontoNanotechnolog.URLwww.nanowerk.com/nanotechnology/introduction/. accesse 19/11/2019.

odd, A., Somerville, J., and Scott, G.(1984) The application of depth of formation damage measurements in predicting water injectivity decline. 1984. doi: <http://dx.doi.org/10.2118/12498-MS>.

Oh, S. and Slattery, J., 1979. Interfacial Tension Required for Significant Displacement of Residual Oil. Society of Petroleum Engineers Journal, 19(02), pp.83-96.

Omar, A. (1983). Effect of Polymer Adsorption on Mobility Ratio. Middle East Oil Technical Conference and Exhibition, 14-17 March, Manama, Bahrain (pp. 509-511). Bahrain: Society of Petroleum Engineers.

Sarem, A. (1970). On the Theory of Polymer Solution Flooding Process. Fall Meeting of the Society of Petroleum Engineers of AIME, 4-7 October, Houston, Texas (pp. 2-5). TEXAS: society of petroleum engineers.

Singh, R. and Mohanty, K., 2015. Synergy between Nanoparticles and Surfactants in Stabilizing Foams for Oil Recovery. *Energy & Fuels*, 29(2), pp.467-479.

Tadros, T. (2013). Gibbs Adsorption Isotherm. In T. Tadros (Ed.), *Encyclopedia of Colloid and Interface Science* (p. 626). Berlin, Heidelberg: Springer Berlin Heidelberg.
https://doi.org/10.1007/978-3-642-20665-8_97

Wisconsin Geological Survey. Rock properties: Porosity and density, 2010. URL
http://wisconsingeologicalsurvey.org/porosity_density/about_porosity_density.html accessed 28/03/2019

Yu, J., Berlin, J. M., Lu, W., Zhang, L., Kan, A. T., Zhang, P., Walsh, E. E., Work, S., Chen, W., Tour, J., Wong, M., and Tomson, M. B. Transport study of nanoparticles for oilfield application. 2010. doi: <http://dx.doi.org/10.2118/131158-ms>.

Appendix A

Drop Image Advanced Software

It is possible to record the evolution of liquid drop into another liquid, or gas bubble into liquid as a function of time using a Pendant Drop system. Live images of the drop or bubble are taken at a specific recurrence that relies upon the experimental duration. The images captured are digitised by a frame grabber, which interface the Rame-Hart camera to the data acquisition system. The contours of the bubbles are evaluated to infer interfacial tension from the captured profile of the bubble using different programs. The whole process of digitisation and analysis of the bubble lasts less than 40 seconds. It consists of four steps:

Capture and digitisation of the image of the pendant bubble.

Extraction of the drop contour, and determination of the radius of curvature at the apex necessary for the calculation of interfacial tension

Smoothing of the extracted curve of the bubble using polynomial.

Profile comparison between the theoretical and experimental bubble, inferring the IFT value.

Steps of the Pendant Drop method are commonly used to measure surface tensions of liquids. It consists in analysing the shape of a drop hanging typically from a capillary tube and about to detach (sometimes the inverse situation of a bubble forming at the bottom of a liquid is preferred, or that of a sessile drop or bubble):

Verify that the instrument is set up according to the instructions provided and has been calibrated.

Fill the quartz cell with de-ionised water.

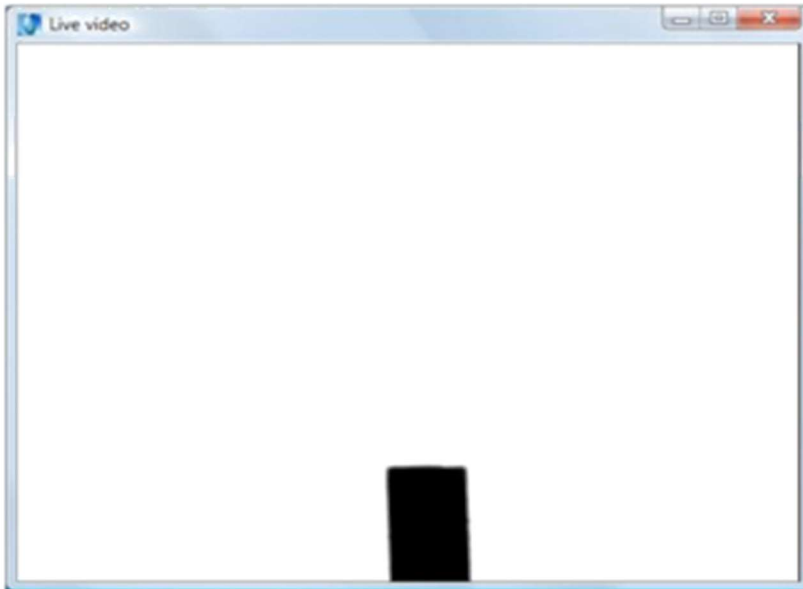
Fill the microsyringe with the test sample of oil.

Attach the inverted needle to the syringe firmly.

Turn the dispensing knob on the microsyringe to remove air from the needle.

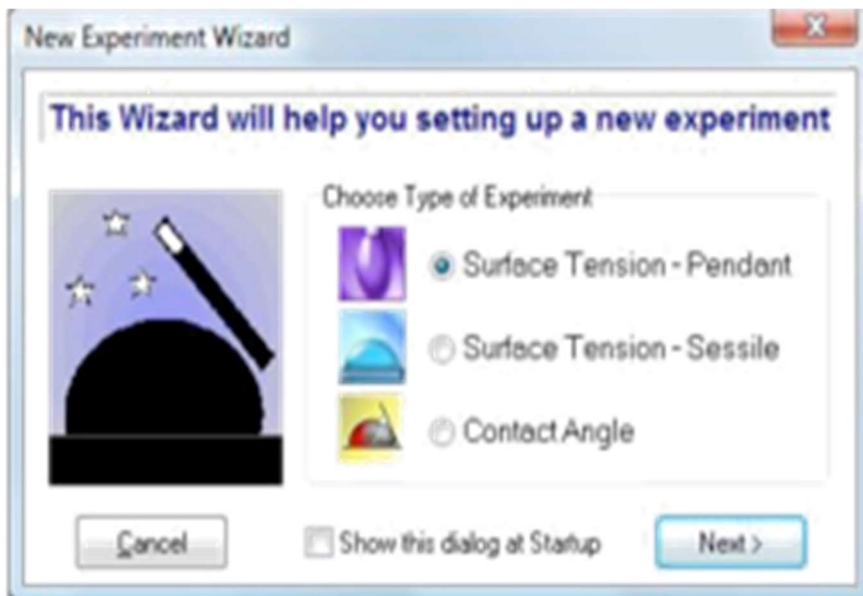
Start the DROP image advanced software.

Install the microsyringe in the fixture and adjust it so that the tip of the needle is visible in the centre bottom of the DROP image live image window as shown below.



A 1 Display Screen Showing Inserted Capillary Tube in the Chamber

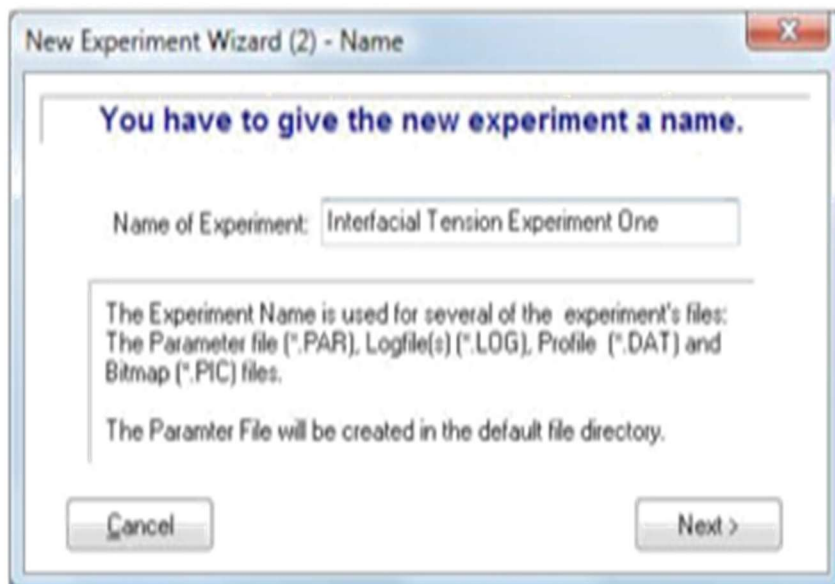
Begin a new experiment using the Experiment Wizard. Click on 'File' – 'New'- 'Experiment Wizard', or simply hit 'Ctrl-T' on the keyboard.



A 2 Screen Displayed for Setting up a New Experiment Dialogue Box

We will use the first choice, 'Surface Tension – Pendant'. This is the appropriate method for both hanging and inverted pendant drop. Click 'Next'.

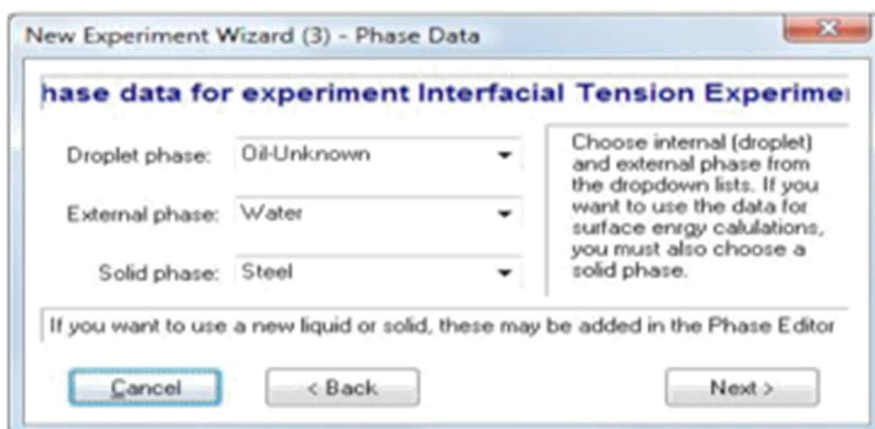
On the next screen enter an experiment name. We will use the ‘Interfacial Tension Experiment’ one.



A 3 Screen Displayed Dialogue Box for Naming the New Experiment

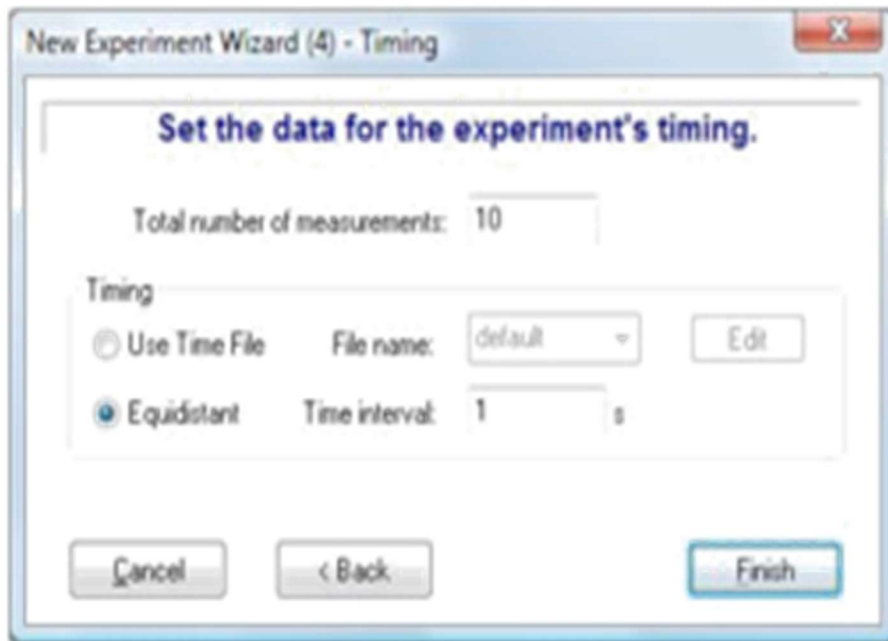
Click on ‘Next’.

On the next screen we will enter the phase data. For the droplet phase, select the liquid you are using from the list. If the liquid is not in the list, you will first need to add it using the phase Editor. Select the ‘External’ phase - in this case, ‘Water’, and then ‘Solid Phase. which is Steel’ (needle).



A 4 Dialogue Box Indicating Phase Input Data for the IFT Measurement

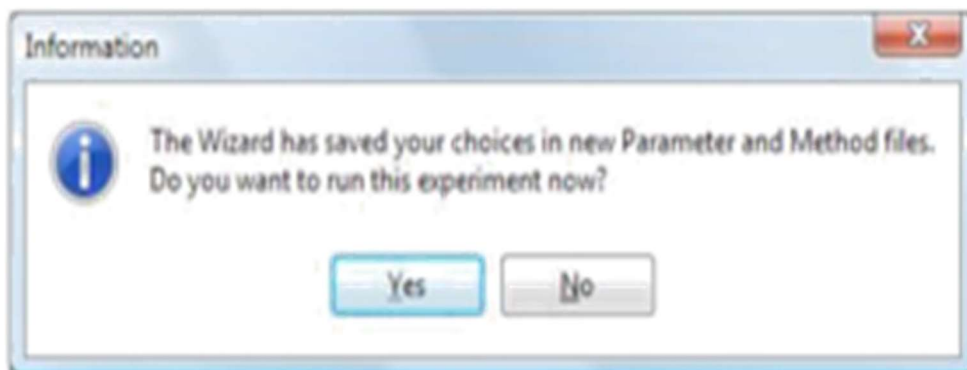
Click on 'Next'



A 5 Dialogue Box Indicating Timing Input Data for the IFT Measurement

Now enter '10' for the number of measurement. For the timing, you can use an existing time file or create a new one. We will use the equidistant option and the 'Time Interval' of '1' which means that the measurements will be taken one second apart.

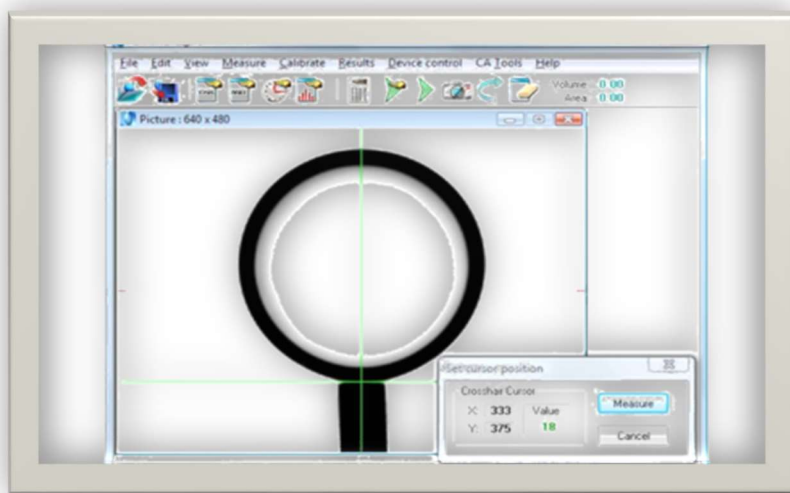
15. Click on 'Next'.



A 6 Information Display Showing Final Step in Setting the New Experiment

At this point, the DROP image has created a parameter and method file for your experiment. Click on 'Yes, to run it.

Now you will need to dispense your test liquid in order to produce a drop similar to the one shown on the next screen. As a rule of thumb, you want to use enough volume to produce a drop that is stable and not so large that it releases itself from the needle. As the interfacial tension decreases, so too will the drop volume.

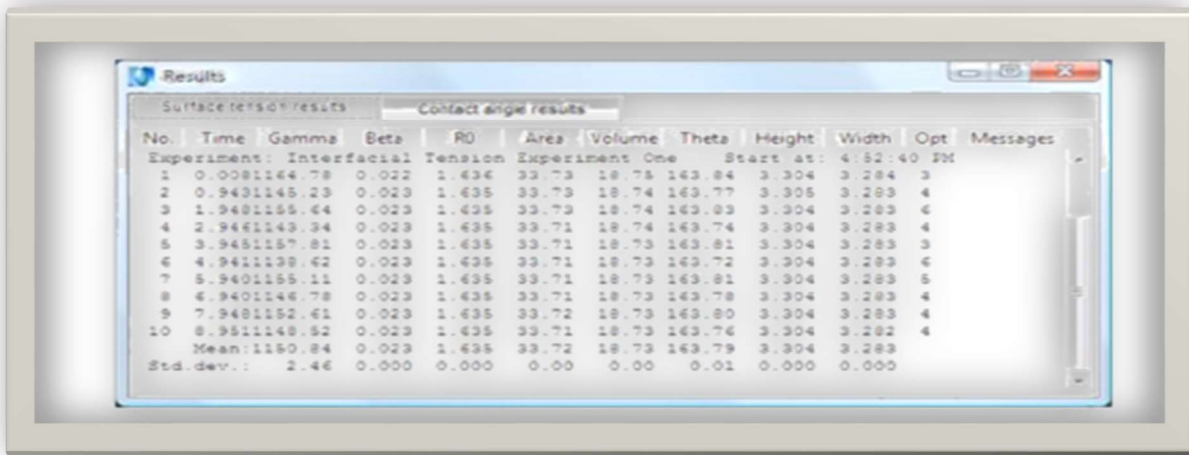


A 7 Drop Film Showing the Crosshair Lines

With the drop created, be sure that your lighting is set properly. The background should be white, while the needle and perimeter of the drop should be black. The interface between the drop and the external phase should be crisp. If not, refocus, and take a new picture.

Place the crosshairs so that the horizontal line passes through the interface between the needle and the drop, and so that the vertical line passes through the centre of the drop and needle as shown above.

When you are ready, click on 'Measure' on the 'Set cursor position' dialogue box. The experiment will now begin.



A 8 IFT/Surface Tension Results Window

The 'Results' window will now appear, if it is not already on your desktop, and it will look similar to the one shown above.

Appendix B

Pendant Drop Method Results

All results from the pendant drop method are usually used to measure the surface tension of a combination of Gum Arabic and silica at different concentrations, pressures and temperatures. The results of surface tension and interfacial tension are the same. Here is some information on each column:

- No: Run number 1,2,3.....
- Time: Precise time in seconds of measurement relative to the start of the current run.
- Gamma: Surface or interfacial tension in N/m.
- Beta: Shape factor - as a rule, a number between 0.2 and 0.4 is good.
- Ro: The radius of curvature at the drops apex in mm.
- Area: The drop surface in mm^2 .
- Volume: The drop volume in mm^3 .
- Theta: The contact angle at the drop limit (horizontal) baseline.
- Height: The total measured distance from baseline to the drop apex in mm.
- Width: The dimension in mm at the maximum width.
- Opt: The number of optimisations performed.

Messages: Errors or Their Messages

0.5 silica and 0.5 Gum Arabic in 500ml at 30°C temperature

Date: 5/21/2019 Remarks : Comments here

Experiment : 088_12 Method : 088.met

Drop phase : Heavy Oil Density : 0.9000

Extern.phase : Brine (15%) Density : 1.0068

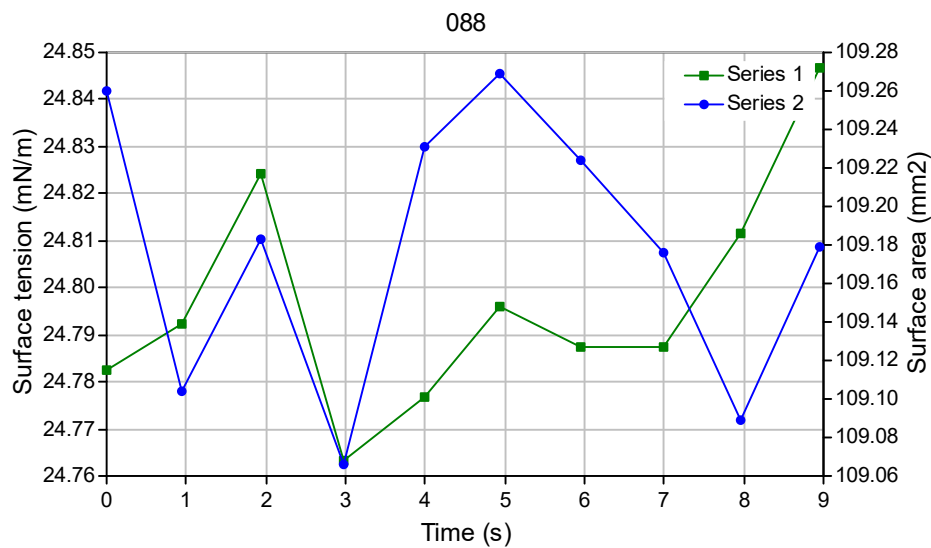
Solid phase : Steel Calculation : Optimized cont.

No.	Time	Gamma	Beta	R0	Area	Volume	Theta	Height	Width	Opt	Messages
-----	------	-------	------	----	------	--------	-------	--------	-------	-----	----------

1	0.0	25.42	0.281	2.612	108.26	106.78	115.24	6.860	5.515	2
2	0.9	25.07	0.284	2.607	108.29	106.67	115.06	6.856	5.519	2
3	2.0	25.12	0.283	2.606	107.64	106.44	115.04	6.852	5.507	2
4	2.9	24.94	0.285	2.603	107.56	106.36	114.61	6.859	5.505	2
5	3.9	25.37	0.281	2.607	107.51	106.06	114.99	6.857	5.519	2
6	5.0	25.44	0.280	2.608	107.90	106.29	114.96	6.859	5.508	2
7	6.0	25.34	0.281	2.608	108.83	106.06	114.82	6.864	5.518	2
8	7.0	25.77	0.278	2.614	108.85	106.37	115.02	6.871	5.511	2
9	7.9	25.88	0.277	2.615	108.20	106.37	115.28	6.863	5.522	2
10	9.0	25.87	0.277	2.615	108.00	106.42	115.36	6.857	5.534	2

Mean: 25.42 0.281 2.610 108.10 106.38 115.04 6.860 5.516

Stand.dev.: 0.11 0.001 0.001 0.15 0.07 0.07 0.002 0.003



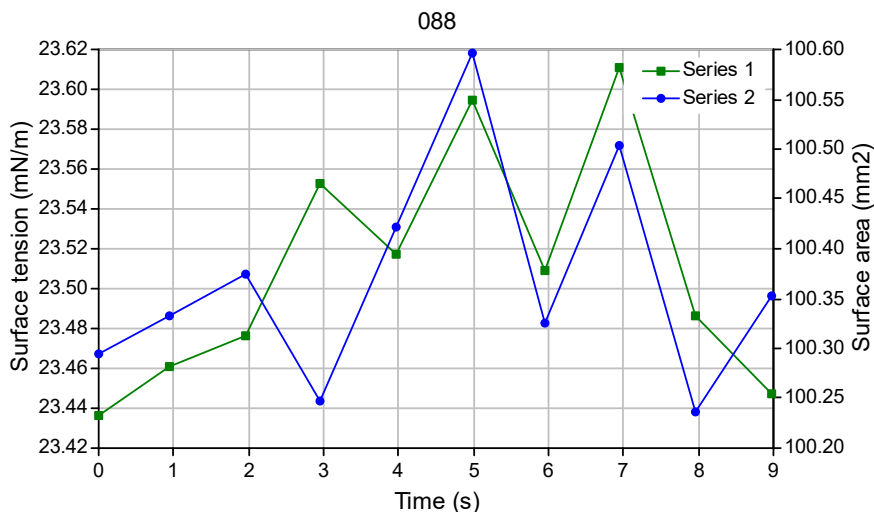
Date : 5/21/2019 Remarks : Comments here
 Experiment : 088_40 Method : 088.met
 Drop phase : Heavy Oil Density : 0.9000
 Extern.phase : Brine (15%) Density : 0.9990
 Solid phase : Steel Calculation : Optimised cont.

No.	Time	Gamma	Beta	R0	Area	Volume	Theta	Height	Width	Opt
-----	------	-------	------	----	------	--------	-------	--------	-------	-----

1	0.0	23.44	0.265	2.530	100.29	94.95	113.67	6.694	5.314	2
2	0.9	23.46	0.265	2.531	100.33	94.93	113.78	6.695	5.314	2
3	2.0	23.48	0.265	2.531	100.38	95.01	113.73	6.695	5.314	2
4	2.9	23.55	0.264	2.532	100.25	95.04	113.79	6.696	5.321	2
5	4.0	23.52	0.265	2.532	100.42	95.11	113.76	6.698	5.322	2
6	5.0	23.59	0.264	2.534	100.60	95.13	113.81	6.700	5.325	2
7	5.9	23.51	0.265	2.532	100.32	95.04	113.92	6.694	5.322	2
8	6.9	23.61	0.264	2.534	100.50	95.21	113.93	6.695	5.326	2
9	8.0	23.49	0.265	2.531	100.24	95.02	113.72	6.697	5.315	2
10	9.0	23.45	0.265	2.530	100.35	94.92	113.58	6.702	5.314	2

Mean: 23.51 0.265 2.532 100.37 95.04 113.77 6.697 5.319

Stand.dev.: 0.02 0.000 0.000 0.04 0.03 0.03 0.001 0.002



At 70°C

Date : 5/21/2019 Remarks : Comments here

Experiment : 088_51 Method : 088.met

Drop phase : Heavy Oil Density : 0.9000

Extern.phase : Brine (15%) Density : 0.9896

Solid phase : Steel Calculation : Optimized cont.

No.	Time	Gamma	Beta	R0	Area	Volume	Theta	Height	Width	Opt
-----	------	-------	------	----	------	--------	-------	--------	-------	-----

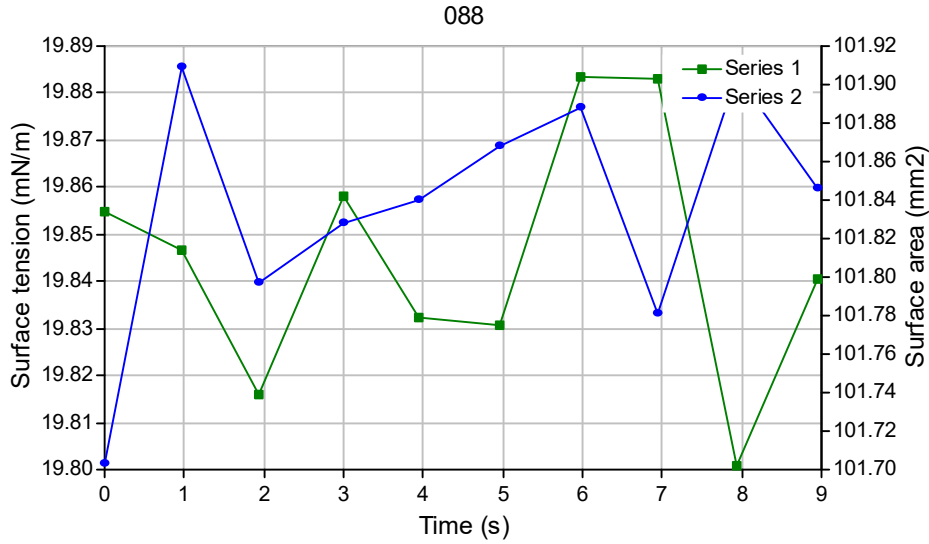
Messages

1	0.0	19.89	0.278	2.510	101.68	95.46	103.05	7.002	5.285	2
2	0.9	19.96	0.278	2.512	101.80	95.72	102.83	7.012	5.289	2
3	2.0	19.92	0.278	2.511	101.75	95.58	102.94	7.009	5.290	2
4	2.9	19.93	0.278	2.512	101.75	95.63	102.86	7.012	5.290	2
5	4.0	19.91	0.278	2.511	101.77	95.55	102.63	7.016	5.290	2
6	5.0	19.90	0.278	2.511	101.72	95.55	102.88	7.010	5.293	2
7	5.9	19.89	0.278	2.510	101.69	95.56	102.87	7.009	5.289	2
8	7.0	19.91	0.278	2.512	101.93	95.72	102.68	7.019	5.289	2
9	8.0	19.91	0.278	2.511	101.75	95.68	102.74	7.014	5.290	2

10 9.0 19.91 0.279 2.512 101.96 95.83 102.49 7.026 5.292 2

Mean: 19.91 0.278 2.511 101.78 95.63 102.80 7.013 5.290

Stand.dev.: 0.01 0.000 0.000 0.03 0.03 0.05 0.002 0.001



At 90°C

Date : 5/21/2019 Remarks : Comments here
 Experiment : 088_62 Method : 088.met
 Drop phase : Heavy Oil Density : 0.9000
 Extern.phase : Brine (15%) Density : 0.9896
 Solid phase : Steel Calculation : Optimized cont.

No.	Time	Gamma	Beta	R0	Area	Volume	Theta	Height	Width	Opt
-----	------	-------	------	----	------	--------	-------	--------	-------	-----

Messages

1	0.0	13.47	0.225	1.858	51.67	35.15	119.13	4.731	3.867	2
2	0.9	13.50	0.225	1.858	51.72	35.16	119.37	4.728	3.873	2
3	2.0	13.42	0.226	1.857	51.72	35.14	119.07	4.730	3.872	2
4	2.9	13.37	0.227	1.857	51.74	35.20	118.99	4.731	3.873	2
5	4.0	13.45	0.225	1.858	51.66	35.13	119.22	4.729	3.874	2
6	5.0	13.43	0.226	1.858	51.65	35.16	119.40	4.727	3.876	2

7	6.0	13.40	0.226	1.856	51.70	35.13	118.95	4.731	3.870	2
8	6.9	13.32	0.227	1.855	51.63	35.10	118.98	4.732	3.864	2
9	8.0	13.40	0.226	1.858	51.72	35.20	118.94	4.737	3.870	2
10	9.0	13.44	0.226	1.858	51.66	35.16	119.34	4.727	3.874	2

=====
Mean: 13.42 0.226 1.857 51.69 35.15 119.14 4.730 3.871

Stand.dev.: 0.02 0.000 0.000 0.01 0.01 0.06 0.001 0.001
=====

At 100°C

Date : 5/21/2019 Remarks : Comments here

Experiment : 088_75 Method : 088.met

Drop phase : Heavy Oil Density : 0.9000

Extern.phase : Brine (15%) Density : 0.9820

Solid phase : Steel Calculation : Optimized cont.

No.	Time	Gamma	Beta	R0	Area	Volume	Theta	Height	Width	Opt
-----	------	-------	------	----	------	--------	-------	--------	-------	-----

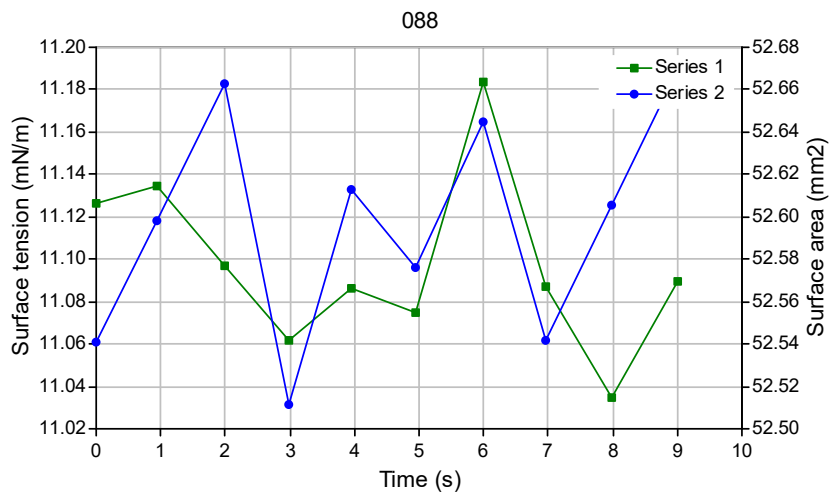
Messages

1	0.0	11.13	0.244	1.838	52.54	35.25	105.02	4.969	3.846	2
2	0.9	11.13	0.245	1.840	52.60	35.39	105.23	4.973	3.846	2
3	2.0	11.10	0.245	1.840	52.66	35.42	105.17	4.977	3.844	2
4	3.0	11.06	0.246	1.839	52.51	35.35	105.38	4.973	3.841	2
5	3.9	11.09	0.246	1.839	52.61	35.36	105.46	4.973	3.842	2
6	4.9	11.08	0.246	1.839	52.58	35.33	104.99	4.978	3.846	2
7	6.0	11.18	0.244	1.841	52.65	35.42	105.47	4.969	3.852	2

8	7.0	11.09	0.245	1.839	52.54	35.35	105.26	4.973	3.841	2
9	8.0	11.03	0.246	1.837	52.61	35.28	104.58	4.980	3.839	2
10	9.0	11.09	0.245	1.839	52.67	35.39	104.70	4.983	3.847	2

Mean: 11.10 0.245 1.839 52.60 35.36 105.13 4.975 3.844

Stand.dev.: 0.01 0.000 0.000 0.02 0.02 0.10 0.001 0.001



Silica 1 g in 500ml at room temperature and pressure 1094 psig

Date : 5/23/2019 Remarks : Comments here
 Experiment : 022_29 Method : 022.met
 Drop phase : Heavy Oil Density : 0.9000
 Extern.phase : Brine (15%) Density : 1.0083
 Solid phase : Steel Calculation : Optimized cont.

No.	Time	Gamma	Beta	R0	Area	Volume	Theta	Height	Width	Opt
-----	------	-------	------	----	------	--------	-------	--------	-------	-----

Messages

1	0.0	0.00	0.000	0.000	0.00	0.00	0.00	0.000	0.000	0	Sides are too differ
2	0.9	0.00	0.000	0.000	0.00	0.00	0.00	0.000	0.000	0	Sides are too differ
3	1.9	15.86	0.245	1.913	56.25	39.25	126.09	4.650	4.025	2	
4	3.0	15.90	0.245	1.913	55.85	39.21	126.13	4.651	4.037	3	
5	4.0	12.43	0.301	1.877	54.76	39.57	119.06	4.656	4.039	3	
6	4.9	15.95	0.244	1.914	56.03	39.22	126.14	4.651	4.027	3	
7	6.0	15.84	0.246	1.914	56.05	39.31	126.07	4.651	4.025	2	
8	7.0	15.93	0.244	1.914	56.24	39.20	126.16	4.649	4.033	3	
9	8.0	16.17	0.241	1.914	55.86	39.22	126.60	4.636	4.034	3	
10	9.0	12.08	0.308	1.872	54.16	39.35	118.23	4.650	4.033	4	

Mean: 15.02 0.259 1.904 55.65 39.29 124.31 4.649 4.031

Stand.dev.: 0.61 0.010 0.006 0.27 0.04 1.24 0.002 0.002

At 2000 psig

Date : 5/23/2019 Remarks : Comments here

Experiment : 022_33 Method : 022.met

Drop phase : Heavy Oil Density : 0.9000

Extern.phase : Brine (15%) Density : 1.0083

Solid phase : Steel Calculation : Optimized cont.

No.	Time	Gamma	Beta	R0	Area	Volume	Theta	Height	Width	Opt
-----	------	-------	------	----	------	--------	-------	--------	-------	-----

Messages

1	0.0	16.88	0.223	1.884	51.90	36.27	130.13	4.442	3.962	3
2	0.9	16.78	0.225	1.883	52.08	36.21	129.99	4.442	3.953	3
3	2.0	0.00	0.000	0.000	0.00	0.00	0.000	0.000	0	Drop is distorted
4	3.0	0.00	0.000	0.000	0.00	0.00	0.000	0.000	0	Error in profile
5	4.0	16.98	0.223	1.887	52.80	36.38	130.24	4.443	3.981	3
6	5.0	16.99	0.222	1.886	53.34	36.26	130.31	4.441	3.980	3
7	6.0	17.35	0.219	1.890	53.43	36.37	130.82	4.440	4.055	3
8	7.0	16.80	0.225	1.884	52.44	36.27	130.03	4.440	3.963	3
9	8.0	16.69	0.226	1.882	51.97	36.20	129.88	4.441	3.955	3
10	9.0	16.82	0.224	1.883	51.76	36.18	130.04	4.440	3.945	2

Mean: 16.91 0.223 1.885 52.46 36.27 130.18 4.441 3.974

Stand.dev.: 0.07 0.001 0.001 0.23 0.03 0.10 0.000 0.012

At 3000 psig

No. Time Gamma Beta R0 Area VolumeTheta Height Width Opt Messages

1	0.0	15.28	0.234	1.834	51.37	34.26	124.25	4.556	3.876	3
2	0.9	15.53	0.231	1.837	51.29	34.25	124.79	4.551	3.872	3
3	2.0	15.51	0.231	1.837	51.38	34.28	124.71	4.551	3.877	3
4	3.0	15.54	0.231	1.837	51.33	34.35	124.67	4.553	3.876	3
5	3.9	15.68	0.229	1.839	52.05	34.23	125.24	4.545	3.868	3
6	5.0	15.37	0.233	1.837	53.05	34.30	124.45	4.562	3.875	3
7	6.0	15.38	0.233	1.836	51.78	34.32	124.42	4.560	3.870	3
8	6.9	15.42	0.232	1.836	51.13	34.32	124.49	4.561	3.874	3
9	8.0	15.30	0.234	1.836	51.77	34.37	124.42	4.559	3.872	3
10	8.9	15.20	0.236	1.836	51.81	34.33	124.11	4.567	3.871	3

Mean: 15.42 0.232 1.836 51.70 34.30 124.55 4.556 3.873

Stand.dev.: 0.05 0.001 0.000 0.18 0.01 0.10 0.002 0.001

At 4000 psig

Date : 5/23/2019 Remarks : Comments here

Experiment : 022_38 Method : 022.met

Drop phase : Heavy Oil Density : 0.9000

Extern.phase : Brine (15%) Density : 1.0083

Solid phase : Steel Calculation : Optimized cont.

No.	Time	Gamma	Beta	R0	Area	Volume	Theta	Height	Width	Opt	Messages
1		0.0	15.18	0.232	1.820	50.50	33.37	124.41	4.517	3.845	3
2		0.9	15.17	0.232	1.820	50.34	33.34	124.48	4.518	3.859	3
3		1.9	15.17	0.232	1.819	50.22	33.33	124.56	4.516	3.851	3
4		3.0	15.07	0.233	1.819	50.80	33.46	123.99	4.521	3.854	3
5		4.0	15.08	0.233	1.819	50.47	33.48	123.99	4.522	3.844	3
6		4.9	15.12	0.233	1.819	50.43	33.36	124.24	4.522	3.854	3
7		6.0	14.88	0.235	1.816	50.72	33.35	124.02	4.523	3.853	3
8		6.9	15.09	0.233	1.820	50.40	33.38	124.28	4.523	3.847	3
9		8.0	15.01	0.234	1.817	50.96	33.40	124.11	4.518	3.848	3
10		8.9	15.12	0.233	1.819	50.69	33.36	124.47	4.517	3.853	3

Mean: 15.09 0.233 1.819 50.55 33.38 124.26 4.520 3.851

Stand.dev.: 0.03 0.000 0.000 0.07 0.02 0.07 0.001 0.001

at 5000psig

Date : 5/23/2019 Remarks : Comments here

Experiment : 022_41 Method : 022.met

Drop phase : Heavy Oil Density : 0.9000

Extern.phase : Brine (15%) Density : 1.0083

Solid phase : Steel Calculation : Optimized cont.

No.	Time	Gamma	Beta	R0	Area	Volume	Theta	Height	Width	Opt	Messages
-----	------	-------	------	----	------	--------	-------	--------	-------	-----	----------

1	0.0	14.51	0.232	1.780	48.30	31.12	127.72	4.296	3.756	3	
2	0.9	14.68	0.230	1.782	48.44	31.15	128.08	4.294	3.752	3	
3	2.0	0.00	0.000	0.000	0.00	0.00	0.000	0.000	0	0	Error in profile
4	3.0	14.51	0.232	1.781	48.13	31.20	127.48	4.304	3.757	3	
5	3.9	14.69	0.230	1.782	47.81	31.19	127.97	4.295	3.757	3	
6	4.9	14.60	0.231	1.783	48.13	31.18	127.72	4.304	3.753	3	
7	6.0	14.62	0.231	1.784	47.78	31.30	127.68	4.305	3.754	3	
8	7.0	14.59	0.231	1.782	48.06	31.15	127.75	4.301	3.756	3	
9	8.0	14.71	0.229	1.782	47.99	31.23	128.05	4.292	3.761	3	
10	9.0	14.80	0.228	1.783	47.83	31.22	128.24	4.289	3.755	3	

Mean: 14.63 0.231 1.782 48.05 31.20 127.85 4.298 3.756

Stand.dev.: 0.03 0.000 0.000 0.08 0.02 0.08 0.002 0.001

At 6000psig

Date : 5/23/2019 Remarks : Comments here

Experiment : 022_45 Method : 022.met

Drop phase : Heavy Oil Density : 0.9000

Extern.phase : Brine (15%) Density : 1.0083

Solid phase : Steel Calculation : Optimized cont.

No.	Time	Gamma	Beta	R0	Area	Volume	Theta	Height	Width	Opt	Messages
-----	------	-------	------	----	------	--------	-------	--------	-------	-----	----------

1	0.0	0.00	0.000	0.000	0.00	0.00	0.00	0.000	0.000	0	Sides are too differ
2	0.9	14.39	0.231	1.769	47.64	30.71	125.43	4.365	3.741	3	
3	2.0	14.42	0.231	1.771	48.57	30.79	125.42	4.370	3.740	3	
4	3.0	14.45	0.230	1.770	47.89	30.85	125.51	4.367	3.743	3	
5	4.0	14.39	0.231	1.770	47.78	30.79	125.22	4.366	3.736	3	
6	4.9	14.52	0.229	1.771	47.96	30.77	125.37	4.368	3.746	3	
7	6.0	14.53	0.230	1.772	48.05	30.79	125.62	4.368	3.747	3	
8	7.0	14.54	0.230	1.772	47.86	30.83	125.62	4.366	3.745	3	
9	8.0	14.66	0.228	1.775	47.94	30.89	125.79	4.366	3.752	3	
10	9.0	14.51	0.230	1.772	48.09	30.86	125.51	4.368	3.747	3	

Mean: 14.49 0.230 1.771 47.98 30.81 125.50 4.367 3.744

Stand.dev.: 0.03 0.000 0.001 0.09 0.02 0.06 0.000 0.002

Gum 0.5g silica 1.5g 500ml at 30°C

Date : 5/22/2019 Remarks : Comments here

Experiment : 025_21 Method : 025.met

Drop phase : Heavy Oil Density : 0.9000

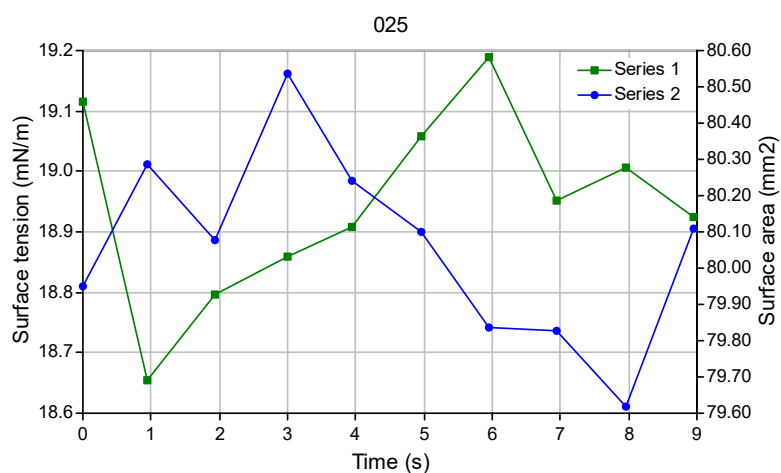
Extern.phase : Brine (15%) Density : 1.0068

Solid phase : Steel Calculation : Optimized cont.

No.	Time	Gamma	Beta	R0	Area	Volume	Theta	Height	Width	Opt
										Messages
1	0.0	18.56	0.290	2.267	80.45	69.91	119.07	5.729	4.815	2
2	0.9	18.74	0.288	2.270	81.51	70.19	119.35	5.728	4.827	3
3	2.0	18.91	0.286	2.273	80.65	70.23	119.65	5.724	4.815	2
4	3.0	18.62	0.289	2.268	80.79	70.20	119.13	5.728	4.817	3
5	4.0	0.00	0.000	0.000	0.00	0.00	0.000	0.000	0	Sides are too differ
6	4.9	18.79	0.287	2.271	81.05	70.09	119.48	5.727	4.816	2
7	6.0	18.44	0.291	2.263	80.75	69.75	118.96	5.720	4.807	2
8	7.0	18.57	0.290	2.267	80.68	70.23	119.00	5.727	4.815	2
9	8.0	18.70	0.288	2.267	80.62	69.98	119.29	5.718	4.811	3
10	9.0	18.45	0.291	2.265	80.58	69.93	118.87	5.727	4.803	2

Mean: 18.64 0.289 2.268 80.79 70.06 119.20 5.725 4.814

Stand.dev.: 0.05 0.001 0.001 0.11 0.06 0.09 0.001 0.002



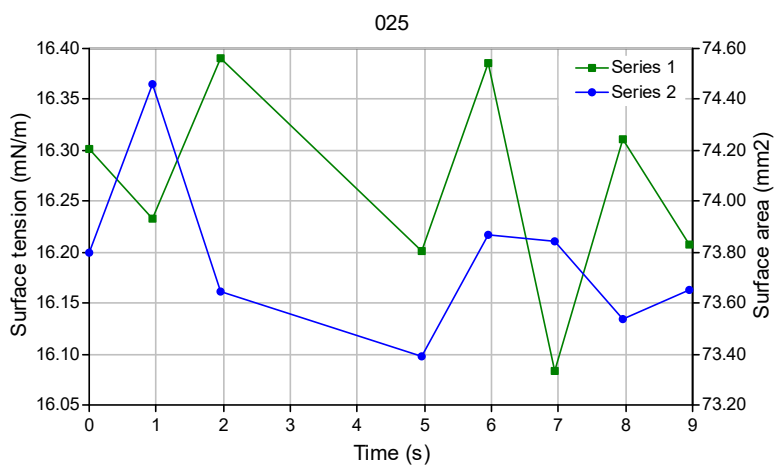
At 50°C

Date : 5/22/2019 Remarks : Comments here
 Experiment : 025_32 Method : 025.met
 Drop phase : Heavy Oil Density : 0.9000
 Extern.phase : Brine (15%) Density : 0.9990
 Solid phase : Steel Calculation : Optimized cont.

No.	Time	Gamma	Beta	R0	Area	Volume	Theta	Height	Width	Opt	Messages
1	0.0	16.07	0.281	2.157	75.04	60.21	115.15	5.669	4.574	2	
2	0.9	16.21	0.279	2.159	74.24	60.33	115.36	5.667	4.577	3	
3	2.0	0.00	0.000	0.000	0.00	0.00	0.000	0.000	0		Error in profile
4	3.0	0.00	0.000	0.000	0.00	0.00	0.000	0.000	0		Error in profile
5	3.9	16.13	0.280	2.156	73.99	60.12	115.20	5.662	4.557	2	
6	5.0	16.13	0.280	2.157	74.51	60.17	115.28	5.670	4.556	2	
7	6.0	16.01	0.282	2.154	73.95	60.13	114.90	5.670	4.561	2	
8	6.9	16.10	0.280	2.156	74.66	60.24	115.42	5.661	4.561	2	
9	8.0	16.12	0.281	2.158	74.21	60.35	115.42	5.666	4.566	2	
10	9.0	16.32	0.278	2.163	74.90	60.36	115.43	5.676	4.577	2	

Mean: 16.13 0.280 2.157 74.44 60.24 115.27 5.668 4.566

Stand.dev.: 0.03 0.000 0.001 0.14 0.03 0.06 0.002 0.003



At 70°C

Drop Shape Image Analysis

Date : 5/22/2019 Remarks : Comments here

Experiment : 025_41 Method : 025.met

Drop phase : Heavy Oil Density : 0.9000

Extern.phase : Brine (15%) Density : 0.9896

Solid phase : Steel Calculation : Optimized cont.

No.	Time	Gamma	Beta	R0	Area	Volume	Theta	Height	Width	Opt
-----	------	-------	------	----	------	--------	-------	--------	-------	-----

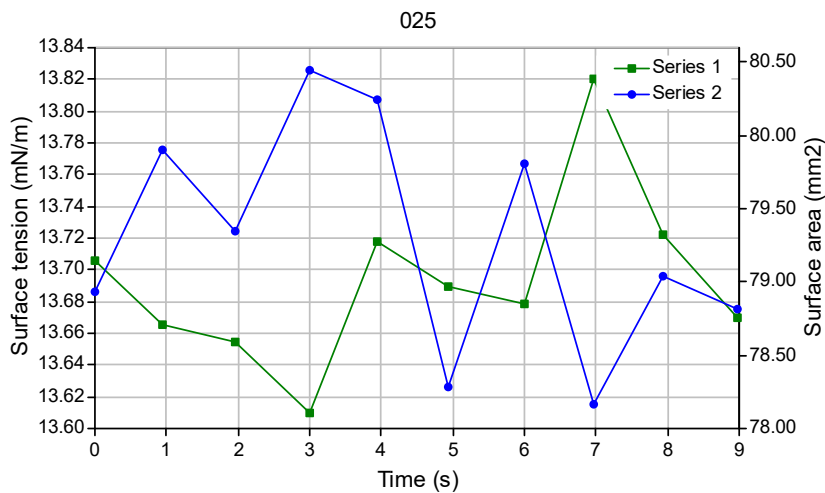
Messages

1	0.0	13.53	0.291	2.118	78.71	58.98	97.07	6.108	4.553	3
2	0.9	13.47	0.292	2.115	79.90	58.74	96.94	6.103	4.571	3
3	2.0	13.57	0.291	2.119	78.72	58.92	96.94	6.110	4.561	3
4	3.0	13.30	0.294	2.109	80.05	58.54	96.59	6.105	4.556	3

5	3.9	13.42	0.292	2.112	77.66	58.53	96.59	6.104	4.559	3
6	4.9	13.39	0.292	2.110	79.08	58.43	96.52	6.101	4.554	3
7	6.0	13.46	0.292	2.113	77.93	58.56	96.63	6.103	4.556	3
8	6.9	13.39	0.293	2.111	77.57	58.50	96.52	6.105	4.556	3
9	8.0	13.38	0.293	2.111	77.77	58.48	96.77	6.100	4.548	3
10	9.0	13.35	0.293	2.110	76.60	58.46	96.47	6.103	4.555	3

Mean: 13.43 0.292 2.113 78.40 58.62 96.70 6.104 4.557

Stand.dev.: 0.03 0.000 0.001 0.35 0.06 0.07 0.001 0.002



At 90°C

Date : 5/22/2019 Remarks : Comments here

Experiment : 025_62 Method : 025.met

Drop phase : Heavy Oil Density : 0.9000

Extern.phase : Brine (15%) Density : 0.9896

Solid phase : Steel Calculation : Optimized cont.

No.	Time	Gamma	Beta	R0	Area	Volume	Theta	Height	Width	Opt
-----	------	-------	------	----	------	--------	-------	--------	-------	-----

Messages

1	0.0	10.82	0.300	1.922	60.04	44.09	108.28	5.278	4.068	2
2	0.9	10.82	0.300	1.923	60.16	44.19	108.25	5.281	4.075	2
3	1.9	10.83	0.300	1.922	60.15	44.18	108.32	5.275	4.074	2
4	3.0	10.84	0.300	1.923	60.12	44.15	108.33	5.277	4.081	2
5	3.9	10.85	0.300	1.923	60.06	44.11	108.39	5.277	4.078	2
6	5.0	10.84	0.300	1.923	60.11	44.13	108.34	5.279	4.076	2
7	6.0	10.83	0.300	1.923	60.15	44.20	108.23	5.281	4.070	2
8	7.0	10.83	0.300	1.923	60.12	44.17	108.38	5.279	4.078	2
9	7.9	10.84	0.300	1.923	60.38	44.15	108.17	5.283	4.081	2
10	9.0	10.79	0.301	1.922	60.09	44.13	108.13	5.283	4.065	2

Mean: 10.83 0.300 1.923 60.14 44.15 108.28 5.279 4.075

Stand.dev.: 0.01 0.000 0.000 0.03 0.01 0.03 0.001 0.002

At 100°C

Date : 5/22/2019 Remarks : Comments here

Experiment : 025_113 Method : 025.met

Drop phase : Heavy Oil Density : 0.9000

Extern.phase : Brine (15%) Density : 0.9820

Solid phase : Steel Calculation : Optimized cont.

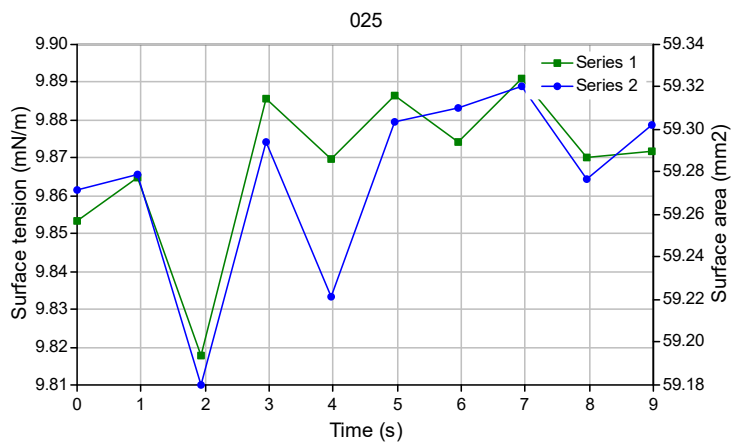
No.	Time	Gamma	Beta	R0	Area	Volume	Theta	Height	Width	Opt
-----	------	-------	------	----	------	--------	-------	--------	-------	-----

Messages

1	0.0	9.87	0.293	1.897	59.07	42.14	101.55	5.370	4.002	3
2	0.9	9.86	0.293	1.896	59.04	42.13	101.41	5.373	4.010	2
3	2.0	9.89	0.292	1.896	59.02	42.09	101.51	5.367	4.010	2
4	2.9	9.90	0.293	1.898	59.05	42.18	101.70	5.367	4.010	3
5	3.9	9.87	0.293	1.896	59.03	42.13	101.34	5.374	4.007	3
6	5.0	9.87	0.293	1.896	59.05	42.11	101.35	5.375	4.008	3
7	6.0	9.87	0.293	1.896	59.08	42.13	101.29	5.375	4.002	3
8	6.9	9.87	0.293	1.896	59.07	42.11	101.09	5.379	4.003	3
9	8.0	9.87	0.293	1.897	59.09	42.13	101.13	5.381	4.008	3
10	9.0	9.88	0.293	1.896	59.03	42.10	101.36	5.371	4.010	2

Mean: 9.87 0.293 1.896 59.05 42.13 101.37 5.373 4.007

Stand.dev.: 0.00 0.000 0.000 0.01 0.01 0.06 0.001 0.001



Gum arabic 3 and Silics 1.5 in 500ml at 30°C

Date : 5/28/2019 Remarks : Comments here

Experiment : 0001_4 Method : 0001.met

Drop phase : Heavy Oil Density : 0.9000

Extern.phase : Brine (15%) Density : 1.0068

Solid phase : Steel Calculation : Optimized cont.

No.	Time	Gamma	Beta	R0	Area	Volume	Theta	Height	Width	Opt	Messages
-----	------	-------	------	----	------	--------	-------	--------	-------	-----	----------

1	0.0	19.72	0.347	2.556	105.86	107.74	112.48	6.569	5.464	3	
---	-----	-------	-------	-------	--------	--------	--------	-------	-------	---	--

2	0.9	19.71	0.347	2.556	105.87	107.84	112.43	6.563	5.488	2	
---	-----	-------	-------	-------	--------	--------	--------	-------	-------	---	--

3	2.0	19.67	0.348	2.555	105.00	107.55	112.37	6.568	5.488	2	
---	-----	-------	-------	-------	--------	--------	--------	-------	-------	---	--

4	3.0	17.46	0.381	2.520	109.27	110.09	108.10	6.575	5.495	3	
---	-----	-------	-------	-------	--------	--------	--------	-------	-------	---	--

5	4.0	19.75	0.347	2.557	108.12	107.52	112.58	6.569	5.476	2	
---	-----	-------	-------	-------	--------	--------	--------	-------	-------	---	--

6	4.9	19.75	0.347	2.556	106.82	107.83	112.55	6.563	5.479	2	
---	-----	-------	-------	-------	--------	--------	--------	-------	-------	---	--

7	5.9	0.00	0.000	0.000	0.00	0.00	0.00	0.000	0.000	0	Error in profile
---	-----	------	-------	-------	------	------	------	-------	-------	---	------------------

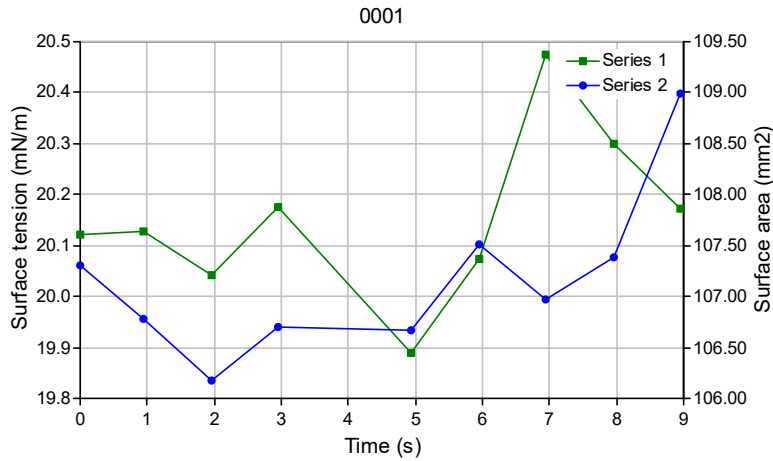
8	7.0	19.77	0.347	2.558	105.11	107.61	112.40	6.573	5.492	2	
---	-----	-------	-------	-------	--------	--------	--------	-------	-------	---	--

9	7.9	19.96	0.345	2.562	108.23	108.10	112.99	6.560	5.487	2	
---	-----	-------	-------	-------	--------	--------	--------	-------	-------	---	--

10	9.0	19.89	0.346	2.562	105.76	107.70	112.56	6.581	5.500	2	
----	-----	-------	-------	-------	--------	--------	--------	-------	-------	---	--

Mean: 19.52 0.350 2.554 106.67 108.00 112.05 6.569 5.485

Stand.dev.: 0.26 0.004 0.004 0.51 0.27 0.50 0.002 0.004



At 50°C

Date : 5/28/2019 Remarks : Comments here

Experiment : 0001_16 Method : 0001.met

Drop phase : Heavy Oil Density : 0.9000

Extern.phase : Brine (15%) Density : 0.9990

Solid phase : Steel Calculation : Optimized cont.

No.	Time	Gamma	Beta	R0	Area	Volume	Theta	Height	Width	Opt	Messages
-----	------	-------	------	----	------	--------	-------	--------	-------	-----	----------

1	0.0	18.12	0.336	2.502	105.07	102.29	106.57	6.928	5.338	2	
---	-----	-------	-------	-------	--------	--------	--------	-------	-------	---	--

2	0.9	18.04	0.337	2.502	105.14	102.68	106.28	6.934	5.342	2	
---	-----	-------	-------	-------	--------	--------	--------	-------	-------	---	--

3	1.9	18.09	0.336	2.502	104.56	102.05	106.49	6.929	5.323	3	
---	-----	-------	-------	-------	--------	--------	--------	-------	-------	---	--

4	3.0	18.10	0.336	2.501	105.47	101.95	106.61	6.921	5.340	2	
---	-----	-------	-------	-------	--------	--------	--------	-------	-------	---	--

5	4.0	17.97	0.337	2.497	104.98	101.61	106.34	6.922	5.338	3	
---	-----	-------	-------	-------	--------	--------	--------	-------	-------	---	--

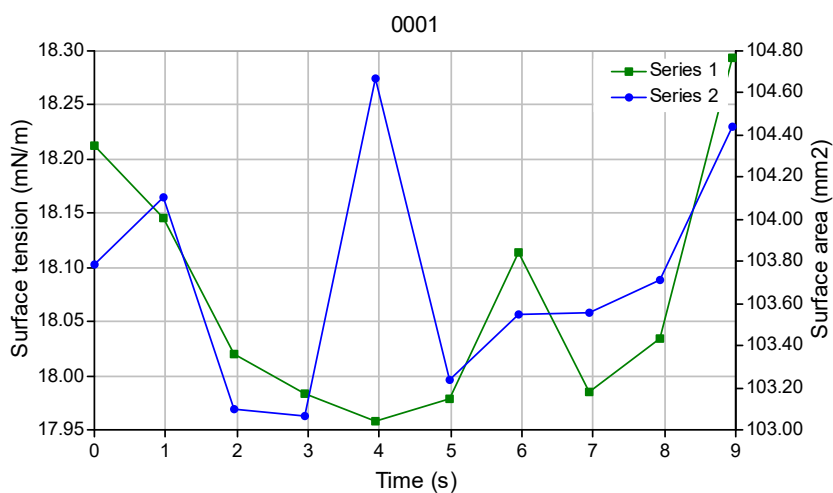
6	5.0	0.00	0.000	0.000	0.00	0.00	0.000	0.000	0		Error in profile
---	-----	------	-------	-------	------	------	-------	-------	---	--	------------------

7	6.0	18.06	0.336	2.500	105.23	101.86	106.37	6.926	5.344	2	
---	-----	-------	-------	-------	--------	--------	--------	-------	-------	---	--

8	7.0	18.01	0.337	2.499	104.95	102.12	106.24	6.928	5.319	3
9	8.0	17.96	0.337	2.498	105.47	101.79	106.32	6.925	5.320	3
10	8.9	18.17	0.335	2.504	105.16	102.27	106.70	6.921	5.329	3

Mean: 18.06 0.336 2.500 105.11 102.07 106.44 6.926 5.333

Stand.dev.: 0.02 0.000 0.001 0.09 0.11 0.05 0.001 0.003



At 70°C

Date : 5/28/2019 Remarks : Comments here

Experiment : 0001_40 Method : 0001.met

Drop phase : Heavy Oil Density : 0.9000

Extern.phase : Brine (15%) Density : 0.9896

Solid phase : Steel Calculation : Optimized cont.

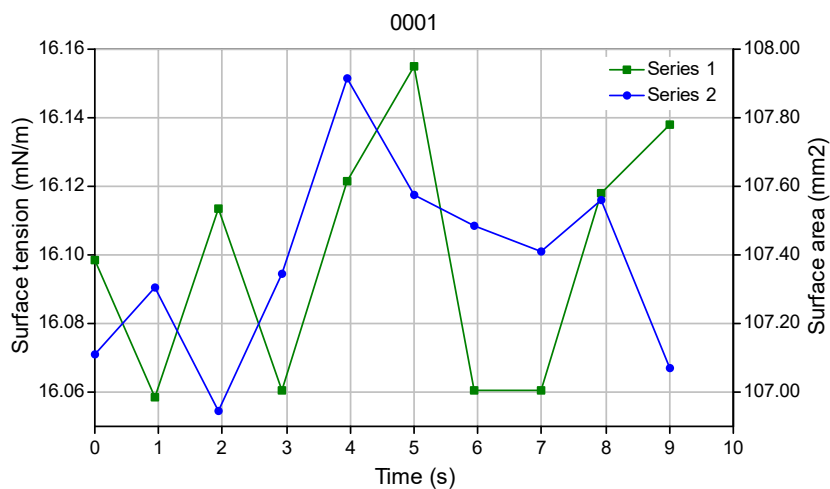
No.	Time	Gamma	Beta	R0	Area	Volume	Theta	Height	Width	Opt
-----	------	-------	------	----	------	--------	-------	--------	-------	-----

Messages

1	0.0	16.21	0.333	2.478	108.27	101.49	92.75	7.469	5.270	3
2	1.0	16.21	0.333	2.479	107.96	101.51	92.62	7.477	5.252	3
3	2.0	16.12	0.334	2.475	107.48	101.33	92.34	7.478	5.241	3
4	3.0	16.19	0.333	2.476	107.73	101.31	92.61	7.464	5.249	3
5	4.0	16.23	0.333	2.479	107.61	101.30	92.88	7.467	5.258	3
6	5.0	16.23	0.333	2.479	108.05	101.70	92.66	7.477	5.269	3
7	5.9	0.00	0.000	0.000	0.00	0.00	0.000	0.000	0	Sides are too differ
8	7.0	16.20	0.333	2.477	107.75	101.33	92.37	7.480	5.245	3
9	8.0	16.17	0.333	2.476	107.34	101.25	92.35	7.473	5.257	3
10	8.9	16.10	0.334	2.474	107.58	101.21	92.19	7.482	5.241	3

Mean: 16.18 0.333 2.477 107.75 101.38 92.53 7.474 5.254

Stand.dev.: 0.02 0.000 0.001 0.10 0.05 0.08 0.002 0.004



At 90°C

Date : 5/28/2019 Remarks : Comments here

Experiment : 0001_66 Method : 0001.met

Drop phase : Heavy Oil Density : 0.9000

Extern.phase : Brine (15%) Density : 0.9824

Solid phase : Steel Calculation : Optimized cont.

No.	Time	Gamma	Beta	R0	Area	Volume	Theta	Height	Width	Opt	
1		0.0	8.73	0.294	1.781	51.26	34.44	109.99	4.837	3.733	3
2		0.9	8.79	0.292	1.782	51.37	34.43	110.24	4.830	3.745	3
3		2.0	8.81	0.291	1.780	51.14	34.30	110.37	4.823	3.759	3
4		2.9	8.70	0.293	1.777	51.27	34.27	109.85	4.830	3.720	3
5		3.9	8.72	0.293	1.779	51.69	34.26	109.92	4.836	3.744	3
6		5.0	8.79	0.292	1.781	51.39	34.42	110.10	4.832	3.753	3
7		5.9	8.81	0.291	1.782	51.32	34.45	110.21	4.828	3.749	3
8		7.0	8.79	0.292	1.781	51.18	34.36	110.71	4.818	3.745	3
9	7.9	0.00	0.000	0.000	0.00	0.00	0.00	0.000	0.000	0	Sides are too differ
10		9.0	8.81	0.291	1.782	51.32	34.44	110.58	4.822	3.745	3

Mean: 8.77 0.292 1.781 51.33 34.38 110.22 4.829 3.744

Stand.dev.: 0.01 0.000 0.001 0.05 0.03 0.10 0.002 0.004

At 100°C

Date : 5/28/2019 Remarks : Comments here

Experiment : 0001_73 Method : 0001.met

Drop phase : Heavy Oil Density : 0.9000

Extern.phase : Brine (15%) Density : 0.9820

Solid phase : Steel Calculation : Optimized cont.

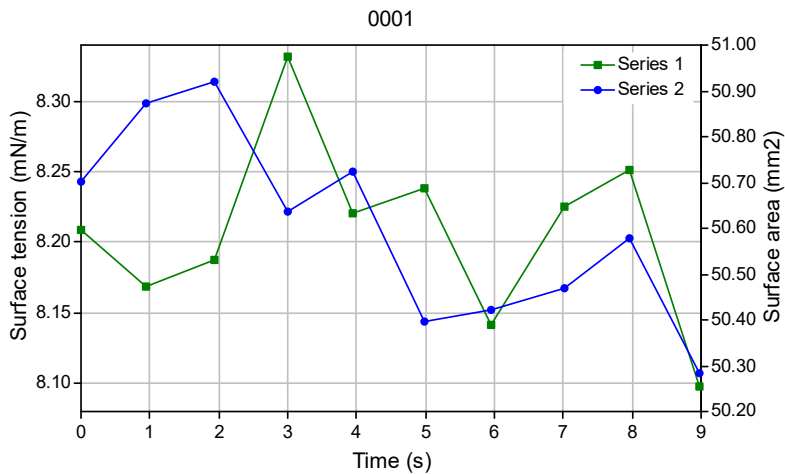
No.	Time	Gamma	Beta	R0	Area	Volume	Theta	Height	Width	Opt
-----	------	-------	------	----	------	--------	-------	--------	-------	-----

Messages

1	0.0	8.32	0.294	1.744	50.60	32.73	95.36	5.068	3.651	3
2	1.0	8.30	0.295	1.745	50.49	32.77	94.92	5.087	3.648	3
3	2.0	8.31	0.295	1.746	50.69	32.87	94.79	5.090	3.644	3
4	2.9	8.35	0.294	1.747	50.90	32.89	95.12	5.082	3.652	3
5	4.0	8.36	0.294	1.748	51.03	32.90	95.19	5.088	3.659	3
6	4.9	8.31	0.294	1.744	50.59	32.69	94.87	5.083	3.646	3
7	6.0	8.30	0.295	1.744	50.49	32.82	95.05	5.081	3.641	3
8	7.0	8.35	0.294	1.747	50.98	32.85	94.92	5.087	3.657	3
9	7.9	8.39	0.293	1.748	50.60	32.86	95.11	5.085	3.656	3
10	9.0	8.38	0.293	1.747	50.93	32.84	95.19	5.081	3.650	3

Mean: 8.34 0.294 1.746 50.73 32.82 95.05 5.083 3.650

Stand.dev.: 0.01 0.000 0.001 0.07 0.02 0.06 0.002 0.002



GUMg 2 SLILICA 0.75g in 500ml AT 30

Date : 5/16/2019 Remarks : Comments here

Experiment : 003_36 Method : 003.met

Drop phase : Heavy Oil Density : 0.9000

Extern.phase : Brine (15%) Density : 1.0068

Solid phase : Steel Calculation : Optimized cont.

No.	Time	Gamma	Beta	R0	Area	Volume	Theta	Height	Width	Opt
-----	------	-------	------	----	------	--------	-------	--------	-------	-----

Messages

1	0.0	17.50	0.288	2.194	77.48	63.58	118.62	5.593	4.676	3
2	0.9	17.53	0.288	2.194	79.30	63.59	118.64	5.591	4.676	3
3	2.0	17.48	0.288	2.194	78.02	63.65	118.51	5.594	4.679	3
4	3.0	17.62	0.287	2.196	77.17	63.58	118.85	5.588	4.675	3
5	4.0	17.61	0.287	2.195	77.33	63.67	118.73	5.592	4.671	3
6	5.0	17.68	0.286	2.197	77.83	63.75	118.95	5.591	4.671	3
7	5.9	17.53	0.288	2.195	77.82	63.79	118.66	5.592	4.678	3

8	7.0	17.52	0.288	2.195	77.18	63.71	118.60	5.593	4.672	3
9	7.9	17.53	0.288	2.196	78.95	63.84	118.71	5.592	4.673	3
10	9.0	17.38	0.290	2.194	78.12	63.79	118.49	5.592	4.671	3

Mean: 17.54 0.288 2.195 77.92 63.69 118.68 5.592 4.674

Stand.dev.: 0.03 0.000 0.000 0.23 0.03 0.04 0.001 0.001

AT 50°C

Date : 5/16/2019 Remarks : Comments here

Experiment : 003_62 Method : 003.met

Drop phase : Heavy Oil Density : 0.9000

Extern.phase : Brine (15%) Density : 0.9990

Solid phase : Steel Calculation : Optimized cont.

No.	Time	Gamma	Beta	R0	Area	Volume	Theta	Height	Width	Opt
-----	------	-------	------	----	------	--------	-------	--------	-------	-----

Messages

1	0.0	13.10	0.263	1.885	53.14	37.93	125.53	4.435	3.969	2
2	0.9	13.27	0.261	1.887	53.20	37.88	125.88	4.436	3.973	2
3	1.9	13.25	0.261	1.887	52.50	37.78	125.86	4.434	3.975	2
4	3.0	13.40	0.259	1.889	53.12	37.89	126.22	4.429	3.983	2
5	4.0	13.17	0.262	1.885	52.76	37.88	125.67	4.436	3.986	2
6	5.0	13.13	0.263	1.885	53.46	37.78	125.61	4.437	3.979	2
7	6.0	13.25	0.261	1.886	52.65	37.75	125.87	4.433	3.984	2
8	7.0	13.20	0.262	1.886	53.35	37.81	125.74	4.438	3.973	2

9	8.0	13.42	0.258	1.886	52.80	37.70	126.32	4.426	3.974	2
10	9.0	13.45	0.258	1.889	52.93	37.89	126.29	4.429	3.975	2

Mean: 13.26 0.261 1.887 52.99 37.83 125.90 4.433 3.977

Stand.dev.: 0.04 0.001 0.000 0.10 0.02 0.09 0.001 0.002

AT 70°C

Date : 5/16/2019 Remarks : Comments here

Experiment : 003_71 Method : 003.met

Drop phase : Heavy Oil Density : 0.9000

Extern.phase : Brine (15%) Density : 0.9990

Solid phase : Steel Calculation : Optimized cont.

No.	Time	Gamma	Beta	R0	Area	Volume	Theta	Height	Width	Opt
-----	------	-------	------	----	------	--------	-------	--------	-------	-----

Messages

1	0.0	13.62	0.257	1.898	53.09	38.39	126.31	4.468	4.000	2
2	0.9	13.68	0.256	1.899	53.63	38.60	126.38	4.468	4.001	2
3	2.0	13.58	0.258	1.899	53.45	38.60	126.14	4.474	4.001	2
4	2.9	13.53	0.259	1.898	53.49	38.33	126.09	4.474	4.004	2
5	3.9	13.35	0.261	1.896	53.49	38.33	125.71	4.476	4.004	2
6	5.0	13.81	0.254	1.902	53.23	38.50	126.67	4.471	4.010	2
7	6.0	13.76	0.255	1.901	54.07	38.49	126.57	4.467	4.001	2
8	7.0	13.67	0.257	1.901	53.15	38.56	126.31	4.476	4.003	2
9	8.0	13.70	0.256	1.900	53.48	38.26	126.46	4.472	4.003	2

10 8.9 13.52 0.259 1.898 53.20 38.58 125.98 4.479 3.993 2

Mean: 13.62 0.257 1.899 53.43 38.46 126.26 4.472 4.002

Stand.dev.: 0.04 0.001 0.001 0.09 0.04 0.09 0.001 0.001

At 90°C

Date : 5/16/2019 Remarks : Comments here

Experiment : 003_113 Method : 003.met

Drop phase : Heavy Oil Density : 0.9000

Extern.phase : Brine (15%) Density : 0.9824

Solid phase : Steel Calculation : Optimized cont.

No.	Time	Gamma	Beta	R0	Area	Volume	Theta	Height	Width	Opt
-----	------	-------	------	----	------	--------	-------	--------	-------	-----

Messages

1 0.0 5.58 0.313 1.468 34.92 19.86 112.76 3.880 3.135 2

2 1.0 5.56 0.314 1.468 34.78 19.83 112.80 3.879 3.141 2

3 2.0 5.57 0.314 1.470 34.91 19.94 112.71 3.882 3.136 2

4 2.9 5.60 0.311 1.468 34.88 19.66 113.35 3.865 3.123 2

5 3.9 5.55 0.313 1.467 34.61 19.70 112.74 3.876 3.120 2

6 5.0 5.58 0.312 1.468 34.56 19.67 112.93 3.878 3.139 2

7 5.9 5.57 0.312 1.467 34.71 19.74 112.95 3.872 3.127 2

8 7.0 5.59 0.312 1.468 34.33 19.49 113.15 3.876 3.128 2

9 8.0 5.51 0.315 1.465 34.92 19.71 112.40 3.880 3.128 2

10 8.9 5.52 0.314 1.465 34.61 19.73 112.44 3.880 3.134 2

Mean: 5.56 0.313 1.467 34.72 19.73 112.82 3.877 3.131

Stand.dev.: 0.01 0.000 0.000 0.06 0.04 0.09 0.002 0.002

At 100°C

Date : 5/16/2019 Remarks : Comments here

Experiment : 003_118 Method : 003.met

Drop phase : Heavy Oil Density : 0.9000

Extern.phase : Brine (15%) Density : 0.9824

Solid phase : Steel Calculation : Optimized cont.

No.	Time	Gamma	Beta	R0	Area	Volume	Theta	Height	Width	Opt	Messages
-----	------	-------	------	----	------	--------	-------	--------	-------	-----	----------

1		0.0	5.84	0.302	1.477	34.04	19.51	117.28	3.759	3.125	2
---	--	-----	------	-------	-------	-------	-------	--------	-------	-------	---

2		0.9	5.84	0.302	1.478	34.03	19.54	117.30	3.756	3.136	2
---	--	-----	------	-------	-------	-------	-------	--------	-------	-------	---

3		2.0	5.83	0.302	1.476	34.03	19.51	117.25	3.755	3.136	2
---	--	-----	------	-------	-------	-------	-------	--------	-------	-------	---

4		2.9	5.92	0.299	1.480	34.11	19.58	117.77	3.755	3.135	2
---	--	-----	------	-------	-------	-------	-------	--------	-------	-------	---

5		4.0	5.86	0.302	1.479	34.11	19.59	117.28	3.759	3.133	2
---	--	-----	------	-------	-------	-------	-------	--------	-------	-------	---

6	4.9	0.00	0.000	0.000	0.00	0.00	0.00	0.000	0.000	0	Sides are too differ
---	-----	------	-------	-------	------	------	------	-------	-------	---	----------------------

7	6.0	0.00	0.000	0.000	0.00	0.00	0.00	0.000	0.000	0	Sides are too differ
---	-----	------	-------	-------	------	------	------	-------	-------	---	----------------------

8		6.9	5.87	0.301	1.478	33.99	19.53	117.40	3.757	3.145	2
---	--	-----	------	-------	-------	-------	-------	--------	-------	-------	---

9		7.9	5.88	0.301	1.479	34.02	19.52	117.39	3.762	3.139	2
---	--	-----	------	-------	-------	-------	-------	--------	-------	-------	---

10 8.9 5.85 0.302 1.478 34.22 19.66 117.15 3.764 3.145 2

Mean: 5.86 0.301 1.478 34.07 19.56 117.35 3.758 3.137

Stand.dev.: 0.01 0.000 0.000 0.03 0.02 0.07 0.001 0.002

Gum Arabic 3g and Silica 0.5 g in 500ml

at 30°C and p 318 psig

Date : 5/10/2019 Remarks : Comments here

Experiment : fluid 01_1 Method : fluid 01.met

Drop phase : Heavy Oil Density : 0.9000

Extern.phase : Brine (15%) Density : 1.0400

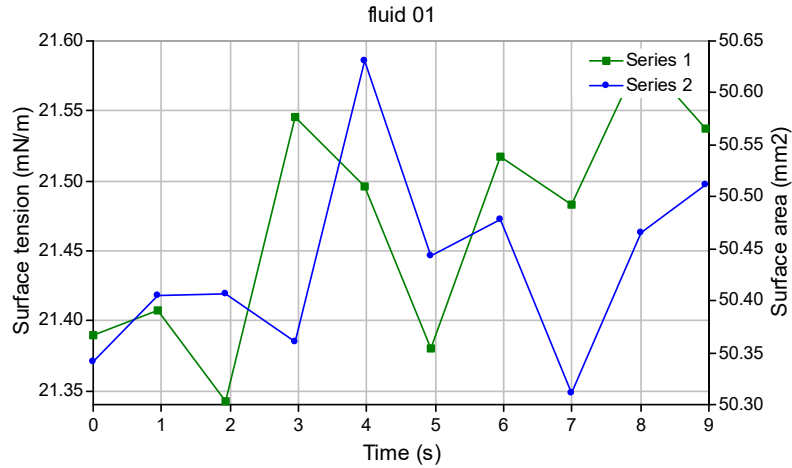
Solid phase : Steel Calculation : Optimized cont.

No.	Time	Gamma	Beta	R0	Area	Volume	Theta	Height	Width	Opt
-----	------	-------	------	----	------	--------	-------	--------	-------	-----

1	0.0	21.39	0.216	1.832	50.34	32.96	102.64	4.857	3.793	3
2	0.9	21.41	0.215	1.832	50.40	33.04	102.87	4.853	3.792	3
3	1.9	21.34	0.216	1.833	50.41	33.05	102.82	4.861	3.792	3
4	2.9	21.55	0.214	1.833	50.36	32.99	102.75	4.850	3.798	2
5	4.0	21.50	0.215	1.833	50.63	33.25	102.53	4.854	3.800	3
6	4.9	21.38	0.216	1.832	50.44	33.07	102.80	4.854	3.799	2
7	6.0	21.52	0.214	1.832	50.48	33.08	102.94	4.847	3.796	3
8	7.0	21.48	0.215	1.833	50.31	32.99	102.88	4.852	3.800	2
9	8.0	21.59	0.214	1.834	50.46	33.01	102.86	4.851	3.811	2
10	8.9	21.54	0.214	1.833	50.51	33.08	103.02	4.848	3.804	2

Mean: 21.47 0.215 1.833 50.44 33.05 102.81 4.853 3.799

Stand.dev.: 0.03 0.000 0.000 0.03 0.03 0.04 0.001 0.002



at 50°C and P 1000 psig

Drop Shape Image Analysis

Date : 5/10/2019 Remarks : Comments here

Experiment : fluid 01_20 Method : fluid 01.met

Drop phase : Heavy Oil Density : 0.9000

Extern.phase : Brine (15%) Density : 1.0400

Solid phase : Steel Calculation : Optimized cont.

No.	Time	Gamma	Beta	R0	Area	Volume	Theta	Height	Width	Opt
-----	------	-------	------	----	------	--------	-------	--------	-------	-----

Messages

1	0.0	18.88	0.206	1.684	41.90	25.30	118.37	4.258	3.492	2
2	0.9	18.89	0.206	1.685	41.88	25.38	118.36	4.260	3.496	2
3	2.0	18.82	0.207	1.684	41.97	25.43	118.16	4.258	3.494	2
4	3.0	18.87	0.207	1.685	41.91	25.41	118.30	4.258	3.489	2
5	3.9	18.84	0.207	1.684	41.82	25.33	118.35	4.258	3.494	2
6	5.0	18.86	0.207	1.684	41.81	25.34	118.39	4.257	3.497	2
7	6.0	18.73	0.208	1.684	41.91	25.32	118.11	4.263	3.491	2
8	7.0	18.69	0.208	1.683	41.87	25.38	117.99	4.261	3.489	2
9	7.9	18.70	0.208	1.684	41.80	25.33	117.95	4.265	3.487	2
10	8.9	18.68	0.208	1.684	42.02	25.45	117.83	4.265	3.493	2

Mean: 18.80 0.207 1.684 41.89 25.37 118.18 4.260 3.492

Stand.dev.: 0.03 0.000 0.000 0.02 0.02 0.06 0.001 0.001

A

At 70 °C

Date : 5/10/2019 Remarks : Comments here

Experiment : 10_9 Method : 10.met

Drop phase : Heavy Oil Density : 0.9000

Extern.phase : G and Silica at 70 Density : 1.0170

Solid phase : Steel Calculation : Optimized cont.

No.	Time	Gamma	Beta	R0	Area	Volume	Theta	Height	Width	Opt
-----	------	-------	------	----	------	--------	-------	--------	-------	-----

Messages

1	0.0	15.36	0.206	1.659	40.87	24.41	116.56	4.207	3.442	2
2	1.0	15.41	0.205	1.660	40.64	24.23	116.92	4.208	3.450	2
3	2.0	15.50	0.204	1.659	40.70	24.26	116.77	4.203	3.442	2
4	2.9	15.48	0.204	1.659	40.69	24.24	116.82	4.204	3.445	2
5	3.9	15.43	0.205	1.659	40.71	24.26	116.67	4.208	3.451	2
6	5.0	15.44	0.205	1.659	40.70	24.25	116.83	4.205	3.452	2
7	6.0	15.41	0.205	1.659	40.71	24.28	116.74	4.208	3.447	2
8	7.0	15.51	0.204	1.660	40.71	24.25	116.87	4.205	3.450	2
9	8.0	15.42	0.205	1.659	40.73	24.27	116.65	4.209	3.453	2
10	8.9	15.41	0.205	1.659	40.72	24.29	116.50	4.210	3.447	2

Mean: 15.44 0.205 1.659 40.72 24.27 116.73 4.207 3.448

Stand.dev.: 0.01 0.000 0.000 0.02 0.02 0.04 0.001 0.001

At 90°C

Date : 5/10/2019 Remarks : Comments here

Experiment : 11_12 Method : 11.met

Drop phase : Heavy Oil Density : 0.9000

Extern.phase : G 3 and Silica 0.5 at Density : 1.0170

Solid phase : Steel Calculation : Optimized cont.

No.	Time	Gamma	Beta	R0	Area	Volume	Theta	Height	Width	Opt
-----	------	-------	------	----	------	--------	-------	--------	-------	-----

Messages

1	0.0	13.58	0.230	1.649	41.63	24.66	92.98	4.538	3.420	3
2	1.0	13.65	0.229	1.650	41.69	24.72	92.62	4.539	3.417	3
3	2.0	13.60	0.229	1.648	41.56	24.60	92.84	4.536	3.412	3
4	3.0	13.66	0.229	1.650	41.61	24.66	92.52	4.541	3.420	3
5	3.9	13.65	0.229	1.651	41.62	24.68	92.35	4.549	3.418	3
6	4.9	13.62	0.229	1.650	41.71	24.74	91.13	4.560	3.416	3
7	6.0	13.67	0.229	1.651	41.69	24.70	91.09	4.559	3.412	3
8	6.9	13.66	0.229	1.651	41.69	24.72	90.26	4.569	3.417	3
9	8.0	13.69	0.228	1.649	41.80	24.53	89.27	4.570	3.416	3
10	9.0	13.69	0.228	1.649	41.73	24.68	88.73	4.576	3.416	3

Mean: 13.65 0.229 1.650 41.67 24.67 91.38 4.554 3.416

Stand.dev.: 0.01 0.000 0.000 0.02 0.02 0.49 0.005 0.001

At 100 °C

Drop Shape Image Analysis

Date : 5/10/2019 Remarks : Comments here

Experiment : 11_29 Method : 11.met

Drop phase : Heavy Oil Density : 0.9000

Extern.phase : G 3 and Silica 0.5 at Density : 1.0170

Solid phase : Steel Calculation : Optimized cont.

No.	Time	Gamma	Beta	R0	Area	Volume	Theta	Height	Width	Opt
-----	------	-------	------	----	------	--------	-------	--------	-------	-----

Messages

1	0.0	11.78	0.195	1.413	28.90	14.85	129.55	3.397	2.937	2
2	0.9	11.58	0.198	1.412	29.02	14.94	128.95	3.401	2.933	2
3	1.9	11.47	0.199	1.411	28.97	14.87	128.76	3.405	2.932	2
4	3.0	11.58	0.198	1.412	28.91	14.78	129.08	3.407	2.932	2
5	3.9	11.52	0.198	1.411	28.93	14.83	128.82	3.406	2.927	2
6	5.0	11.66	0.196	1.412	28.90	14.79	129.23	3.404	2.931	2
7	6.0	11.50	0.199	1.411	29.02	14.80	128.89	3.407	2.929	2
8	7.0	11.71	0.195	1.412	28.88	14.82	129.37	3.398	2.931	2
9	8.0	11.51	0.198	1.410	28.86	14.80	128.88	3.405	2.929	2
10	9.0	11.70	0.196	1.412	28.91	14.81	129.16	3.406	2.933	2

Mean: 11.60 0.197 1.412 28.93 14.83 129.07 3.404 2.931

Stand.dev.: 0.03 0.000 0.000 0.02 0.01 0.08 0.001 0.001

Fluid 5 distilled water at 30°C

Date : 6/7/2019 Remarks : Comments here

Experiment : 015_62 Method : 015.met

Drop phase : Heavy Oil Density : 0.9000

Extern.phase : distilled water Density : 0.9957

Solid phase : Steel Calculation : Optimized cont.

No.	Time	Gamma	Beta	R0	Area	Volume	Theta	Height	Width	Opt
-----	------	-------	------	----	------	--------	-------	--------	-------	-----

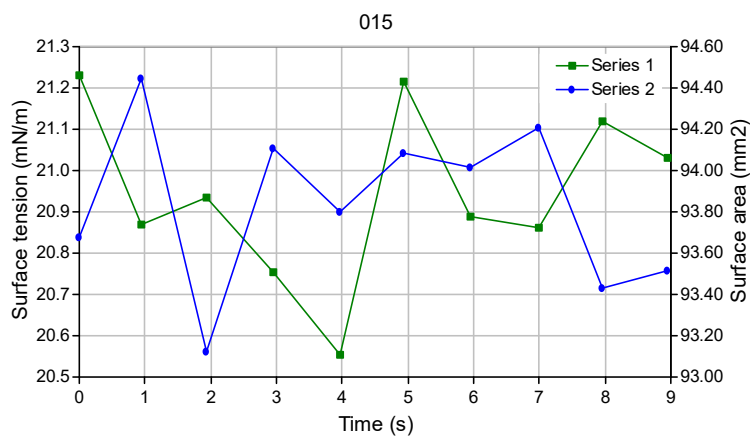
Messages

1	0.0	20.32	0.281	2.465	94.41	87.23	119.40	6.230	5.229	2
2	1.0	20.31	0.281	2.467	94.10	87.50	119.37	6.236	5.225	2
3	2.0	20.56	0.279	2.472	94.03	87.20	119.70	6.242	5.236	2
4	3.0	20.46	0.280	2.470	93.96	87.78	119.71	6.225	5.231	2
5	4.0	20.06	0.283	2.461	94.06	86.99	118.91	6.246	5.207	2
6	5.0	20.30	0.281	2.465	93.37	87.64	119.33	6.233	5.214	2
7	6.0	20.10	0.283	2.463	94.13	87.31	119.24	6.234	5.207	2
8	6.9	20.44	0.280	2.468	93.69	87.05	119.43	6.244	5.224	2
9	8.0	20.30	0.280	2.463	93.37	87.02	119.57	6.217	5.203	2
10	9.0	20.57	0.278	2.467	93.40	86.99	119.90	6.220	5.211	2

Mean: 20.34 0.281 2.466 93.85 87.27 119.46 6.233 5.219

Stand.dev.: 0.05 0.001 0.001 0.12 0.09 0.09 0.003 0.004

At 50°C



Date : 6/7/2019 Remarks : Comments here
 Experiment : 015_103 Method : 015.met
 Drop phase : Heavy Oil Density : 0.9000
 Extern.phase : distilled water Density : 0.9881
 Solid phase : Steel Calculation : Optimized cont.

No.	Time	Gamma	Beta	R0	Area	Volume	Theta	Height	Width	Opt	Messages	
1		0.0	19.73	0.267	2.469	94.29	86.59	115.47	6.442	5.231	3	
2	0.9	0.00	0.000	0.000	0.00	0.00	0.00	0.000	0.000	0	Sides are too differ	
3	2.0	19.75	0.266	2.468	94.19	85.43	115.91	6.436	5.205	2		
4	2.9	19.70	0.267	2.466	93.85	85.57	115.60	6.439	5.205	2		
5	4.0	19.78	0.266	2.467	93.93	85.59	116.06	6.424	5.190	2		
6	5.0	19.55	0.268	2.464	94.54	85.79	115.11	6.446	5.189	2		
7	5.9	19.31	0.271	2.460	94.04	85.70	114.84	6.443	5.210	2		
8	7.0	0.00	0.000	0.000	0.00	0.00	0.000	0.000	0.000	0	Sides are too differ	
9	7.9	19.34	0.270	2.459	94.30	85.38	115.07	6.442	5.186	2		
10	8.9	19.75	0.266	2.466	93.66	85.69	115.65	6.438	5.188	2		

Mean: 19.61 0.268 2.465 94.10 85.72 115.46 6.439 5.201

Stand.dev.: 0.07 0.001 0.001 0.10 0.13 0.15 0.002 0.005

At 70°C

Drop Shape Image Analysis

Date : 6/7/2019 Remarks : Comments here
Experiment : 015_130 Method : 015.met
Drop phase : Heavy Oil Density : 0.9000
Extern.phase : distilled water Density : 0.9785
Solid phase : Steel Calculation : Optimized cont.

No.	Time	Gamma	Beta	R0	Area	Volume	Theta	Height	Width	Opt
-----	------	-------	------	----	------	--------	-------	--------	-------	-----

Messages

1	0.0	18.79	0.258	2.511	97.12	89.35	111.08	6.681	5.269	2
2	0.9	19.05	0.255	2.513	97.06	89.19	112.13	6.649	5.298	2
3	2.0	18.92	0.256	2.510	96.67	88.66	111.43	6.669	5.259	2
4	3.0	18.73	0.258	2.505	96.86	88.70	111.33	6.660	5.281	2
5	3.9	18.85	0.257	2.509	97.51	89.46	111.73	6.656	5.280	2
6	5.0	18.84	0.257	2.510	97.65	89.25	111.02	6.677	5.265	2
7	6.0	18.70	0.259	2.506	97.00	89.10	111.25	6.663	5.246	2
8	6.9	18.73	0.258	2.505	96.87	88.74	111.21	6.666	5.247	2
9	8.0	18.71	0.258	2.506	96.67	88.61	111.20	6.669	5.260	2
10	9.0	18.57	0.260	2.503	97.14	88.36	111.27	6.665	5.247	2

Mean: 18.79 0.258 2.508 97.05 88.94 111.37 6.665 5.265

Stand.dev.: 0.04 0.000 0.001 0.10 0.12 0.10 0.003 0.006

At 90°C

Date : 6/7/2019 Remarks : Comments here
 Experiment : 015_141 Method : 015.met
 Drop phase : Heavy Oil Density : 0.9000
 Extern.phase : distilled water Density : 0.9704
 Solid phase : Steel Calculation : Optimized cont.

No.	Time	Gamma	Beta	R0	Area	Volume	Theta	Height	Width	Opt	Messages
1	0.0	17.50	0.253	2.532	99.03	90.40	97.58	7.029	5.281	2	
2	0.9	17.35	0.255	2.530	99.18	89.45	97.41	7.041	5.257	3	
3	2.0	17.45	0.253	2.530	99.30	89.86	96.93	7.043	5.285	2	
4	3.0	17.47	0.253	2.530	99.25	89.79	97.10	7.038	5.281	2	
5	3.9	17.38	0.254	2.529	99.10	89.75	96.94	7.041	5.276	2	
6	5.0	17.29	0.255	2.526	99.05	89.48	96.67	7.047	5.256	3	
7	6.0	17.25	0.256	2.527	99.62	89.86	97.47	7.038	5.270	2	
8	7.0	17.39	0.254	2.527	99.03	89.44	96.81	7.040	5.257	2	
9	7.9	17.30	0.255	2.525	98.48	89.56	96.52	7.041	5.260	2	
10	8.9	0.00	0.000	0.000	0.00	0.00	0.000	0.000	0		Sides are too differ

Mean: 17.37 0.254 2.528 99.12 89.73 97.05 7.040 5.269

Stand.dev.: 0.03 0.000 0.001 0.10 0.10 0.12 0.002 0.004

At 100°C

Date : 6/7/2019 Remarks : Comments here

Experiment : 015_166 Method : 015.met

Drop phase : Heavy Oil Density : 0.9000

Extern.phase : distilled water Density : 0.9692

Solid phase : Steel Calculation : Optimized cont.

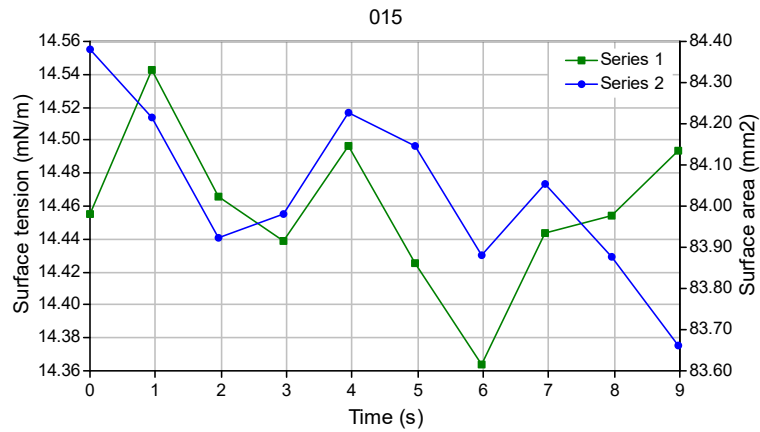
No.	Time	Gamma	Beta	R0	Area	Volume	Theta	Height	Width	Opt
-----	------	-------	------	----	------	--------	-------	--------	-------	-----

Messages

1	0.0	14.46	0.256	2.334	84.38	68.51	78.09	6.879	4.851	3
2	0.9	14.54	0.255	2.337	84.22	68.50	78.20	6.874	4.834	3
3	2.0	14.47	0.256	2.335	83.92	68.29	78.50	6.873	4.822	3
4	2.9	14.44	0.256	2.333	83.98	68.35	77.94	6.876	4.831	3
5	4.0	14.50	0.256	2.337	84.23	68.70	78.52	6.876	4.827	3
6	5.0	14.43	0.257	2.335	84.15	68.50	78.31	6.884	4.849	3
7	6.0	14.36	0.257	2.333	83.88	68.11	78.11	6.889	4.822	3
8	6.9	14.44	0.256	2.335	84.05	68.20	77.53	6.893	4.825	3
9	7.9	14.45	0.256	2.333	83.88	68.29	77.54	6.884	4.828	3
10	9.0	14.49	0.255	2.336	83.66	68.07	77.90	6.884	4.811	3

Mean: 14.08 0.256 2.335 84.03 68.35 78.06 6.881 4.830

Stand.dev.: 0.02 0.000 0.000 0.07 0.06 0.11 0.002 0.004



Fluid 5 10%salt water at 30

Date : 6/3/2019 Remarks : Comments here

Experiment : 000_37 Method : 000.met

Drop phase : Heavy Oil Density : 0.9000

Extern.phase : Brine (10%) Density : 1.0031

Solid phase : Steel Calculation : Optimized cont.

No.	Time	Gamma	Beta	R0	Area	Volume	Theta	Height	Width	Opt
-----	------	-------	------	----	------	--------	-------	--------	-------	-----

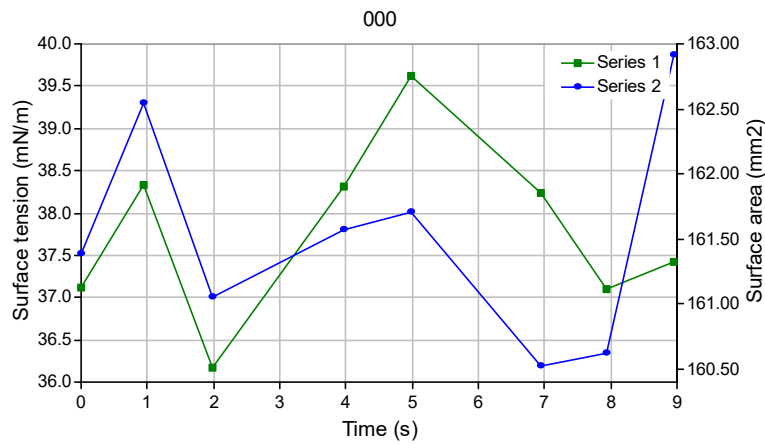
Messages

1	0.0	36.80	0.305	3.329	166.34	217.73	120.65	7.687	7.125	3
2	0.9	36.55	0.306	3.325	166.48	218.81	120.49	7.681	7.137	3
3	2.0	36.54	0.306	3.324	169.72	216.94	120.50	7.695	7.094	2
4	3.0	36.74	0.305	3.327	169.63	217.31	120.63	7.698	7.097	3
5	3.9	37.16	0.301	3.327	166.47	216.82	121.05	7.691	7.111	3

6	5.0	37.77	0.298	3.335	166.84	217.12	121.49	7.687	7.093	2
7	6.0	35.46	0.313	3.314	167.86	216.80	119.57	7.708	7.071	2
8	7.0	37.02	0.302	3.326	168.16	215.70	120.93	7.686	7.093	2
9	7.9	36.28	0.307	3.319	168.08	215.95	120.34	7.682	7.079	2
10	9.0	36.92	0.303	3.327	166.84	216.70	120.80	7.704	7.079	2

Mean: 36.72 0.305 3.325 167.64 216.99 120.65 7.692 7.098

Stand.dev.: 0.19 0.001 0.002 0.40 0.28 0.16 0.003 0.007



At 50°C

Date : 6/3/2019 Remarks : Comments here
 Experiment : 000_67 Method : 000.met
 Drop phase : Heavy Oil Density : 0.9000
 Extern.phase : Brine (10%) Density : 1.0031
 Solid phase : Steel Calculation : Optimized cont.

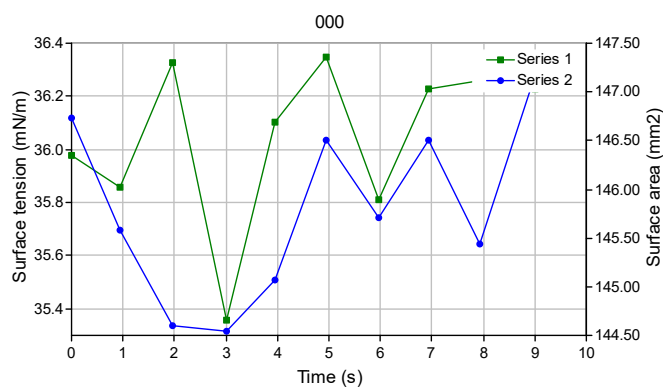
No.	Time	Gamma	Beta	R0	Area	Volume	Theta	Height	Width	Opt
-----	------	-------	------	----	------	--------	-------	--------	-------	-----

Messages

1	0.0	35.98	0.268	3.086	146.73	169.83	122.36	7.663	6.507	2
2	1.0	35.86	0.268	3.084	145.59	169.88	122.26	7.660	6.507	2
3	2.0	36.32	0.265	3.085	144.60	169.15	122.81	7.641	6.505	2
4	3.0	35.36	0.271	3.076	144.54	168.82	121.95	7.655	6.489	2
5	3.9	36.10	0.266	3.081	145.07	168.69	122.57	7.644	6.503	2
6	4.9	36.35	0.265	3.087	146.51	169.42	122.73	7.651	6.530	3
7	6.0	35.81	0.268	3.081	145.71	169.28	122.21	7.657	6.542	3
8	6.9	36.23	0.266	3.085	146.51	168.98	122.59	7.655	6.530	3
9	7.9	36.26	0.266	3.087	145.44	169.27	122.74	7.649	6.538	3
10	9.0	36.23	0.266	3.084	147.18	169.19	122.64	7.649	6.507	2

Mean: 36.05 0.267 3.084 145.79 169.25 122.48 7.652 6.516

Stand.dev.: 0.10 0.001 0.001 0.29 0.12 0.09 0.002 0.006



70°C

Date : 6/3/2019 Remarks : Comments here

Experiment : 000_103 Method : 000.met
 Drop phase : Heavy Oil Density : 0.9000
 Extern.phase : Brine (10%) Density : 0.9859
 Solid phase : Steel Calculation : Optimized cont.

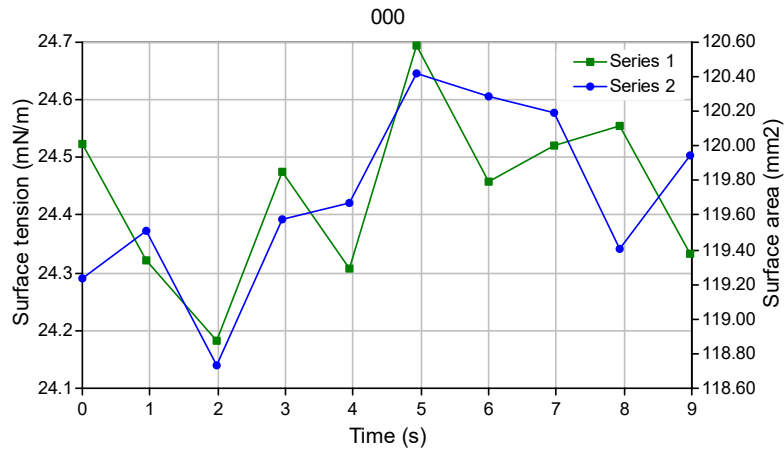
No.	Time	Gamma	Beta	R0	Area	Volume	Theta	Height	Width	Opt
-----	------	-------	------	----	------	--------	-------	--------	-------	-----

Messages

1	0.0	24.52	0.262	2.762	119.23	121.52	114.53	7.259	5.814	2
2	1.0	24.32	0.263	2.757	119.51	121.38	114.31	7.256	5.799	2
3	2.0	24.18	0.264	2.754	118.74	121.03	113.97	7.261	5.803	2
4	2.9	24.48	0.262	2.759	119.58	121.94	114.24	7.256	5.833	2
5	3.9	24.31	0.264	2.758	119.67	122.37	113.81	7.269	5.805	2
6	4.9	24.69	0.261	2.765	120.42	123.02	114.29	7.265	5.833	2
7	6.0	24.46	0.263	2.762	120.29	122.76	113.76	7.276	5.792	2
8	7.0	24.52	0.262	2.762	120.19	122.73	114.10	7.264	5.829	2
9	7.9	24.56	0.262	2.766	119.41	122.33	114.14	7.282	5.823	2
10	9.0	24.33	0.264	2.760	119.95	122.32	113.44	7.289	5.830	2

Mean: 24.44 0.263 2.760 119.70 122.14 114.06 7.268 5.816

Stand.dev.: 0.05 0.000 0.001 0.16 0.21 0.10 0.004 0.005



At 90°C

Date : 6/3/2019 Remarks : Comments here

Experiment : 000_146 Method : 000.met

Drop phase : Heavy Oil Density : 0.9000

Extern.phase : Brine (10%) Density : 0.9784

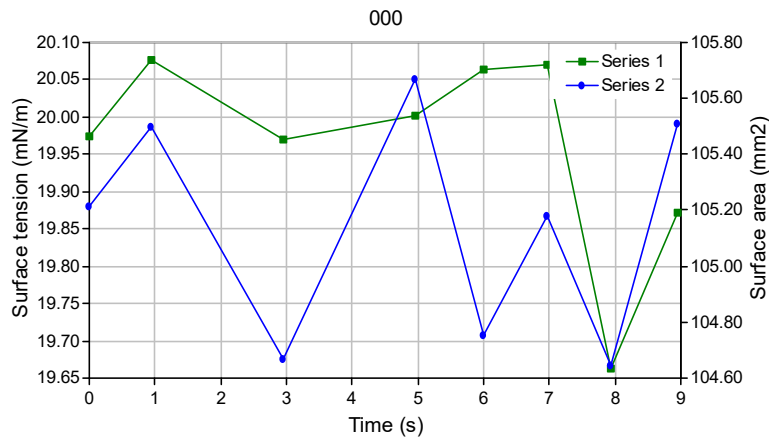
Solid phase : Steel Calculation : Optimized cont.

No.	Time	Gamma	Beta	R0	Area	Volume	Theta	Height	Width	Opt	Messages
1	0.0	19.97	0.260	2.599	105.21	100.53	113.76	6.857	5.461	2	
2	0.9	20.08	0.260	2.606	105.50	101.46	113.81	6.871	5.461	2	
3	2.0	0.00	0.000	0.000	0.00	0.00	0.000	0.000	0		Sides are too differ
4	2.9	19.97	0.260	2.600	104.67	100.73	113.39	6.869	5.443	3	
5	4.0	0.00	0.000	0.000	0.00	0.00	0.000	0.000	0		Error in profile
6	4.9	20.00	0.259	2.596	105.67	100.67	113.40	6.858	5.452	2	

7	6.0	20.06	0.259	2.600	104.75	100.76	113.31	6.870	5.457	2
8	7.0	20.07	0.258	2.597	105.18	100.39	113.34	6.865	5.430	3
9	7.9	19.66	0.263	2.591	104.64	100.27	112.45	6.883	5.435	2
10	8.9	19.87	0.261	2.597	105.51	100.60	112.89	6.877	5.436	2

Mean: 19.96 0.260 2.598 105.14 100.68 113.29 6.869 5.447

Stand.dev.: 0.05 0.000 0.002 0.14 0.13 0.16 0.003 0.004



At 100°C

Date : 6/3/2019 Remarks : Comments here

Experiment : 000_189 Method : 000.met

Drop phase : Heavy Oil Density : 0.9000

Extern.phase : Brine (10%) Density : 0.9778

Solid phase : Steel Calculation : Optimized cont.

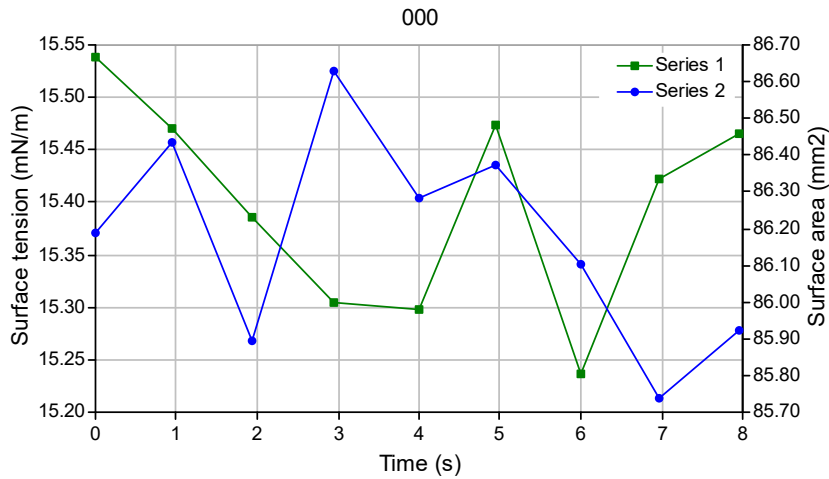
No.	Time	Gamma	Beta	R0	Area	Volume	Theta	Height	Width	Opt	Messages
-----	------	-------	------	----	------	--------	-------	--------	-------	-----	----------

1	0.0	15.54	0.268	2.336	86.19	74.45	110.24	6.261	4.931	2
---	-----	-------	-------	-------	-------	-------	--------	-------	-------	---

2	0.9	15.47	0.268	2.333	86.44	74.08	110.34	6.250	4.956	3
3	1.9	15.39	0.269	2.328	85.89	73.23	110.51	6.245	4.935	3
4	2.9	15.30	0.271	2.329	86.63	73.76	110.10	6.261	4.925	2
5	4.0	15.30	0.270	2.328	86.28	73.64	109.88	6.259	4.917	2
6	4.9	15.47	0.269	2.334	86.37	74.11	110.45	6.257	4.939	2
7	6.0	15.24	0.272	2.328	86.10	73.86	109.67	6.270	4.933	2
8	7.0	15.42	0.269	2.331	85.74	73.62	110.29	6.256	4.943	3
9	8.0	15.47	0.268	2.330	85.92	74.16	110.08	6.250	4.921	2
10	9.0	0.00	0.000	0.000	0.00	0.00	0.000	0.000	0	Sides are too differ

Mean: 15.40 0.269 2.331 86.17 73.88 110.17 6.257 4.933

Stand.dev.: 0.03 0.000 0.001 0.10 0.12 0.09 0.002 0.004



Fluid 4 salt water 10% at 30°C

Date : 6/4/2019 Remarks : Comments here

Experiment : 00000_59 Method : 00000.met

Drop phase : Heavy Oil Density : 0.9000

Extern.phase : Brine (10%) Density : 1.0031

Solid phase : Steel Calculation : Optimized cont.

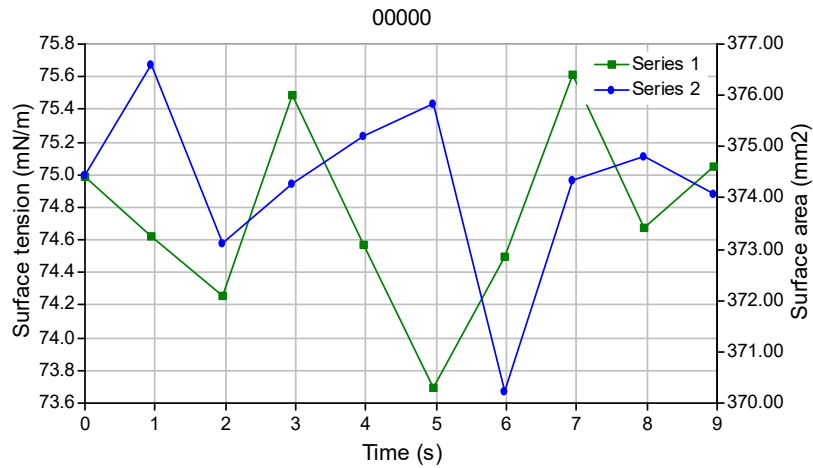
No.	Time	Gamma	Beta	R0	Area	Volume	Theta	Height	Width	Opt
-----	------	-------	------	----	------	--------	-------	--------	-------	-----

Messages

1	0.0	74.99	0.309	4.786	374.44	684.70	112.35	12.761	10.249	3
2	0.9	74.62	0.310	4.783	376.60	683.67	112.36	12.752	10.209	2
3	2.0	74.25	0.311	4.779	373.12	684.17	112.18	12.751	10.177	2
4	2.9	75.49	0.308	4.795	374.27	686.41	112.76	12.744	10.216	2
5	4.0	74.57	0.311	4.786	375.20	684.55	112.15	12.776	10.202	2
6	4.9	73.69	0.313	4.778	375.85	684.20	111.68	12.787	10.230	2
7	6.0	74.50	0.311	4.784	370.24	680.60	112.20	12.771	10.170	2
8	6.9	75.62	0.307	4.793	374.35	684.27	113.04	12.729	10.167	2
9	8.0	74.67	0.310	4.785	374.81	685.78	112.36	12.751	10.181	2
10	8.9	75.05	0.309	4.788	374.07	685.27	112.47	12.756	10.242	2

Mean: 74.74 0.310 4.786 374.30 684.36 112.36 12.758 10.204

Stand.dev.: 0.18 0.001 0.002 0.54 0.49 0.11 0.005 0.009



AT 50°C

Date : 6/4/2019 Remarks : Comments here

Experiment : 00000_73 Method : 00000.met

Drop phase : Heavy Oil Density : 0.9000

Extern.phase : Brine (10%) Density : 0.9954

Solid phase : Steel Calculation : Optimized cont.

No.	Time	Gamma	Beta	R0	Area	Volume	Theta	Height	Width	Opt
-----	------	-------	------	----	------	--------	-------	--------	-------	-----

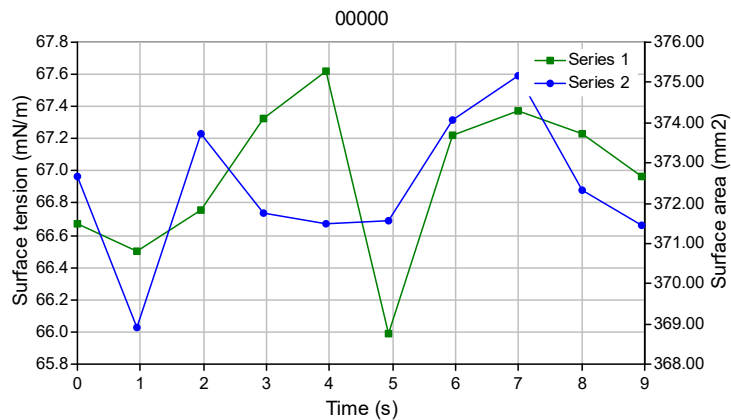
=====

1	0.0	66.68	0.313	4.725	372.65	668.24	106.02	13.166	10.022	2
2	0.9	66.50	0.314	4.720	368.91	666.52	105.76	13.167	10.015	2
3	2.0	66.75	0.314	4.730	373.72	670.96	105.87	13.181	10.060	2
4	2.9	67.33	0.311	4.734	371.74	669.74	106.27	13.159	10.090	2
5	4.0	67.62	0.310	4.733	371.51	667.95	106.69	13.134	10.085	2
6	4.9	65.99	0.316	4.719	371.58	666.80	105.60	13.186	10.043	2
7	6.0	67.22	0.312	4.734	374.08	669.86	105.86	13.198	10.047	2
8	7.0	67.37	0.312	4.736	375.17	673.12	106.24	13.172	10.119	2

9	8.0	67.23	0.312	4.733	372.31	673.10	106.42	13.137	10.108	2
10	8.9	66.97	0.313	4.732	371.43	669.94	105.91	13.184	10.068	2

Mean: 66.97 0.313 4.730 372.31 669.62 106.06 13.168 10.066

Stand.dev.: 0.15 0.000 0.002 0.55 0.73 0.11 0.007 0.011



AT 70°C

Date : 6/4/2019 Remarks : Comments here
 Experiment : 00000_87 Method : 00000.met
 Drop phase : Heavy Oil Density : 0.9000
 Extern.phase : Brine (10%) Density : 0.9859
 Solid phase : Steel Calculation : Optimized cont.

No.	Time	Gamma	Beta	R0	Area	Volume	Theta	Height	Width	Opt
-----	------	-------	------	----	------	--------	-------	--------	-------	-----

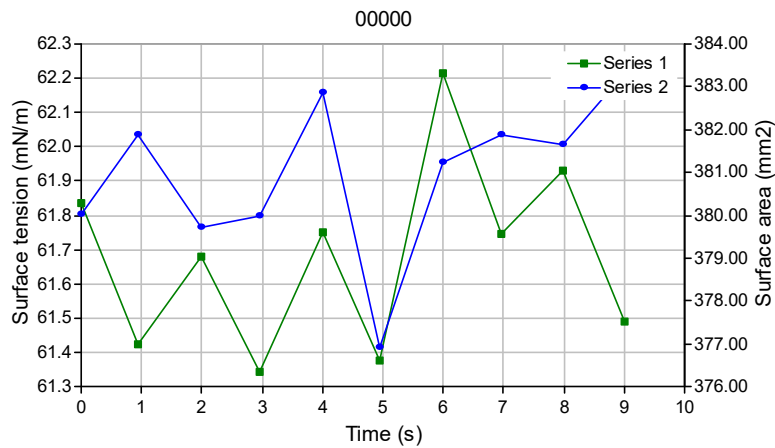
Messages

1	0.0	61.84	0.308	4.754	380.01	679.68	100.57	13.626	10.037	3
---	-----	-------	-------	-------	--------	--------	--------	--------	--------	---

2	1.0	61.42	0.310	4.751	381.87	678.02	100.57	13.626	10.029	3
3	2.0	61.68	0.308	4.749	379.72	677.80	100.38	13.619	10.048	3
4	3.0	61.34	0.310	4.751	379.98	678.52	99.91	13.669	10.097	2
5	4.0	61.75	0.308	4.755	382.86	679.48	100.54	13.632	10.051	3
6	4.9	61.38	0.309	4.747	376.90	677.34	100.00	13.640	10.029	3
7	6.0	62.21	0.307	4.762	381.22	682.47	100.56	13.630	10.095	2
8	7.0	61.74	0.308	4.754	381.89	680.12	100.46	13.631	10.112	2
9	8.0	61.93	0.307	4.750	381.64	678.54	100.61	13.598	10.071	2
10	9.0	61.49	0.309	4.751	383.32	678.96	100.36	13.629	10.076	3

Mean: 61.68 0.309 4.752 380.94 679.09 100.40 13.630 10.064

Stand.dev.: 0.09 0.000 0.001 0.59 0.47 0.08 0.006 0.009



AT 90°C

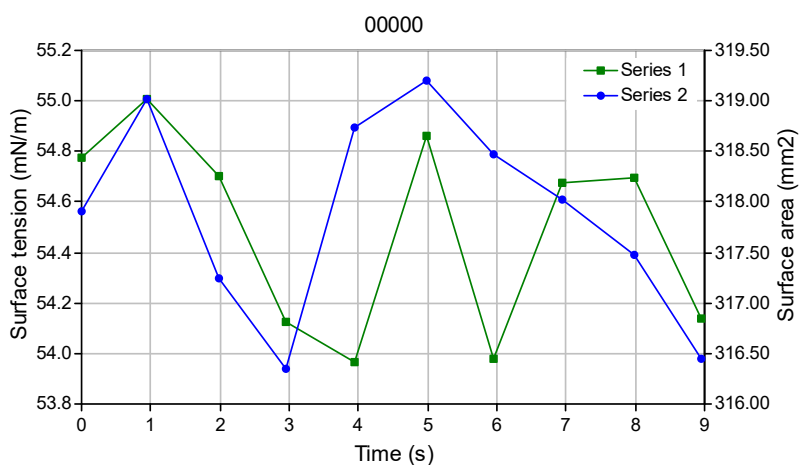
No.	Time	Gamma	Beta	R0	Area	Volume	Theta	Height	Width	Opt
-----	------	-------	------	----	------	--------	-------	--------	-------	-----

Messages

1	0.0	54.77	0.280	4.462	317.90	529.98	108.85	12.129	9.414	2
2	0.9	55.01	0.279	4.465	319.03	530.98	108.59	12.141	9.463	2
3	2.0	54.70	0.280	4.462	317.24	529.42	108.52	12.143	9.432	2
4	2.9	54.13	0.281	4.450	316.34	526.12	108.00	12.146	9.362	2
5	3.9	53.96	0.283	4.456	318.73	528.67	108.08	12.170	9.378	3
6	5.0	54.86	0.279	4.464	319.20	530.77	108.45	12.160	9.415	2
7	5.9	53.98	0.282	4.453	318.48	529.03	107.77	12.171	9.392	2
8	7.0	54.68	0.280	4.458	318.02	527.09	108.30	12.152	9.434	2
9	8.0	54.70	0.279	4.458	317.48	527.51	108.22	12.155	9.390	2
10	9.0	54.14	0.281	4.449	316.45	526.99	107.86	12.151	9.415	2

Mean: 54.49 0.280 4.458 317.89 528.66 108.26 12.152 9.410

Stand.dev.: 0.12 0.000 0.002 0.32 0.53 0.11 0.004 0.009



At 100°C

Date : 6/4/2019 Remarks : Comments here

Experiment : 00000_152 Method : 00000.met

Drop phase : Heavy Oil Density : 0.9000

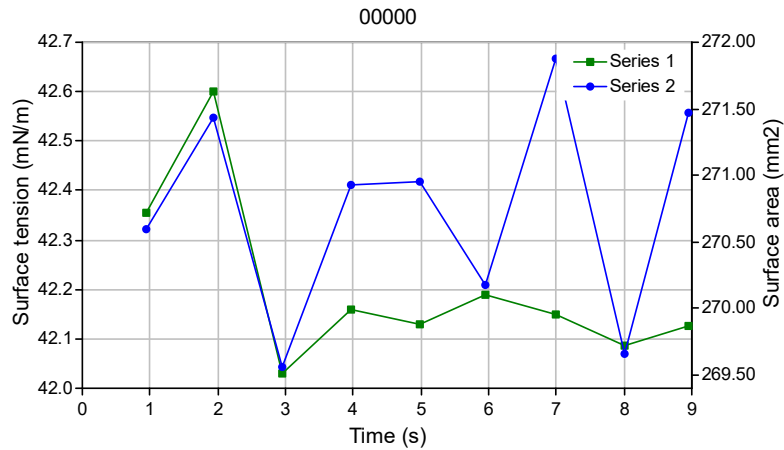
Extern.phase : Brine (10%) Density : 0.9778

Solid phase : Steel Calculation : Optimized cont.

No.	Time	Gamma	Beta	R0	Area	Volume	Theta	Height	Width	Opt	Messages
1	0.0	0.00	0.000	0.000	0.00	0.00	0.000	0.000	0		Sides are too differ
2	0.9	42.36	0.296	4.051	270.60	409.96	100.20	11.528	8.611	2	
3	1.9	42.60	0.295	4.056	271.44	411.51	100.44	11.526	8.545	3	
4	2.9	42.03	0.297	4.046	269.55	407.21	100.32	11.524	8.528	3	
5	4.0	42.16	0.297	4.051	270.93	409.10	100.25	11.539	8.598	2	
6	5.0	42.13	0.297	4.048	270.96	409.73	100.08	11.538	8.567	2	
7	5.9	42.19	0.297	4.049	270.18	409.84	99.92	11.541	8.597	2	
8	7.0	42.15	0.297	4.053	271.88	410.87	99.81	11.564	8.589	2	
9	8.0	42.09	0.298	4.051	269.65	410.55	99.89	11.554	8.583	2	
10	9.0	42.13	0.296	4.045	271.47	408.45	100.20	11.519	8.568	2	

Mean: 42.20 0.297 4.050 270.74 409.69 100.12 11.537 8.576

Stand.dev.: 0.06 0.000 0.001 0.27 0.43 0.07 0.005 0.009



fluid 4 0.5%salt water at 30°C

Date : 5/31/2019 Remarks : Comments here

Experiment : 33_29 Method : 33.met

Drop phase : Heavy Oil Density : 0.9000

Extern.phase : Brine (05%) Density : 0.9994

Solid phase : Steel Calculation : Optimized cont.

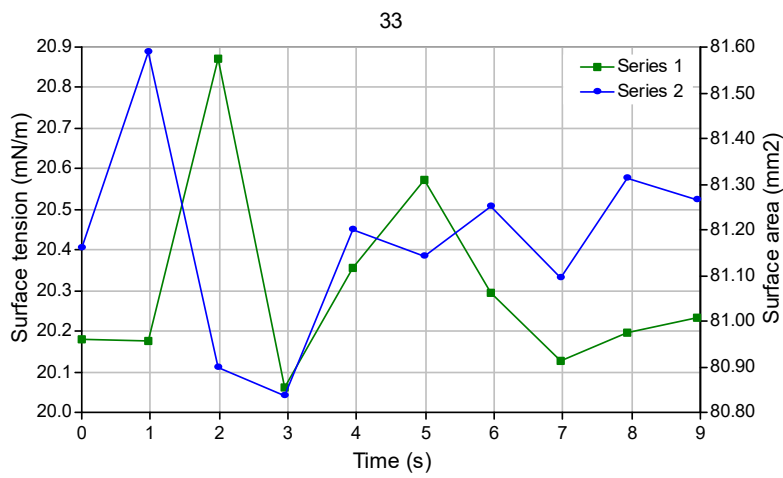
No.	Time	Gamma	Beta	R0	Area	Volume	Theta	Height	Width	Opt
-----	------	-------	------	----	------	--------	-------	--------	-------	-----

1	0.0	19.46	0.274	2.338	82.25	73.74	123.16	5.683	4.948	3
2	0.9	19.46	0.274	2.340	82.93	73.95	123.06	5.691	4.955	2
3	1.9	19.38	0.275	2.337	82.60	73.86	123.08	5.675	4.948	3
4	3.0	19.64	0.272	2.340	82.34	73.94	123.40	5.676	4.953	3
5	4.0	19.46	0.274	2.340	82.33	73.85	123.13	5.686	4.957	3
6	5.0	19.46	0.274	2.337	82.48	73.92	123.21	5.667	4.949	3
7	6.0	19.57	0.273	2.339	82.67	73.79	123.34	5.675	4.954	3
8	7.0	19.64	0.272	2.341	83.20	73.68	123.46	5.684	4.955	3

9	7.9	19.46	0.274	2.338	82.33	73.80	123.18	5.678	4.945	3
10	8.9	19.50	0.274	2.339	82.16	73.74	123.20	5.685	4.942	2

Mean: 19.50 0.273 2.339 82.53 73.83 123.22 5.680 4.951

Stand.dev.: 0.03 0.000 0.000 0.10 0.03 0.04 0.002 0.002



AT 50°C

Date : 5/31/2019 Remarks : Comments here

Experiment : 33_38 Method : 33.met

Drop phase : Heavy Oil Density : 0.9000

Extern.phase : Brine (05%) Density : 0.9917

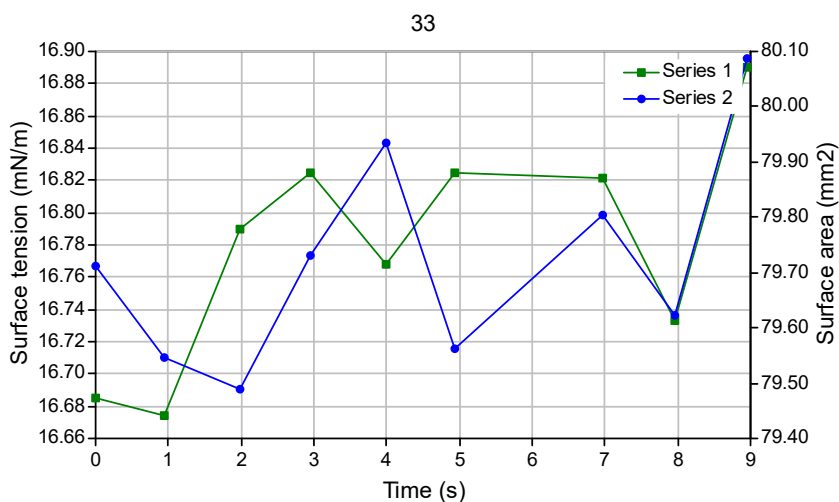
Solid phase : Steel Calculation : Optimized cont.

No. Time Gamma Beta R0 Area Volume Theta Height Width Opt
 Messages

1	0.0	16.75	0.280	2.285	81.04	70.69	119.39	5.794	4.839	2
2	1.0	16.65	0.281	2.282	80.78	70.24	119.29	5.792	4.841	2
3	2.0	16.66	0.281	2.282	80.78	70.64	119.28	5.791	4.828	2
4	2.9	16.61	0.282	2.282	81.17	70.41	119.35	5.793	4.829	2
5	3.9	16.70	0.281	2.283	81.13	70.42	119.35	5.792	4.834	2
6	5.0	16.52	0.283	2.279	80.76	70.23	119.09	5.793	4.825	2
7	6.0	16.63	0.282	2.281	80.79	70.23	119.31	5.791	4.837	2
8	6.9	16.80	0.279	2.283	80.86	70.30	119.80	5.778	4.842	2
9	7.9	16.66	0.281	2.282	81.37	70.24	119.34	5.795	4.829	2
10	9.0	16.64	0.281	2.280	80.92	70.13	119.33	5.790	4.843	2

Mean: 16.66 0.281 2.282 80.96 70.35 119.35 5.791 4.835

Stand.dev.: 0.02 0.000 0.001 0.07 0.06 0.06 0.001 0.002



AT 70°C

Date : 5/31/2019 Remarks : Comments here
 Experiment : 33_46 Method : 33.met
 Drop phase : Heavy Oil Density : 0.9000
 Extern.phase : Brine (05%) Density : 0.9822
 Solid phase : Steel Calculation : Optimized cont.

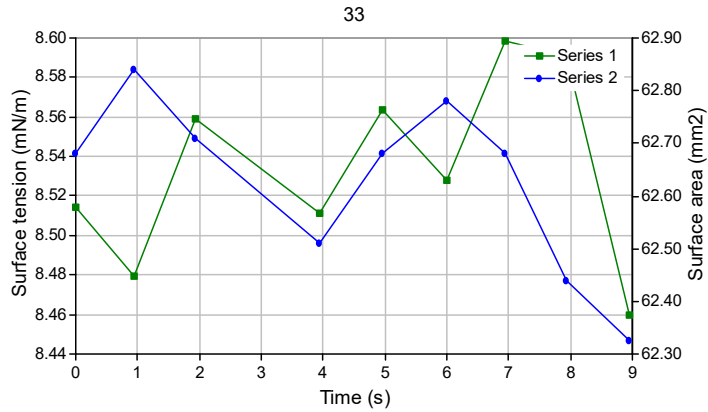
No.	Time	Gamma	Beta	R0	Area	Volume	Theta	Height	Width	Opt
-----	------	-------	------	----	------	--------	-------	--------	-------	-----

Messages

1	0.0	14.95	0.278	2.268	80.29	68.92	119.24	5.776	4.788	2
2	1.0	14.84	0.279	2.265	79.88	68.64	119.06	5.773	4.778	2
3	1.9	14.91	0.278	2.267	80.15	68.92	119.10	5.776	4.783	2
4	3.0	15.08	0.275	2.270	80.23	68.80	119.68	5.760	4.784	2
5	3.9	14.93	0.278	2.267	80.06	68.77	119.19	5.776	4.773	2
6	5.0	14.75	0.280	2.264	79.98	68.71	118.77	5.783	4.772	2
7	5.9	14.79	0.279	2.263	79.73	68.46	118.93	5.775	4.785	2
8	7.0	14.81	0.279	2.265	80.25	68.74	118.88	5.782	4.770	2
9	7.9	14.76	0.280	2.262	79.88	68.55	118.83	5.774	4.775	2
10	9.0	14.95	0.277	2.267	79.76	68.71	119.22	5.774	4.780	2

Mean: 14.88 0.278 2.266 80.02 68.72 119.09 5.775 4.779

Stand.dev.: 0.03 0.000 0.001 0.06 0.05 0.08 0.002 0.002



AT 100°C

Date : 5/31/2019 Remarks : Comments here

Experiment : 33_83 Method : 33.met

Drop phase : Heavy Oil Density : 0.9000

Extern.phase : Brine (05%) Density : 0.9736

Solid phase : Steel Calculation : Optimized cont.

No.	Time	Gamma	Beta	R0	Area	Volume	Theta	Height	Width	Opt
-----	------	-------	------	----	------	--------	-------	--------	-------	-----

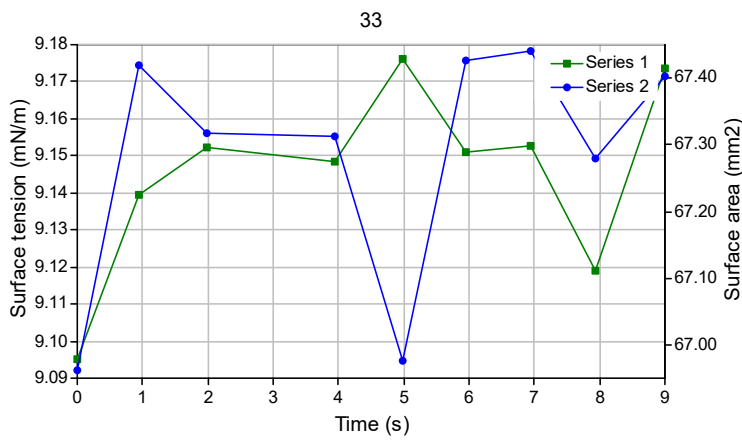
Messages

1	0.0	9.18	0.307	1.976	66.27	48.92	91.45	5.893	4.150	3
2	0.9	9.11	0.308	1.971	66.18	48.73	90.89	5.897	4.152	3
3	2.0	9.21	0.306	1.976	66.44	49.02	91.57	5.892	4.168	3
4	2.9	9.15	0.307	1.973	66.37	48.85	91.04	5.893	4.143	3
5	4.0	9.13	0.308	1.973	66.49	48.86	90.77	5.904	4.160	3
6	4.9	9.13	0.307	1.971	66.58	48.69	91.27	5.887	4.146	3
7	6.0	9.17	0.307	1.974	66.54	48.91	91.52	5.885	4.165	3
8	7.0	9.19	0.306	1.974	66.20	48.84	91.13	5.895	4.168	3
9	8.0	9.18	0.307	1.977	66.59	49.18	91.14	5.903	4.165	3

10 8.9 9.15 0.308 1.974 66.24 48.90 91.18 5.900 4.153 3

Mean: 9.16 0.307 1.974 66.39 48.89 91.20 5.895 4.157

Stand.dev.: 0.01 0.000 0.001 0.05 0.04 0.08 0.002 0.003



Gum 1.5g and Silica 1g in 500ml

At 30°C

Date : 5/14/2019 Remarks : Comments here

Experiment : 03_180 Method : 03.met

Drop phase : Heavy Oil Density : 0.9000

Extern.phase : Brine (15%) Density : 1.0068

Solid phase : Steel Calculation : Optimized cont.

No. Time Gamma Beta R0 Area Volume Theta Height Width Opt
Messages

1	0.0	12.12	0.257	1.724	47.96	28.96	71.44	5.203	3.542	3
2	0.9	12.22	0.255	1.725	47.95	29.12	71.26	5.194	3.552	3
3	2.0	12.33	0.254	1.727	47.83	29.01	70.60	5.197	3.562	3
4	3.0	12.30	0.254	1.726	47.80	28.87	70.36	5.200	3.554	3
5	4.0	12.38	0.252	1.726	48.27	29.08	70.41	5.187	3.565	3
6	5.0	12.27	0.253	1.723	47.21	28.67	70.18	5.194	3.566	3
7	5.9	12.24	0.254	1.723	47.81	29.06	69.53	5.204	3.541	3
8	7.0	12.36	0.253	1.726	47.94	29.01	68.96	5.215	3.546	3
9	8.0	12.25	0.253	1.720	47.64	28.96	68.54	5.204	3.534	3
10	9.0	12.36	0.251	1.722	47.79	29.11	67.96	5.208	3.534	3

Mean: 12.28 0.254 1.724 47.82 28.99 69.92 5.201 3.550

Stand.dev.: 0.03 0.001 0.001 0.09 0.04 0.36 0.002 0.004

At 50°C

Date : 5/14/2019 Remarks : Comments here

Experiment : 03_210 Method : 03.met

Drop phase : Heavy Oil Density : 0.9000

Extern.phase : Brine (15%) Density : 0.9990

Solid phase : Steel Calculation : Optimized cont.

No.	Time	Gamma	Beta	R0	Area	Volume	Theta	Height	Width	Opt
-----	------	-------	------	----	------	--------	-------	--------	-------	-----

Messages

1	0.0	7.47	0.279	1.466	33.44	18.45	118.44	3.749	3.112	2
2	0.9	7.70	0.272	1.468	33.28	18.41	119.61	3.729	3.096	2
3	2.0	7.50	0.278	1.466	33.78	18.50	118.47	3.750	3.096	2
4	2.9	7.53	0.277	1.466	33.36	18.38	118.61	3.746	3.108	2
5	3.9	7.62	0.275	1.467	33.60	18.52	119.00	3.741	3.099	2
6	5.0	7.58	0.275	1.466	33.78	18.40	118.95	3.740	3.106	2
7	6.0	7.44	0.280	1.464	33.36	18.49	118.17	3.749	3.095	2
8	7.0	7.51	0.277	1.464	33.37	18.53	118.54	3.741	3.100	2
9	8.0	7.56	0.276	1.466	33.33	18.39	118.85	3.743	3.088	2
10	9.0	7.49	0.278	1.464	33.47	18.57	118.29	3.747	3.097	2

Mean: 7.54 0.277 1.466 33.48 18.46 118.69 3.743 3.100

Stand.dev.: 0.02 0.001 0.000 0.06 0.02 0.13 0.002 0.002

At 70°C

Date : 5/14/2019 Remarks : Comments here

Experiment : 03_228 Method : 03.met

Drop phase : Light Crude Density : 0.8800

Extern.phase : Brine (15%) Density : 0.9896

Solid phase : Steel Calculation : Optimized cont.

No.	Time	Gamma	Beta	R0	Area	Volume	Theta	Height	Width	Opt
-----	------	-------	------	----	------	--------	-------	--------	-------	-----

Messages

1	0.0	13.37	0.233	1.701	43.59	27.15	120.64	4.306	3.551	2
2	0.9	13.32	0.234	1.701	43.87	27.25	120.48	4.313	3.558	2
3	2.0	13.55	0.230	1.703	43.80	27.30	121.06	4.300	3.570	2
4	3.0	13.48	0.231	1.702	43.77	27.19	120.93	4.308	3.562	2
5	4.0	13.38	0.232	1.700	43.72	27.12	120.77	4.305	3.556	2
6	5.0	13.38	0.232	1.700	43.63	27.07	120.52	4.308	3.539	2
7	6.0	13.29	0.234	1.702	43.74	27.27	120.24	4.319	3.556	2
8	6.9	13.19	0.236	1.700	43.84	27.04	120.20	4.319	3.557	2
9	8.0	13.36	0.233	1.701	43.72	27.20	120.51	4.310	3.555	2
10	9.0	13.36	0.233	1.700	43.91	27.25	120.58	4.304	3.557	2

Mean: 13.37 0.233 1.701 43.76 27.19 120.59 4.309 3.556

Stand.dev.: 0.03 0.000 0.000 0.03 0.03 0.09 0.002 0.002

At 90°C

Drop Shape Image Analysis

Date : 5/14/2019 Remarks : Comments here

Experiment : 03_247 Method : 03.met

Drop phase : Heavy Oil Density : 0.9000

Extern.phase : Brine (15%) Density : 0.9824

Solid phase : Steel Calculation : Optimized cont.

No.	Time	Gamma	Beta	R0	Area	Volume	Theta	Height	Width	Opt
										Messages

1	0.0	7.40	0.253	1.520	36.66	20.11	92.30	4.294	3.172	3	
2	0.9	7.30	0.256	1.519	36.71	20.15	92.15	4.306	3.175	3	
3	1.9	7.37	0.254	1.521	36.74	20.31	91.43	4.309	3.162	3	
4	3.0	7.41	0.253	1.522	37.05	20.38	91.41	4.309	3.183	3	
5	3.9	7.39	0.254	1.523	36.81	20.26	91.10	4.319	3.192	2	
6	5.0	0.00	0.000	0.000	0.00	0.00	0.00	0.000	0.000	0	Sides are too differ
7	6.0	7.43	0.252	1.521	36.63	20.16	90.37	4.314	3.191	2	
8	7.0	7.38	0.254	1.523	36.93	20.24	90.00	4.337	3.186	3	
9	7.9	7.41	0.252	1.522	36.59	20.08	90.04	4.326	3.171	3	
10	9.0	7.39	0.253	1.520	36.69	20.05	89.59	4.327	3.163	3	

=====
Mean: 7.39 0.253 1.521 36.76 20.19 90.93 4.316 3.177

Stand.dev.: 0.01 0.000 0.000 0.05 0.04 0.33 0.004 0.004
=====

At 100°C

Date : 5/14/2019 Remarks : Comments here

Experiment : 03_257 Method : 03.met

Drop phase : Heavy Oil Density : 0.9000

Extern.phase : Brine (15%) Density : 0.9824

Solid phase : Steel Calculation : Optimized cont.

No.	Time	Gamma	Beta	R0	Area	Volume	Theta	Height	Width	Opt	Messages
-----	------	-------	------	----	------	--------	-------	--------	-------	-----	----------

=====
=====

1	0.0	5.78	0.230	1.283	24.46	11.41	126.02	3.139	2.698	2	
2	0.9	5.75	0.231	1.282	24.37	11.51	125.87	3.137	2.695	2	
3	1.9	5.83	0.228	1.282	24.27	11.42	126.12	3.135	2.696	3	
4	3.0	5.83	0.228	1.284	24.41	11.51	126.09	3.137	2.700	3	
5	3.9	5.84	0.228	1.285	24.61	11.57	126.19	3.139	2.696	2	
6	4.9	6.01	0.223	1.288	24.40	11.56	127.14	3.129	2.709	3	
7	6.0	5.84	0.228	1.283	24.47	11.47	126.40	3.135	2.707	3	
8	7.0	0.00	0.000	0.000	0.00	0.00	0.00	0.000	0.000	0	Sides are too differ
9	8.0	5.87	0.227	1.285	24.60	11.53	126.31	3.139	2.709	3	
10	9.0	5.82	0.229	1.283	24.44	11.45	126.22	3.135	2.692	2	

=====
Mean: 5.84 0.228 1.284 24.45 11.49 126.26 3.136 2.700

Stand.dev.: 0.02 0.001 0.001 0.04 0.02 0.12 0.001 0.002
=====

Fluid 3 salt water 10 % at 30 °C

Date : 5/31/2019 Remarks : Comments here

Experiment : 1_69 Method : 1.met

Drop phase : Heavy Oil Density : 0.9000

Extern.phase : Brine (10%) Density : 1.0031

Solid phase : Steel Calculation : Optimized cont.

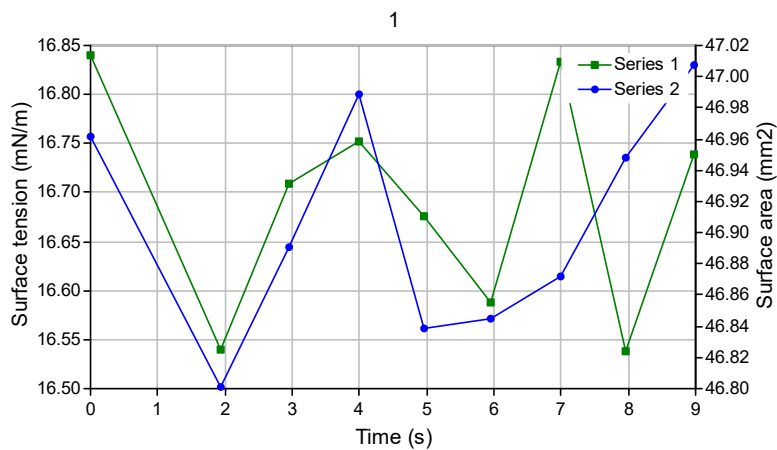
No.	Time	Gamma	Beta	R0	Area	Volume	Theta	Height	Width	Opt
-----	------	-------	------	----	------	--------	-------	--------	-------	-----

Messages

1	0.0	16.52	0.199	1.805	47.09	31.06	130.99	4.311	3.757	2
2	0.9	16.47	0.200	1.805	47.07	31.04	130.78	4.316	3.745	2
3	1.9	16.66	0.198	1.805	47.12	30.96	131.02	4.311	3.749	2
4	2.9	16.51	0.200	1.805	47.21	31.01	130.68	4.319	3.746	2
5	4.0	16.61	0.199	1.806	47.19	31.05	130.89	4.314	3.751	2
6	5.0	16.81	0.197	1.808	47.23	31.04	131.15	4.315	3.754	2
7	6.0	16.52	0.200	1.805	47.25	31.01	130.72	4.319	3.756	2
8	7.0	16.67	0.198	1.807	47.18	31.10	130.84	4.318	3.745	2
9	7.9	16.40	0.201	1.805	47.20	31.03	130.48	4.323	3.748	2
10	9.0	16.68	0.198	1.806	47.12	31.05	130.82	4.317	3.750	2

Mean: 16.59 0.199 1.806 47.17 31.03 130.84 4.316 3.750

Stand.dev.: 0.04 0.000 0.000 0.02 0.01 0.06 0.001 0.001



AT 50°C

Date : 5/31/2019 Remarks : Comments here

Experiment : 1_84 Method : 1.met
 Drop phase : Heavy Oil Density : 0.9000
 Extern.phase : Brine (10%) Density : 0.9954
 Solid phase : Steel Calculation : Optimized cont.

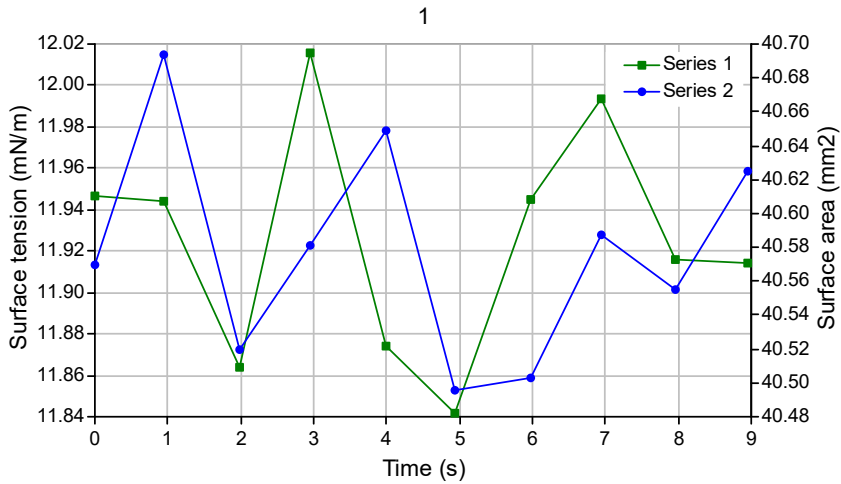
No.	Time	Gamma	Beta	R0	Area	Volume	Theta	Height	Width	Opt
-----	------	-------	------	----	------	--------	-------	--------	-------	-----

Messages

1	0.0	11.76	0.217	1.653	40.69	24.53	121.83	4.152	3.445	2
2	0.9	11.86	0.216	1.653	40.73	24.50	122.27	4.143	3.447	2
3	2.0	11.91	0.215	1.655	40.89	24.57	122.38	4.145	3.457	2
4	2.9	11.85	0.216	1.653	40.73	24.53	122.15	4.143	3.446	2
5	4.0	11.73	0.218	1.652	40.86	24.56	121.57	4.153	3.456	2
6	5.0	11.83	0.216	1.654	40.93	24.55	122.23	4.148	3.457	2
7	6.0	11.82	0.217	1.655	40.78	24.64	121.86	4.156	3.453	2
8	7.0	11.75	0.218	1.653	40.76	24.54	121.85	4.154	3.446	2
9	8.0	11.83	0.216	1.654	40.74	24.58	122.16	4.150	3.454	2
10	9.0	11.85	0.216	1.655	40.89	24.62	122.08	4.150	3.458	2

Mean: 11.82 0.216 1.653 40.80 24.56 122.04 4.149 3.452

Stand.dev.: 0.02 0.000 0.000 0.03 0.01 0.08 0.001 0.002



AT 70°C

Date : 5/31/2019 Remarks : Comments here

Experiment : 1_105 Method : 1.met

Drop phase : Heavy Oil Density : 0.9000

Extern.phase : Brine (10%) Density : 0.9859

Solid phase : Steel Calculation : Optimized cont.

No.	Time	Gamma	Beta	R0	Area	Volume	Theta	Height	Width	Opt
-----	------	-------	------	----	------	--------	-------	--------	-------	-----

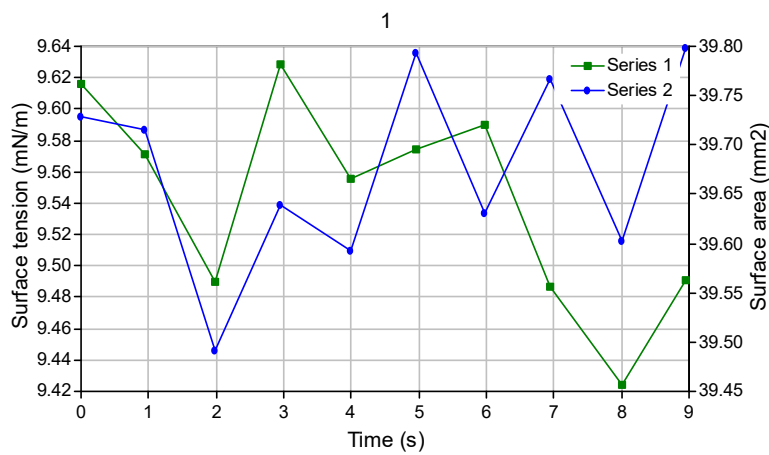
Messages

1	0.0	9.62	0.227	1.611	39.73	23.14	115.26	4.168	3.376	2
2	0.9	9.57	0.229	1.611	39.72	23.19	114.92	4.177	3.372	2
3	2.0	9.49	0.230	1.609	39.49	23.13	114.75	4.178	3.369	2
4	2.9	9.63	0.227	1.612	39.64	23.22	115.26	4.172	3.357	2
5	4.0	9.56	0.229	1.612	39.59	23.29	114.55	4.183	3.368	2
6	5.0	9.57	0.228	1.610	39.79	23.19	114.83	4.176	3.373	2
7	6.0	9.59	0.228	1.611	39.63	23.14	115.16	4.172	3.366	2

8	7.0	9.49	0.230	1.609	39.77	23.21	114.25	4.183	3.364	2
9	8.0	9.42	0.232	1.609	39.60	23.15	114.35	4.189	3.373	2
10	8.9	9.49	0.230	1.610	39.80	23.18	114.32	4.185	3.361	2

Mean: 9.54 0.229 1.610 39.68 23.18 114.76 4.179 3.368

Stand.dev.: 0.02 0.000 0.000 0.03 0.02 0.12 0.002 0.002



AT 90°C

Date : 5/31/2019 Remarks : Comments here

Experiment : 1_134 Method : 1.met

Drop phase : Heavy Oil Density : 0.9000

Extern.phase : Brine (10%) Density : 0.9859

Solid phase : Steel Calculation : Optimized cont.

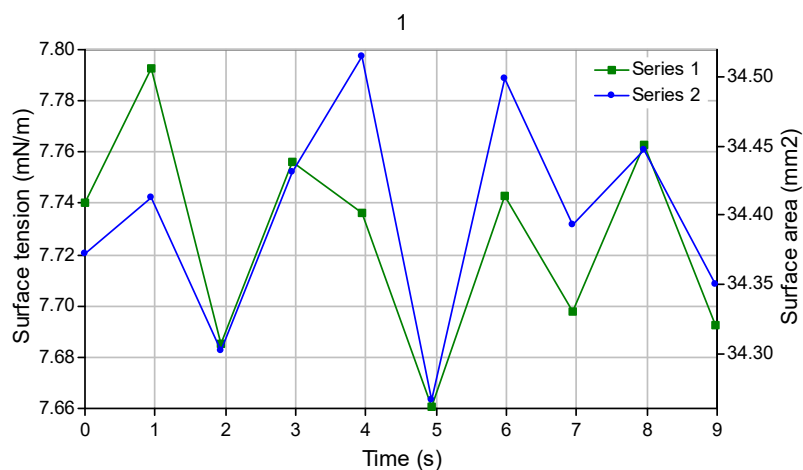
No.	Time	Gamma	Beta	R0	Area	Volume	Theta	Height	Width	Opt
-----	------	-------	------	----	------	--------	-------	--------	-------	-----

Messages

1	0.0	7.74	0.239	1.482	34.37	18.44	105.60	3.987	3.098	2
2	1.0	7.79	0.239	1.486	34.41	18.52	105.64	3.994	3.113	2
3	1.9	7.69	0.241	1.484	34.30	18.46	105.21	4.004	3.117	2
4	2.9	7.76	0.240	1.485	34.43	18.51	105.26	4.000	3.106	2
5	3.9	7.74	0.240	1.484	34.51	18.51	105.58	3.995	3.114	2
6	4.9	7.66	0.242	1.482	34.27	18.41	105.41	3.998	3.102	2
7	6.0	7.74	0.240	1.485	34.50	18.51	105.22	4.003	3.118	2
8	7.0	7.70	0.241	1.482	34.39	18.44	105.25	3.997	3.117	2
9	7.9	7.76	0.239	1.484	34.45	18.47	105.54	3.995	3.116	2
10	9.0	7.69	0.241	1.482	34.35	18.44	105.06	3.997	3.109	2

Mean: 7.73 0.240 1.484 34.40 18.47 105.38 3.997 3.111

Stand.dev.: 0.01 0.000 0.000 0.03 0.01 0.06 0.002 0.002



AT 100°C

Date : 5/31/2019 Remarks : Comments here

Experiment : 1_160 Method : 1.met

Drop phase : Heavy Oil Density : 0.9000

Extern.phase : Brine (10%) Density : 0.9778

Solid phase : Steel Calculation : Optimized cont.

No.	Time	Gamma	Beta	R0	Area	Volume	Theta	Height	Width	Opt	Messages
1	0.0	0.00	0.000	0.000	0.00	0.00	0.000	0.000	0		Sides are too differ
2	0.9	5.51	0.175	1.125	17.61	7.24	137.17	2.550	2.341	3	
3	2.0	5.58	0.173	1.126	17.57	7.24	137.37	2.558	2.348	3	
4	2.9	5.51	0.176	1.126	17.67	7.26	137.00	2.561	2.348	3	
5	4.0	5.28	0.182	1.124	17.67	7.27	136.04	2.568	2.344	3	
6	5.0	5.68	0.171	1.129	17.62	7.25	137.76	2.558	2.347	3	
7	6.0	5.37	0.180	1.125	17.62	7.25	136.52	2.564	2.344	3	
8	7.0	5.57	0.174	1.128	17.64	7.28	137.29	2.557	2.358	3	
9	8.0	0.00	0.000	0.000	0.00	0.00	0.000	0.000	0		Sides are too differ
10	9.0	5.46	0.177	1.125	17.59	7.23	136.83	2.561	2.337	3	

Mean: 5.50 0.176 1.126 17.62 7.25 137.00 2.560 2.346

Stand.dev.: 0.04 0.001 0.001 0.01 0.01 0.19 0.002 0.002

Date : 5/31/2019 Remarks : Comments here

Experiment : 1_163 Method : 1.met

Drop phase : Heavy Oil Density : 0.9000

Extern.phase : Brine (10%) Density : 0.9778

Solid phase : Steel Calculation : Optimized cont.

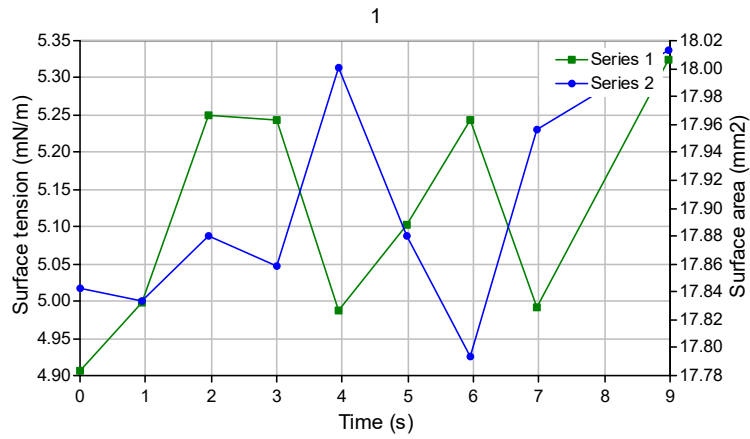
No.	Time	Gamma	Beta	R0	Area	Volume	Theta	Height	Width	Opt
-----	------	-------	------	----	------	--------	-------	--------	-------	-----

Messages

1	0.0	4.91	0.195	1.120	17.84	7.35	133.01	2.623	2.354	3
2	1.0	5.00	0.193	1.123	17.83	7.34	133.57	2.624	2.357	4
3	2.0	5.25	0.184	1.125	17.88	7.36	134.68	2.612	2.359	3
4	3.0	5.24	0.184	1.125	17.86	7.33	134.78	2.612	2.352	3
5	4.0	4.99	0.193	1.123	18.00	7.40	133.19	2.628	2.341	3
6	5.0	5.10	0.189	1.125	17.88	7.37	133.95	2.623	2.358	3
7	5.9	5.24	0.184	1.124	17.79	7.30	134.83	2.609	2.349	3
8	7.0	4.99	0.193	1.124	17.96	7.39	133.23	2.629	2.359	3
9	7.9	0.00	0.000	0.000	0.00	0.00	0.000	0.000	0	Error in profile
10	9.0	5.32	0.182	1.127	18.01	7.39	135.05	2.612	2.347	4

Mean: 5.12 0.189 1.124 17.90 7.36 134.03 2.619 2.353

Stand.dev.: 0.05 0.002 0.001 0.03 0.01 0.27 0.003 0.002



fluid 2

At 30°C

Date : 5/13/2019 Remarks : Comments here

Experiment : 03_34 Method : 03.met

Drop phase : Light Crude Density : 0.8800

Extern.phase : Brine (15%) Density : 1.0155

Solid phase : Steel Calculation : Optimized cont.

No.	Time	Gamma	Beta	R0	Area	Volume	Theta	Height	Width	Opt
-----	------	-------	------	----	------	--------	-------	--------	-------	-----

Messages

1	0.0	8.84	0.305	1.424	34.29	18.33	100.06	4.077	3.037	2
2	1.0	8.76	0.307	1.422	34.08	18.25	99.90	4.081	3.008	3
3	2.0	8.88	0.304	1.425	34.01	18.25	99.99	4.082	3.037	2
4	3.0	8.87	0.305	1.426	34.01	18.25	100.15	4.083	3.043	2
5	3.9	8.79	0.307	1.424	34.02	18.24	99.59	4.092	3.026	2

6	5.0	8.76	0.308	1.424	34.45	18.28	98.81	4.108	3.028	2
7	6.0	8.76	0.306	1.421	34.23	18.37	99.18	4.086	3.021	2
8	7.0	8.74	0.308	1.423	34.10	18.16	98.27	4.120	3.022	2
9	7.9	8.90	0.304	1.426	34.19	18.21	99.02	4.102	3.019	3
10	9.0	8.79	0.306	1.423	34.26	18.17	98.43	4.109	3.024	2

=====
Mean: 8.81 0.306 1.424 34.16 18.25 99.34 4.094 3.026

Stand.dev.: 0.02 0.000 0.001 0.05 0.02 0.22 0.005 0.003
=====

At 50°C

Date : 5/13/2019 Remarks : Comments here

Experiment : 03_79 Method : 03.met

Drop phase : Light Crude Density : 0.8800

Extern.phase : Brine (15%) Density : 1.0118

Solid phase : Steel Calculation : Optimized cont.

No.	Time	Gamma	Beta	R0	Area	Volume	Theta	Height	Width	Opt
-----	------	-------	------	----	------	--------	-------	--------	-------	-----

Messages

1	0.0	6.49	0.307	1.243	25.31	12.11	108.87	3.390	2.623	3
2	0.9	6.56	0.305	1.244	25.28	12.07	109.10	3.391	2.628	2
3	2.0	6.47	0.308	1.242	25.24	12.01	108.41	3.400	2.631	2
4	3.0	6.54	0.305	1.243	25.33	12.07	109.28	3.387	2.631	2
5	4.0	6.62	0.303	1.245	25.26	12.05	109.54	3.387	2.634	2
6	5.0	6.53	0.305	1.242	25.23	11.95	109.39	3.384	2.633	2

7	6.0	6.48	0.308	1.243	25.32	12.05	108.67	3.398	2.631	2
8	6.9	6.57	0.304	1.244	25.33	12.03	109.49	3.384	2.633	2
9	8.0	6.59	0.304	1.245	25.35	12.02	109.29	3.392	2.631	3
10	8.9	6.55	0.305	1.243	25.27	12.04	109.11	3.390	2.622	3

=====
Mean: 6.54 0.306 1.243 25.29 12.04 109.11 3.391 2.630

Stand.dev.: 0.02 0.001 0.000 0.01 0.01 0.12 0.002 0.001
=====

At 70°C

Date : 5/13/2019 Remarks : Comments here

Experiment : 03_122 Method : 03.met

Drop phase : Light Crude Density : 0.8800

Extern.phase : Brine (15%) Density : 1.0185

Solid phase : Steel Calculation : Optimized cont.

No.	Time	Gamma	Beta	R0	Area	Volume	Theta	Height	Width	Opt
-----	------	-------	------	----	------	--------	-------	--------	-------	-----

Messages

1	0.0	10.16	0.227	1.303	24.68	11.97	129.92	3.053	2.723	2
2	0.9	9.92	0.231	1.298	24.58	12.02	129.28	3.053	2.708	2
3	2.0	10.02	0.229	1.299	24.49	11.97	129.49	3.055	2.706	2
4	2.9	9.99	0.230	1.301	24.69	12.00	129.32	3.061	2.716	2
5	4.0	10.17	0.227	1.302	24.62	11.94	129.86	3.057	2.722	3
6	4.9	9.86	0.232	1.298	24.47	11.97	129.02	3.060	2.713	2
7	6.0	9.89	0.232	1.299	24.61	11.90	129.10	3.063	2.709	2
8	6.9	10.20	0.226	1.302	24.55	12.02	129.92	3.054	2.725	3

9	8.0	9.85	0.232	1.298	24.64	11.95	129.02	3.060	2.707	2
10	9.0	10.00	0.229	1.300	24.55	12.06	129.37	3.059	2.720	3

Mean: 10.01 0.230 1.300 24.59 11.98 129.43 3.057 2.715

Stand.dev.: 0.04 0.001 0.001 0.02 0.01 0.11 0.001 0.002

At 90°C

Date : 5/13/2019 Remarks : Comments here

Experiment : 03_140 Method : 03.met

Drop phase : Light Crude Density : 0.8800

Extern.phase : Brine (15%) Density : 1.0185

Solid phase : Steel Calculation : Optimized cont.

No.	Time	Gamma	Beta	R0	Area	Volume	Theta	Height	Width	Opt
-----	------	-------	------	----	------	--------	-------	--------	-------	-----

Messages

1	0.0	10.06	0.240	1.333	26.23	13.09	127.67	3.178	2.788	2
2	0.9	10.01	0.241	1.333	26.21	13.18	127.39	3.182	2.795	2
3	1.9	10.17	0.238	1.334	26.23	13.12	127.94	3.173	2.803	3
4	3.0	10.11	0.239	1.333	26.15	13.15	127.65	3.182	2.797	2
5	3.9	10.23	0.237	1.336	26.38	13.17	127.99	3.183	2.804	2
6	5.0	10.23	0.237	1.335	26.15	13.13	128.16	3.173	2.806	3
7	5.9	10.16	0.239	1.335	26.32	13.14	127.90	3.180	2.802	2
8	7.0	10.22	0.237	1.335	26.22	13.16	127.99	3.176	2.804	2
9	8.0	10.10	0.240	1.334	26.42	13.12	127.76	3.179	2.805	2
10	8.9	10.26	0.236	1.335	26.42	13.09	128.17	3.177	2.800	2

Mean: 10.15 0.238 1.334 26.27 13.13 127.86 3.178 2.800

Stand.dev.: 0.03 0.001 0.000 0.03 0.01 0.08 0.001 0.002

At 100°C

Drop Shape Image Analysis

Date : 5/13/2019 Remarks : Comments here

Experiment : 03_158 Method : 03.met

Drop phase : Light Crude Density : 0.8800

Extern.phase : Brine (15%) Density : 1.0185

Solid phase : Steel Calculation : Optimized cont.

No.	Time	Gamma	Beta	R0	Area	Volume	Theta	Height	Width	Opt
-----	------	-------	------	----	------	--------	-------	--------	-------	-----

Messages

1	0.0	9.46	0.280	1.396	31.14	16.42	111.03	3.756	2.953	2
2	0.9	9.47	0.280	1.396	31.17	16.46	111.07	3.756	2.952	2
3	2.0	9.49	0.279	1.397	31.20	16.48	111.35	3.750	2.957	2
4	3.0	9.49	0.279	1.397	31.15	16.43	111.36	3.752	2.956	2
5	4.0	9.57	0.277	1.398	31.20	16.46	111.40	3.750	2.959	2
6	4.9	9.46	0.280	1.396	31.25	16.49	110.98	3.756	2.953	2
7	6.0	9.56	0.278	1.398	31.23	16.48	111.56	3.747	2.956	2
8	7.0	9.57	0.278	1.398	31.19	16.46	111.54	3.749	2.958	2

9	8.0	9.56	0.278	1.398	31.19	16.44	111.56	3.748	2.957	2
10	9.0	9.55	0.278	1.398	31.12	16.44	111.94	3.745	2.959	2

Mean: 9.52 0.279 1.397 31.18 16.45 111.38 3.751 2.956

Stand.dev.: 0.01 0.000 0.000 0.01 0.01 0.09 0.001 0.001

Distilled water Fluid 4 at 30°C

Date : 6/5/2019 Remarks : Comments here

Experiment : 100_74 Method : 100.met

Drop phase : Heavy Oil Density : 0.9000

Extern.phase : Water Density : 0.9987

Solid phase : Steel Calculation : Optimized cont.

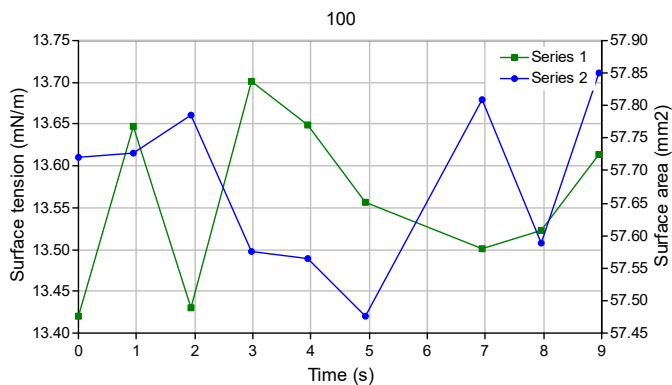
No.	Time	Gamma	Beta	R0	Area	Volume	Theta	Height	Width	Opt
-----	------	-------	------	----	------	--------	-------	--------	-------	-----

Messages

1	0.0	13.80	0.268	1.954	58.14	43.04	121.23	4.906	4.120	2
2	1.0	13.60	0.271	1.953	58.27	43.12	120.59	4.921	4.117	2
3	2.0	13.79	0.268	1.954	58.07	42.97	121.02	4.913	4.096	3
4	2.9	13.64	0.270	1.951	58.15	42.95	120.64	4.917	4.099	2
5	4.0	13.59	0.271	1.951	58.21	43.12	120.65	4.912	4.113	2
6	5.0	13.69	0.269	1.951	58.17	43.01	120.69	4.916	4.094	2
7	6.0	13.63	0.271	1.952	58.54	43.11	120.65	4.917	4.103	2
8	7.0	13.72	0.269	1.952	58.24	43.06	120.88	4.910	4.098	2
9	7.9	13.79	0.268	1.954	58.32	43.14	120.90	4.916	4.101	2
10	8.9	13.66	0.270	1.950	58.22	42.89	120.78	4.912	4.088	2

Mean: 13.69 0.270 1.952 58.23 43.04 120.80 4.914 4.103

Stand.dev.: 0.03 0.000 0.000 0.04 0.03 0.07 0.001 0.003



At 50°C

Date : 6/5/2019 Remarks : Comments here

Experiment : 100_94 Method : 100.met

Drop phase : Heavy Oil Density : 0.9000

Extern.phase : distilled water Density : 0.9881

Solid phase : Steel Calculation : Optimized cont.

No.	Time	Gamma	Beta	R0	Area	Volume	Theta	Height	Width	Opt
-----	------	-------	------	----	------	--------	-------	--------	-------	-----

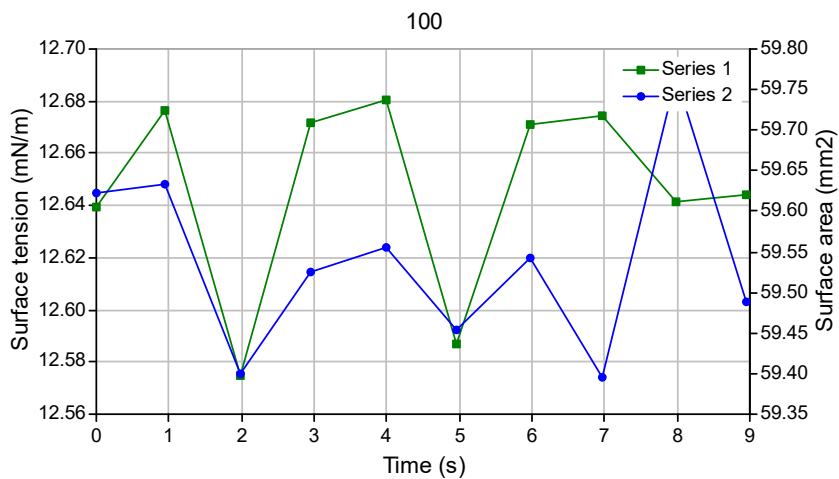
Messages

1	0.0	12.58	0.265	1.964	60.10	43.72	109.57	5.282	4.101	3
2	0.9	12.61	0.265	1.966	60.17	43.86	109.84	5.278	4.113	3
3	1.9	12.57	0.265	1.963	60.22	43.78	109.60	5.277	4.112	3
4	3.0	12.53	0.266	1.963	60.18	43.70	109.55	5.282	4.109	3
5	4.0	12.59	0.265	1.964	60.43	43.73	109.70	5.278	4.098	3

6	4.9	12.53	0.266	1.962	60.20	43.76	109.48	5.279	4.098	3
7	6.0	12.61	0.265	1.965	60.21	43.84	109.69	5.279	4.107	3
8	6.9	12.71	0.263	1.967	60.45	43.82	109.77	5.278	4.120	3
9	8.0	12.54	0.266	1.964	60.14	43.72	109.79	5.279	4.102	3
10	8.9	0.00	0.000	0.000	0.00	0.00	0.000	0.000	0	Sides are too differ

Mean: 12.58 0.265 1.964 60.23 43.77 109.67 5.279 4.107

Stand.dev.: 0.02 0.000 0.000 0.04 0.02 0.04 0.001 0.003



At 70°C

Date : 6/5/2019 Remarks : Comments here

Experiment : 100_126 Method : 100.met

Drop phase : Heavy Oil Density : 0.9000

Extern.phase : distilled water Density : 0.9785

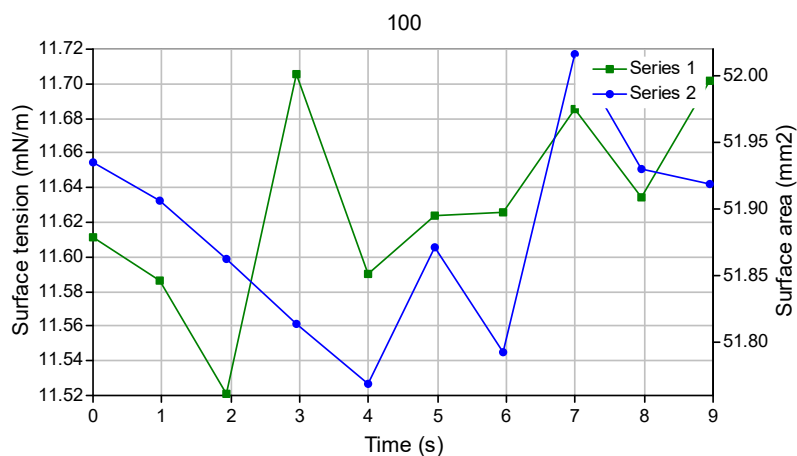
Solid phase : Steel Calculation : Optimized cont.

No.	Time	Gamma	Beta	R0	Area	Volume	Theta	Height	Width	Opt Messages
-----	------	-------	------	----	------	--------	-------	--------	-------	--------------

1	0.0	11.61	0.233	1.874	51.93	35.86	124.06	4.644	3.901	2
2	1.0	11.59	0.233	1.872	51.91	35.84	124.05	4.640	3.899	2
3	1.9	11.52	0.234	1.873	51.86	35.74	123.85	4.651	3.910	2
4	2.9	11.71	0.231	1.876	51.81	35.83	124.28	4.643	3.923	2
5	4.0	11.59	0.233	1.874	51.77	35.81	123.97	4.647	3.907	2
6	4.9	11.62	0.233	1.874	51.87	35.80	124.12	4.642	3.904	2
7	5.9	11.63	0.233	1.874	51.79	35.81	123.98	4.646	3.905	2
8	7.0	11.69	0.232	1.875	52.02	35.73	124.14	4.648	3.903	2
9	7.9	11.63	0.233	1.876	51.93	35.96	124.05	4.649	3.904	2
10	8.9	11.70	0.231	1.874	51.92	35.73	124.23	4.643	3.904	2

Mean: 11.63 0.233 1.874 51.88 35.81 124.07 4.645 3.906

Stand.dev.: 0.02 0.000 0.000 0.02 0.02 0.04 0.001 0.002

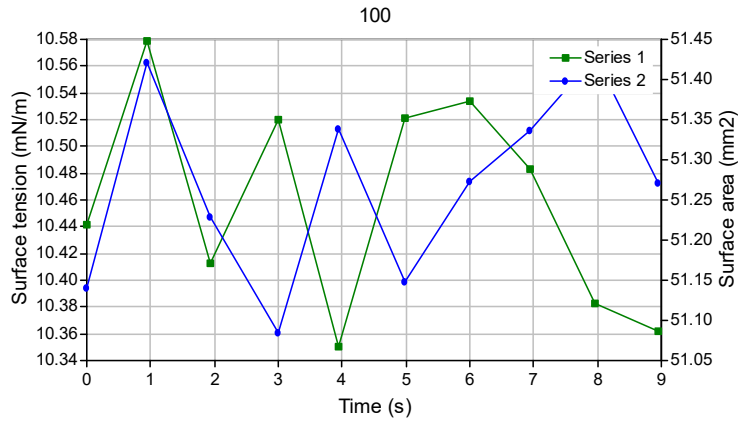


At 90°C

Date : 6/5/2019 Remarks : Comments here

Experiment : 100_150 Method : 100.met
 Drop phase : Heavy Oil Density : 0.9000
 Extern.phase : distilled water Density : 0.9704
 Solid phase : Steel Calculation : Optimized cont.

No.	Time	Gamma	Beta	R0	Area	Volume	Theta	Height	Width	Opt	Messages
1	0.0	10.61	0.225	1.860	51.05	34.67	121.71	4.671	3.868	2	
2	1.0	0.00	0.000	0.000	0.00	0.00	0.000	0.000	0		Sides are too differ
3	1.9	10.73	0.223	1.863	51.29	34.72	121.95	4.672	3.854	3	
4	3.0	10.68	0.224	1.862	51.05	34.74	122.00	4.669	3.879	2	
5	4.0	10.62	0.225	1.860	51.41	34.78	121.71	4.670	3.856	3	
6	5.0	10.60	0.225	1.859	51.31	34.66	121.72	4.671	3.855	3	
7	6.0	10.51	0.227	1.858	51.21	34.65	121.35	4.675	3.852	3	
8	7.0	10.56	0.226	1.858	51.07	34.64	121.59	4.670	3.856	2	
9	8.0	10.54	0.226	1.858	51.25	34.65	121.31	4.675	3.862	2	
10	9.0	10.72	0.223	1.862	51.35	34.79	121.99	4.671	3.872	2	
Mean: 10.62 0.225 1.860 51.22 34.70 121.70 4.672 3.862 Stand.dev.: 0.03 0.000 0.001 0.05 0.02 0.09 0.001 0.003											



At 100°C

Date : 6/5/2019 Remarks : Comments here
 Experiment : 100_181 Method : 100.met
 Drop phase : Heavy Oil Density : 0.9000
 Extern.phase : distilled water Density : 0.9692
 Solid phase : Steel Calculation : Optimized cont.

No.	Time	Gamma	Beta	R0	Area	Volume	Theta	Height	Width	Opt
-----	------	-------	------	----	------	--------	-------	--------	-------	-----

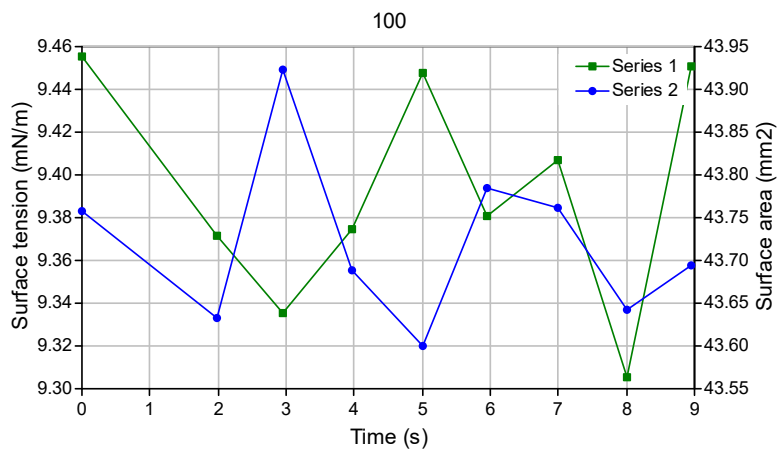


1	0.0	9.67	0.211	1.733	43.30	27.41	129.78	4.147	3.597	2
2	0.9	9.60	0.212	1.733	43.42	27.55	129.51	4.152	3.583	3
3	2.0	9.58	0.213	1.733	43.36	27.53	129.47	4.153	3.605	2
4	2.9	9.64	0.212	1.733	43.56	27.46	129.80	4.145	3.608	2
5	4.0	9.65	0.211	1.734	43.32	27.47	129.79	4.149	3.594	2
6	4.9	0.00	0.000	0.000	0.00	0.00	0.000	0.000	0	Error in profile
7	6.0	9.60	0.213	1.734	43.23	27.49	129.48	4.157	3.605	2

8	7.0	9.56	0.213	1.731	43.27	27.40	129.36	4.152	3.602	2
9	8.0	9.57	0.213	1.732	43.36	27.48	129.38	4.156	3.598	2
10	9.0	9.51	0.214	1.732	43.36	27.44	129.20	4.159	3.590	2

Mean: 9.60 0.212 1.733 43.35 27.47 129.53 4.152 3.598

Stand.dev.: 0.02 0.000 0.000 0.03 0.02 0.07 0.002 0.003



Distilled water Fluid 3 at 30°C

Date : 6/6/2019 Remarks : Comments here

Experiment : 022_343 Method : 022.met

Drop phase : Heavy Oil Density : 0.9000

Extern.phase : distilled water Density : 0.9957

Solid phase : Steel Calculation : Optimized cont.

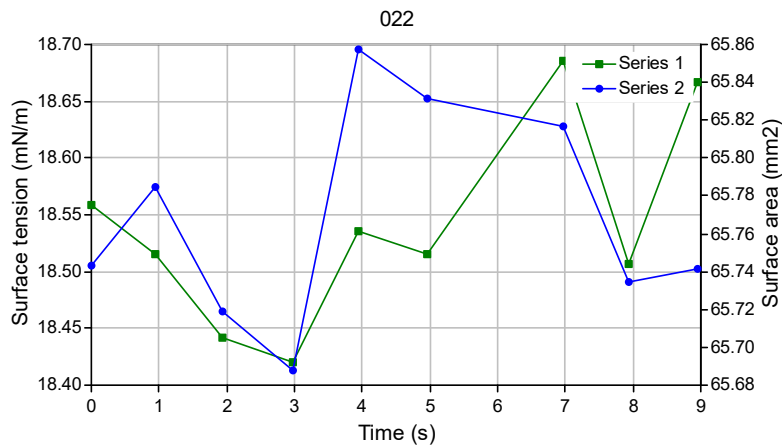
No.	Time	Gamma	Beta	R0	Area	Volume	Theta	Height	Width	Opt
-----	------	-------	------	----	------	--------	-------	--------	-------	-----

1	0.0	17.63	0.239	2.118	66.74	52.70	126.53	5.139	4.435	2
---	-----	-------	-------	-------	-------	-------	--------	-------	-------	---

2	1.0	17.67	0.239	2.119	66.74	52.80	126.51	5.142	4.432	2
3	1.9	17.91	0.236	2.122	66.94	52.83	126.93	5.137	4.453	2
4	3.0	17.75	0.238	2.120	66.81	52.79	126.64	5.141	4.446	2
5	3.9	17.66	0.239	2.119	66.78	52.82	126.44	5.144	4.437	2
6	5.0	17.66	0.239	2.119	66.66	52.68	126.56	5.143	4.436	2
7	6.0	17.61	0.239	2.117	66.93	52.57	126.46	5.141	4.432	2
8	7.0	17.41	0.241	2.116	66.48	52.84	126.14	5.140	4.449	3
9	7.9	17.65	0.239	2.119	67.10	52.63	126.42	5.149	4.439	2
10	9.0	17.69	0.239	2.120	66.76	52.66	126.63	5.143	4.434	2

Mean: 17.66 0.239 2.119 66.79 52.73 126.52 5.142 4.439

Stand.dev.: 0.04 0.000 0.001 0.05 0.03 0.06 0.001 0.002



AT 50°C

Date : 6/6/2019 Remarks : Comments here

Experiment : 022_363 Method : 022.met

Drop phase : Heavy Oil Density : 0.9000

Extern.phase : distilled water Density : 0.9881

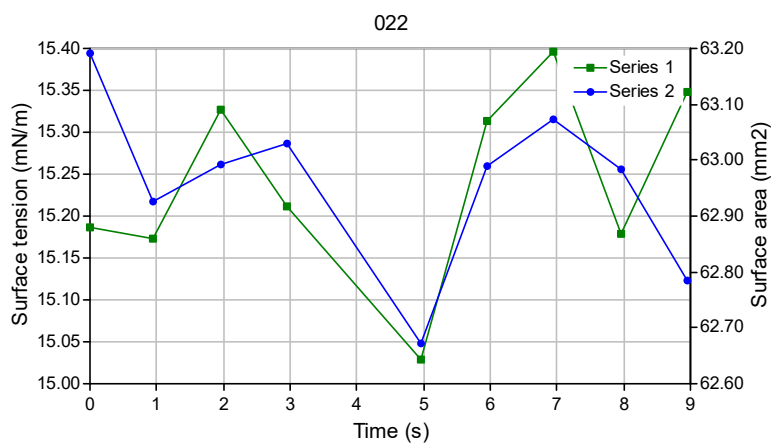
Solid phase : Steel Calculation : Optimized cont.

No. Time Gamma Beta R0 Area Volume Theta Height Width Opt
Messages

1	0.0	14.83	0.248	2.062	62.28	48.18	126.12	4.980	4.328	2
2	0.9	14.79	0.248	2.062	62.27	48.28	125.96	4.986	4.329	2
3	2.0	14.71	0.250	2.063	62.38	48.30	125.79	4.990	4.336	2
4	3.0	14.65	0.250	2.060	62.31	48.25	125.75	4.985	4.322	2
5	4.0	14.57	0.252	2.061	62.34	48.30	125.42	4.997	4.328	2
6	4.9	14.78	0.249	2.064	62.46	48.33	126.04	4.981	4.328	2
7	6.0	14.51	0.253	2.061	62.32	48.29	125.38	4.995	4.328	2
8	6.9	14.64	0.251	2.061	62.30	48.25	125.70	4.989	4.331	2
9	8.0	14.60	0.252	2.062	62.52	48.23	125.52	4.999	4.328	2
10	9.0	14.68	0.251	2.063	62.21	48.40	125.77	4.988	4.342	2

Mean: 14.67 0.250 2.062 62.34 48.28 125.75 4.989 4.330

Stand.dev.: 0.03 0.001 0.000 0.03 0.02 0.08 0.002 0.002



AT 70°C

Date : 6/6/2019 Remarks : Comments here

Experiment : 022_372 Method : 022.met

Drop phase : Heavy Oil Density : 0.9000

Extern.phase : distilled water Density : 0.9739

Solid phase : Steel Calculation : Optimized cont.

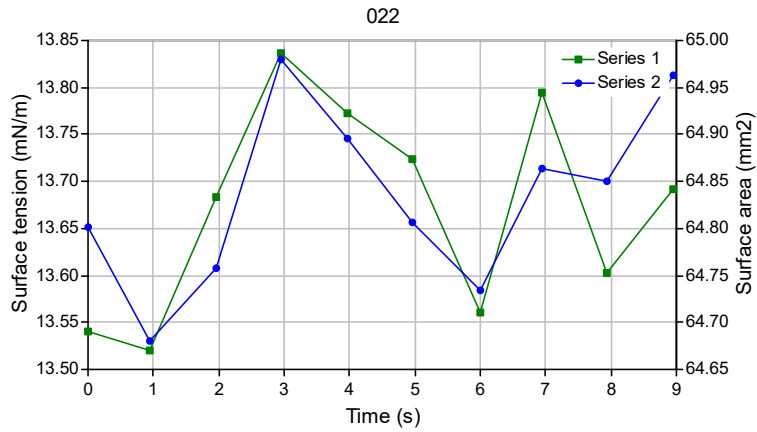
No.	Time	Gamma	Beta	R0	Area	Volume	Theta	Height	Width	Opt
-----	------	-------	------	----	------	--------	-------	--------	-------	-----

Messages

1		0.0	13.51	0.236	2.099	64.94	50.64	125.45	5.153	4.389	2
2		0.9	13.51	0.237	2.100	65.06	50.68	125.49	5.157	4.400	2
3		1.9	13.67	0.234	2.101	64.92	50.68	125.76	5.151	4.394	2
4		3.0	13.59	0.235	2.100	64.96	50.66	125.84	5.145	4.399	2
5		4.0	13.70	0.234	2.101	65.07	50.71	125.73	5.153	4.390	2
6	5.0	0.00	0.000	0.000	0.00	0.00	0.00	0.000	0.000	0	Error in profile
7		5.9	13.63	0.234	2.099	64.80	50.50	125.92	5.142	4.394	2
8		6.9	13.65	0.235	2.102	65.15	50.74	125.69	5.156	4.394	2
9		7.9	13.80	0.232	2.101	64.91	50.51	126.33	5.134	4.387	2
10		9.0	13.63	0.234	2.098	64.96	50.51	125.66	5.148	4.383	2

Mean: 13.63 0.235 2.100 64.97 50.63 125.76 5.149 4.392

Stand.dev.: 0.03 0.000 0.000 0.03 0.03 0.09 0.002 0.002



AT 90°C

Date : 6/6/2019 Remarks : Comments here

Experiment : 022_397 Method : 022.met

Drop phase : Heavy Oil Density : 0.9000

Extern.phase : distilled water Density : 0.9704

Solid phase : Steel Calculation : Optimized cont.

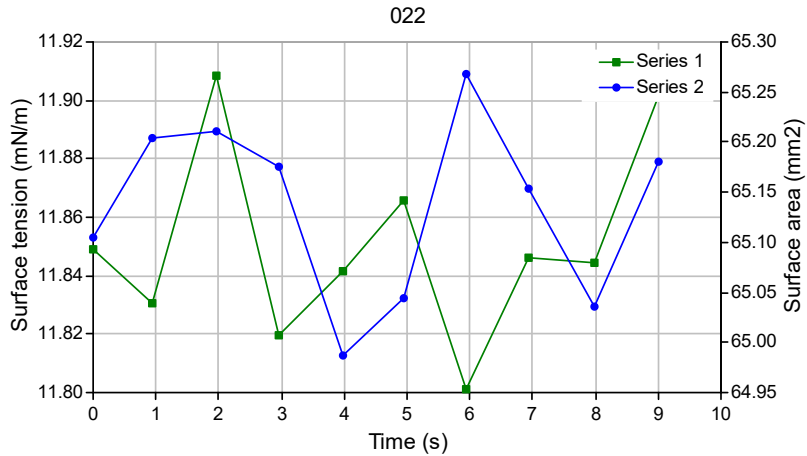
No.	Time	Gamma	Beta	R0	Area	Volume	Theta	Height	Width	Opt	Messages
-----	------	-------	------	----	------	--------	-------	--------	-------	-----	----------

1	0.0	12.02	0.244	2.059	65.24	49.26	109.17	5.481	4.311	2	
2	1.0	12.06	0.243	2.058	65.05	48.98	109.17	5.476	4.309	2	
3	2.0	11.96	0.245	2.058	65.09	49.05	109.18	5.482	4.316	2	
4	3.0	12.08	0.243	2.060	65.12	49.06	109.39	5.475	4.313	2	
5	3.9	12.00	0.244	2.058	65.07	48.91	109.20	5.481	4.315	2	
6	5.0	11.95	0.245	2.057	65.15	49.06	108.83	5.484	4.309	2	
7	5.9	11.97	0.244	2.057	64.93	48.96	109.10	5.482	4.298	2	
8	7.0	11.94	0.244	2.056	65.11	48.92	108.87	5.481	4.302	2	
9	7.9	11.98	0.244	2.057	64.90	48.82	108.80	5.487	4.314	2	

10 8.9 11.94 0.245 2.057 65.12 48.93 109.08 5.482 4.300 2

Mean: 11.99 0.244 2.058 65.08 48.99 109.08 5.481 4.309

Stand.dev.: 0.02 0.000 0.000 0.03 0.04 0.06 0.001 0.002



AT 100°C

Date : 6/6/2019 Remarks : Comments here

Experiment : 022_437 Method : 022.met

Drop phase : Heavy Oil Density : 0.9000

Extern.phase : distilled water Density : 0.9692

Solid phase : Steel Calculation : Optimized cont.

No.	Time	Gamma	Beta	R0	Area	Volume	Theta	Height	Width	Opt
-----	------	-------	------	----	------	--------	-------	--------	-------	-----

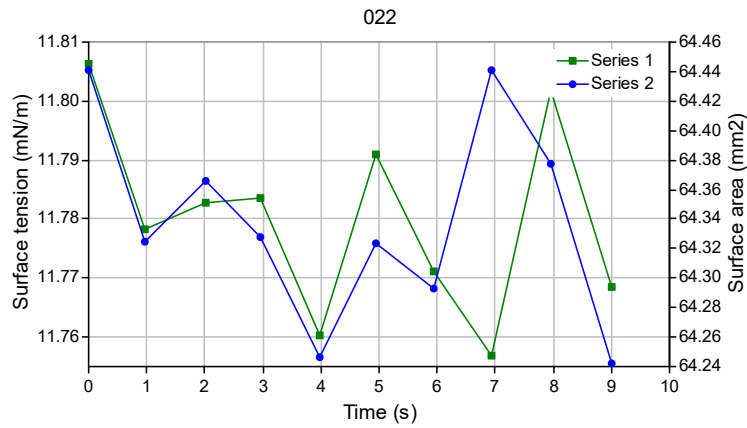
Messages

1	0.0	11.69	0.241	2.037	64.19	47.01	89.69	5.717	4.230	3
2	0.9	11.67	0.241	2.035	64.19	47.00	89.69	5.714	4.237	3
3	2.0	11.75	0.240	2.039	64.31	47.15	89.98	5.713	4.243	3
4	2.9	11.74	0.240	2.038	64.15	47.03	89.66	5.715	4.230	3
5	4.0	11.68	0.241	2.036	64.11	46.96	90.07	5.709	4.243	3

6	4.9	11.71	0.241	2.038	64.31	47.16	90.58	5.706	4.233	3
7	6.0	11.68	0.241	2.036	64.18	47.04	89.76	5.714	4.233	3
8	6.9	11.73	0.240	2.037	64.17	47.01	90.11	5.710	4.235	3
9	8.0	11.72	0.241	2.038	64.34	47.13	90.30	5.710	4.237	3
10	8.9	11.74	0.240	2.038	64.26	47.07	90.41	5.708	4.237	3

Mean: 11.71 0.241 2.037 64.22 47.06 90.02 5.712 4.236

Stand.dev.: 0.01 0.000 0.000 0.02 0.02 0.10 0.001 0.001



Brine 05% fluid 3 at 30t p 1560 psig

Date : 5/29/2019 Remarks : Comments here

Experiment : 101_14 Method : 101.met

Drop phase : Heavy Oil Density : 0.9000

Extern.phase : Brine (05%) Density : 0.9994

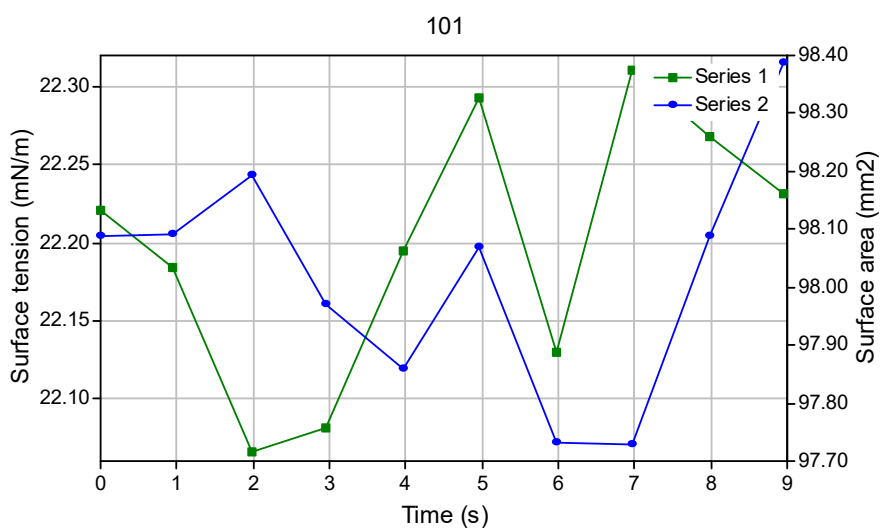
Solid phase : Steel Calculation : Optimized cont.

No.	Time	Gamma	Beta	R0	Area	Volume	Theta	Height	Width	Opt	Messages
-----	------	-------	------	----	------	--------	-------	--------	-------	-----	----------

1	0.0	22.75	0.279	2.553	97.07	96.46	123.40	6.080	5.390	2
2	1.0	22.56	0.281	2.551	97.45	96.36	123.14	6.082	5.399	2
3	2.0	22.62	0.281	2.551	97.46	96.33	123.24	6.078	5.385	2
4	3.0	22.62	0.281	2.552	97.26	96.58	123.19	6.079	5.398	2
5	3.9	22.56	0.281	2.551	96.95	96.43	123.12	6.082	5.391	2
6	5.0	22.56	0.281	2.551	97.22	96.52	123.14	6.080	5.395	2
7	5.9	22.64	0.281	2.553	97.16	96.55	123.23	6.082	5.395	2
8	7.0	22.66	0.280	2.552	97.33	96.45	123.28	6.077	5.393	2
9	7.9	22.55	0.281	2.550	97.33	96.35	123.14	6.076	5.393	2
10	9.0	22.75	0.279	2.553	97.26	96.45	123.43	6.072	5.392	2

Mean: 22.63 0.281 2.552 97.25 96.45 123.23 6.079 5.393

Stand.dev.: 0.02 0.000 0.000 0.05 0.03 0.03 0.001 0.001



At 50°C

Drop Shape Image Analysis

Date : 5/29/2019 Remarks : Comments here

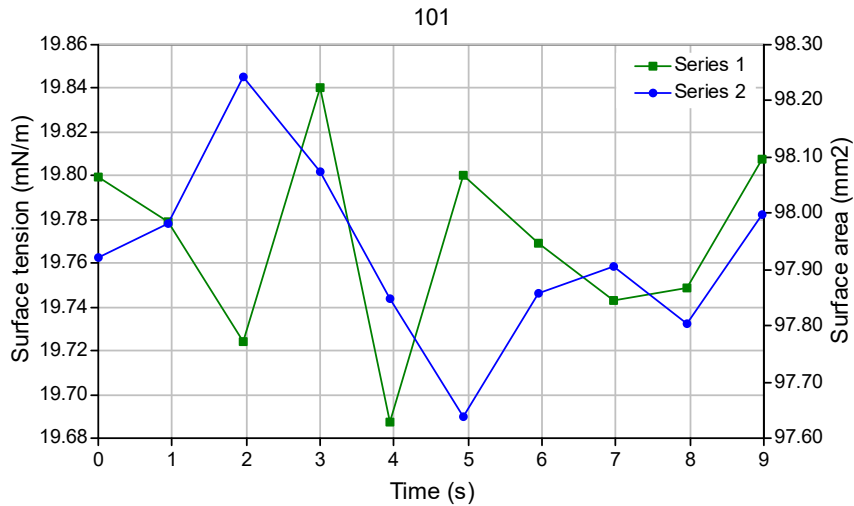
Experiment : 101_22 Method : 101.met
 Drop phase : Heavy Oil Density : 0.9000
 Extern.phase : Brine (05%) Density : 0.9917
 Solid phase : Steel Calculation : Optimized cont.

No. Time Gamma Beta R0 Area Volume Theta Height Width Opt
 Messages

1	0.0	19.72	0.292	2.530	98.03	96.62	120.48	6.252	5.362	2
2	0.9	19.69	0.292	2.529	98.20	96.51	120.48	6.252	5.351	2
3	2.0	19.77	0.291	2.531	98.42	96.75	120.56	6.251	5.363	2
4	2.9	19.55	0.293	2.526	98.16	96.40	120.26	6.251	5.354	2
5	4.0	19.74	0.292	2.529	97.96	96.51	120.59	6.249	5.353	2
6	4.9	19.77	0.291	2.528	98.16	96.37	120.67	6.244	5.359	2
7	6.0	19.68	0.292	2.528	98.00	96.41	120.52	6.248	5.362	2
8	7.0	19.66	0.292	2.528	98.17	96.47	120.44	6.250	5.358	2
9	7.9	19.68	0.292	2.527	98.27	96.35	120.53	6.247	5.357	2
10	9.0	19.66	0.292	2.527	98.06	96.43	120.48	6.245	5.356	2

Mean: 19.69 0.292 2.528 98.14 96.48 120.50 6.249 5.358

Stand.dev.: 0.02 0.000 0.000 0.04 0.04 0.03 0.001 0.001



At 70 °C and 1700p

Date : 5/29/2019 Remarks : Comments here

Experiment : 101_36 Method : 101.met

Drop phase : Heavy Oil Density : 0.9000

Extern.phase : Brine (05%) Density : 0.9822

Solid phase : Steel Calculation : Optimized cont.

No.	Time	Gamma	Beta	R0	Area	Volume	Theta	Height	Width	Opt
-----	------	-------	------	----	------	--------	-------	--------	-------	-----

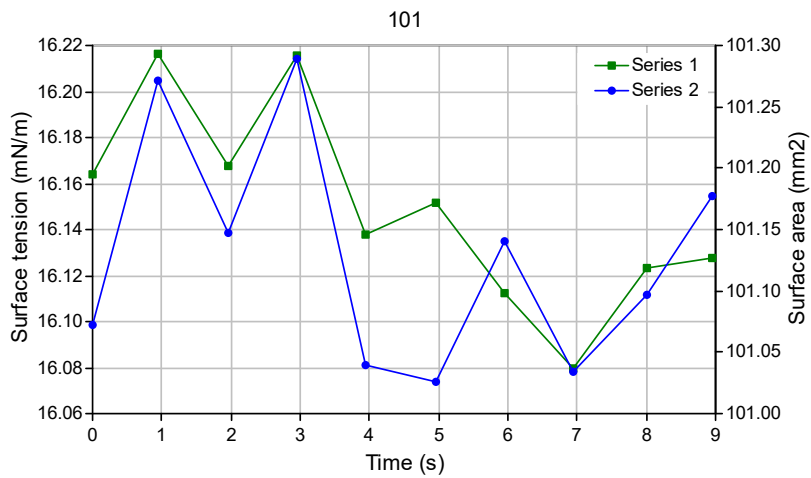
Messages

1	0.0	16.29	0.314	2.517	100.53	99.40	115.73	6.476	5.353	2
2	1.0	16.12	0.316	2.512	100.18	99.04	115.46	6.473	5.349	2
3	2.0	16.21	0.315	2.515	100.44	99.22	115.63	6.474	5.355	2
4	3.0	16.18	0.315	2.514	100.29	99.12	115.56	6.476	5.347	2
5	4.0	16.18	0.314	2.511	100.12	98.81	115.62	6.468	5.350	2
6	4.9	16.13	0.315	2.512	100.35	99.07	115.41	6.478	5.348	2
7	6.0	16.19	0.315	2.514	100.29	99.12	115.59	6.477	5.346	2
8	6.9	16.14	0.315	2.513	100.26	99.06	115.46	6.479	5.351	2

9	8.0	16.20	0.315	2.514	100.51	99.16	115.59	6.476	5.347	2
10	9.0	16.25	0.314	2.515	100.38	99.31	115.63	6.476	5.359	2

Mean: 16.19 0.315 2.514 100.34 99.13 115.57 6.475 5.350

Stand.dev.: 0.02 0.000 0.001 0.04 0.05 0.03 0.001 0.001



At 90°C and 1700p

Date : 5/29/2019 Remarks : Comments here

Experiment : 101_71 Method : 101.met

Drop phase : Heavy Oil Density : 0.9000

Extern.phase : Brine (05%) Density : 0.9745

Solid phase : Steel Calculation : Optimized cont.

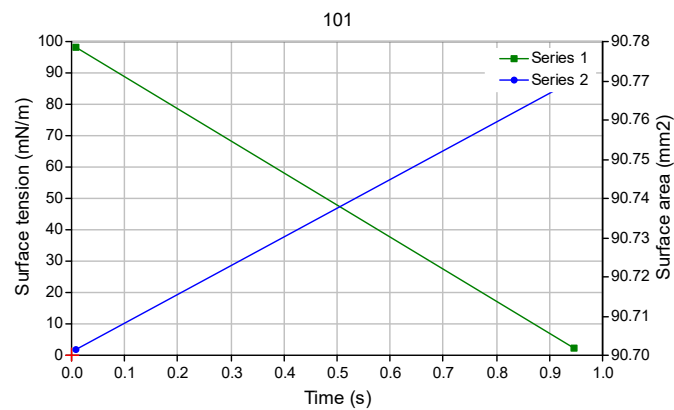
No.	Time	Gamma	Beta	R0	Area	Volume	Theta	Height	Width	Opt
-----	------	-------	------	----	------	--------	-------	--------	-------	-----

1	0.0	11.08	0.330	2.238	88.84	75.77	84.54	7.013	4.742	3
---	-----	-------	-------	-------	-------	-------	-------	-------	-------	---

2	0.9	11.17	0.329	2.243	89.68	76.20	84.55	7.025	4.747	3
3	2.0	11.14	0.329	2.241	89.29	75.93	84.54	7.020	4.743	3
4	2.9	0.00	0.000	0.000	0.00	0.00	0.000	0.000	0	Sides are too differ
5	4.0	0.00	0.000	0.000	0.00	0.00	0.000	0.000	0	Drop is distorted
6	5.0	11.16	0.329	2.241	89.62	75.96	83.90	7.038	4.738	3
7	6.0	11.11	0.329	2.238	88.84	75.75	83.52	7.041	4.753	3
8	7.0	11.12	0.329	2.238	88.98	75.92	83.58	7.041	4.734	3
9	8.0	11.16	0.329	2.241	89.26	75.91	83.54	7.050	4.739	3
10	9.0	11.12	0.329	2.239	89.09	75.84	83.26	7.055	4.743	3

Mean: 11.13 0.329 2.240 89.20 75.91 83.93 7.035 4.742

Stand.dev.: 0.01 0.000 0.001 0.12 0.05 0.19 0.005 0.002



At 100°C

Date : 5/29/2019 Remarks : Comments here

Experiment : 101_139 Method : 101.met
 Drop phase : Heavy Oil Density : 0.9000
 Extern.phase : Brine (05%) Density : 0.9736
 Solid phase : Steel Calculation : Optimized cont.

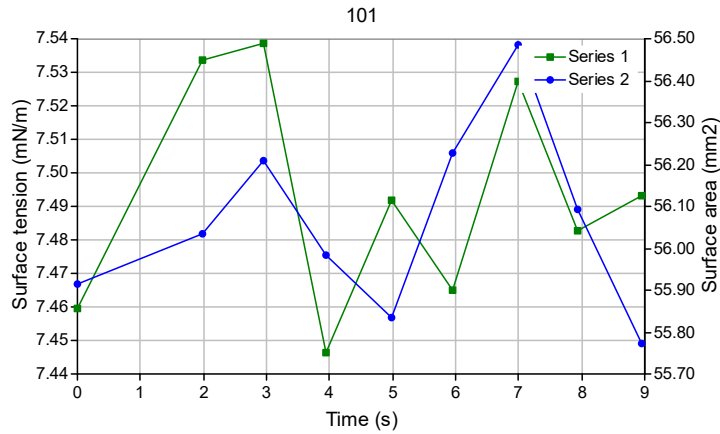
No.	Time	Gamma	Beta	R0	Area	Volume	Theta	Height	Width	Opt
-----	------	-------	------	----	------	--------	-------	--------	-------	-----

Messages

1	0.0	7.43	0.330	1.845	56.25	40.46	111.55	4.909	3.971	2
2	0.9	7.46	0.329	1.845	56.03	40.45	111.92	4.895	3.971	3
3	2.0	7.46	0.330	1.846	55.97	40.52	111.66	4.906	3.960	2
4	2.9	7.40	0.331	1.843	56.34	40.51	111.40	4.910	3.963	2
5	4.0	7.43	0.330	1.844	55.86	40.45	111.57	4.904	3.953	2
6	4.9	7.47	0.329	1.845	56.18	40.49	111.78	4.903	3.954	2
7	6.0	7.45	0.330	1.845	55.66	40.46	111.59	4.906	3.959	2
8	6.9	7.39	0.332	1.843	56.03	40.46	111.38	4.908	3.960	2
9	8.0	7.42	0.331	1.843	55.91	40.45	111.43	4.907	3.965	2
10	8.9	7.41	0.331	1.844	55.99	40.43	111.41	4.910	3.959	2

Mean: 7.43 0.330 1.844 56.02 40.47 111.57 4.906 3.961

Stand.dev.: 0.01 0.000 0.000 0.06 0.01 0.06 0.001 0.002



Fluid 5 at 30°C and 1730p

Date : 5/29/2019 Remarks : Comments here

Experiment : 022_216 Method : 022.met

Drop phase : Heavy Oil Density : 0.9000

Extern.phase : Brine (05%) Density : 0.9994

Solid phase : Steel Calculation : Optimized cont.

No.	Time	Gamma	Beta	R0	Area	Volume	Theta	Height	Width	Opt
-----	------	-------	------	----	------	--------	-------	--------	-------	-----

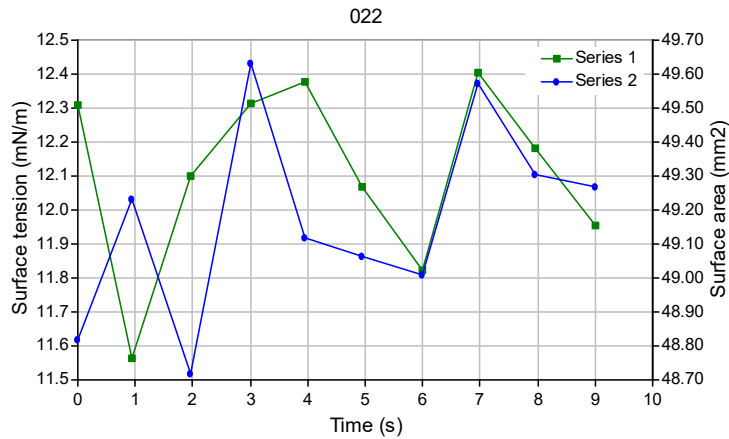
Messages

1	0.0	12.34	0.261	1.818	48.52	33.52	126.10	4.166	3.841	2
2	1.0	12.48	0.259	1.820	50.06	33.54	126.43	4.167	3.849	3
3	1.9	12.55	0.258	1.821	49.41	33.50	126.53	4.162	3.845	2
4	2.9	12.84	0.252	1.823	48.80	33.46	127.23	4.152	3.836	2
5	4.0	12.79	0.253	1.821	49.43	33.38	127.16	4.151	3.843	3
6	4.9	12.96	0.251	1.825	48.53	33.52	127.43	4.154	3.844	2
7	5.9	12.70	0.255	1.821	48.84	33.42	126.95	4.160	3.838	2

8	7.0	0.00	0.000	0.000	0.00	0.00	0.00	0.000	0.000	10	Not converging
9	8.0	13.07	0.249	1.826	48.57	33.48	127.67	4.148	3.838	2	
10	9.0	12.85	0.252	1.824	48.66	33.39	127.24	4.160	3.833	2	

Mean: 12.73 0.254 1.822 48.98 33.47 126.97 4.158 3.841

Stand.dev.: 0.08 0.001 0.001 0.18 0.02 0.17 0.002 0.002



At 50 °C and 1700p

Date : 5/29/2019 Remarks : Comments here

Experiment : 022_244 Method : 022.met

Drop phase : Heavy Oil Density : 0.9000

Extern.phase : Brine (05%) Density : 0.9917

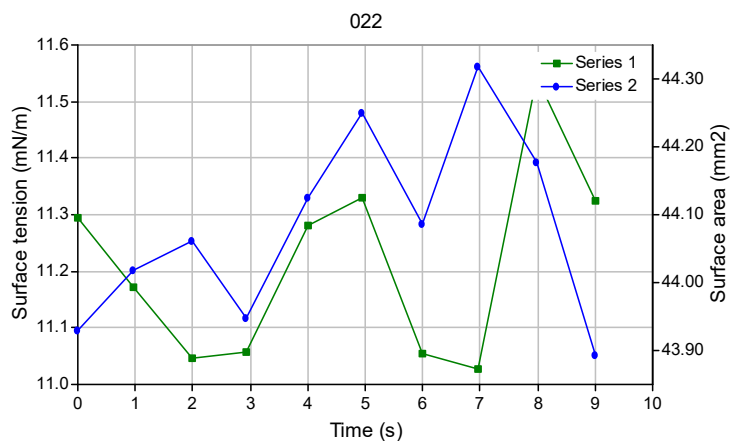
Solid phase : Steel Calculation : Optimized cont.

No.	Time	Gamma	Beta	R0	Area	Volume	Theta	Height	Width	Opt	Messages
-----	------	-------	------	----	------	--------	-------	--------	-------	-----	----------

1	0.0	12.06	0.227	1.743	43.34	28.41	130.58	3.977	3.659	3
2	0.9	12.38	0.222	1.746	43.28	28.41	131.25	3.971	3.651	2
3	2.0	12.07	0.226	1.742	43.41	28.40	130.63	3.972	3.653	3
4	2.9	12.23	0.224	1.745	43.55	28.34	130.95	3.975	3.648	2
5	3.9	12.15	0.225	1.744	43.81	28.38	130.78	3.971	3.650	2
6	4.9	12.34	0.222	1.746	43.28	28.42	131.16	3.973	3.653	2
7	5.9	12.11	0.226	1.745	43.39	28.41	130.62	3.982	3.651	2
8	7.0	12.08	0.226	1.744	43.27	28.39	130.62	3.972	3.636	2
9	8.0	12.14	0.225	1.744	43.10	28.37	130.76	3.971	3.649	3
10	8.9	12.23	0.224	1.746	43.21	28.46	130.91	3.967	3.653	2

=====
Mean: 12.18 0.225 1.744 43.36 28.40 130.82 3.973 3.650

Stand.dev.: 0.04 0.001 0.000 0.06 0.01 0.07 0.001 0.002
=====



At 70°C and 1550p

Date : 5/29/2019 Remarks : Comments here

Experiment : 022_271 Method : 022.met

Drop phase : Heavy Oil Density : 0.9000

Extern.phase : Brine (05%) Density : 0.9822

Solid phase : Steel Calculation : Optimized cont.

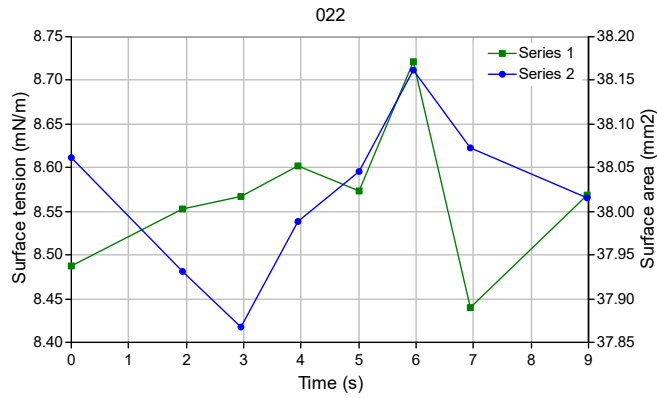
No.	Time	Gamma	Beta	R0	Area	Volume	Theta	Height	Width	Opt
-----	------	-------	------	----	------	--------	-------	--------	-------	-----

Messages

1	0.0	9.52	0.221	1.614	37.51	22.50	130.81	3.764	3.380	3
2	0.9	9.47	0.221	1.613	37.32	22.45	130.69	3.767	3.380	3
3	1.9	9.62	0.219	1.616	37.35	22.62	131.03	3.762	3.381	2
4	3.0	9.58	0.220	1.616	37.48	22.57	130.89	3.768	3.380	3
5	4.0	9.72	0.217	1.617	37.57	22.55	131.32	3.764	3.381	3
6	5.0	9.48	0.221	1.612	37.29	22.45	130.72	3.761	3.380	3
7	6.0	9.50	0.221	1.615	37.62	22.51	130.69	3.770	3.383	2
8	7.0	9.64	0.218	1.616	37.44	22.48	131.17	3.762	3.375	3
9	7.9	9.53	0.221	1.615	37.41	22.57	130.79	3.765	3.374	3
10	9.0	9.66	0.218	1.617	37.53	22.59	131.14	3.764	3.372	2

Mean: 9.57 0.220 1.615 37.45 22.53 130.93 3.765 3.379

Stand.dev.: 0.03 0.000 0.001 0.03 0.02 0.07 0.001 0.001



At 90 °C

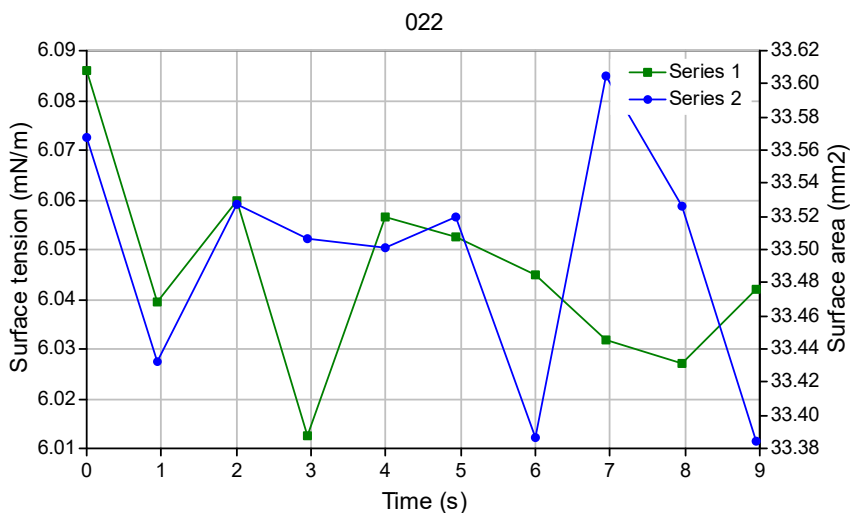
Date : 5/29/2019 Remarks : Comments here
 Experiment : 022_303 Method : 022.met
 Drop phase : Heavy Oil Density : 0.9000
 Extern.phase : Brine (05%) Density : 0.9822
 Solid phase : Steel Calculation : Optimized cont.

No. Time Gamma Beta R0 Area Volume Theta Height Width Opt
 Messages

1	0.0	6.09	0.274	1.439	33.57	17.71	108.10	3.910	3.053	3
2	1.0	6.04	0.275	1.436	33.43	17.65	107.65	3.912	3.045	3
3	2.0	6.06	0.275	1.437	33.53	17.70	107.86	3.908	3.042	2
4	2.9	6.01	0.277	1.437	33.51	17.62	107.53	3.924	3.033	2
5	4.0	6.06	0.275	1.438	33.50	17.62	107.83	3.917	3.051	3
6	4.9	6.05	0.275	1.437	33.52	17.65	107.44	3.915	3.051	3
7	6.0	6.04	0.275	1.436	33.39	17.57	107.73	3.913	3.031	2
8	6.9	6.03	0.276	1.436	33.60	17.70	107.38	3.916	3.049	3
9	8.0	6.03	0.276	1.435	33.53	17.68	107.19	3.914	3.045	3
10	8.9	6.04	0.275	1.437	33.38	17.65	107.54	3.917	3.046	3

Mean: 6.05 0.275 1.437 33.50 17.66 107.62 3.914 3.045

Stand.dev.: 0.01 0.000 0.000 0.02 0.01 0.08 0.001 0.002



At 100

Date : 5/29/2019 Remarks : Comments here

Experiment : 022_333 Method : 022.met

Drop phase : Heavy Oil Density : 0.9000

Extern.phase : Brine (05%) Density : 0.9822

Solid phase : Steel Calculation : Optimized cont.

No.	Time	Gamma	Beta	R0	Area	Volume	Theta	Height	Width	Opt	Messages
-----	------	-------	------	----	------	--------	-------	--------	-------	-----	----------

1	0.0	0.00	0.000	0.000	0.00	0.00	0.000	0.000	0		Sides are too differ
---	-----	------	-------	-------	------	------	-------	-------	---	--	----------------------

2	0.9	0.00	0.000	0.000	0.00	0.00	0.000	0.000	0		Sides are too differ
---	-----	------	-------	-------	------	------	-------	-------	---	--	----------------------

3	2.0	6.11	0.266	1.420	32.89	16.95	102.87	3.919	3.006	2	
---	-----	------	-------	-------	-------	-------	--------	-------	-------	---	--

4	2.9	6.07	0.267	1.417	33.03	16.78	103.14	3.909	2.994	2
5	3.9	6.08	0.267	1.417	32.98	16.85	103.26	3.904	2.998	2
6	5.0	6.13	0.265	1.418	32.96	16.78	103.48	3.900	3.001	3
7	6.0	0.00	0.000	0.000	0.00	0.00	0.000	0.000	0	Sides are too differ
8	6.9	6.13	0.264	1.417	32.71	16.71	103.71	3.897	2.993	2
9	8.0	6.05	0.268	1.417	32.68	16.79	103.29	3.912	2.998	2
10	9.0	6.10	0.265	1.417	32.77	16.75	103.91	3.898	3.003	3

Mean: 6.09 0.266 1.418 32.86 16.80 103.38 3.906 2.999

Stand.dev.: 0.01 0.000 0.000 0.05 0.03 0.13 0.003 0.002

